THE UNIVERSITY OF CHICAGO

SINGLE CELL RNA SEQUENCING OF PROSTATE SAMPLES YIELDS CANDIDATE FACTORS NECESSARY FOR PROSTATE REGENERATION

A DISSERTATION SUBMITTED TO

THE FACULTY OF THE DIVISION OF THE BIOLOGICAL SCIENCES

AND THE PRITZKER SCHOOL OF MEDICINE

IN CANDIDACY FOR THE DEGREE OF

DOCTOR OF PHILOSOPHY

COMMITTEE ON DEVELOPMENT, REGENERATION, AND STEM CELL BIOLOGY

BY

DANIEL CLARK MOLINE

CHICAGO, ILLINOIS

MARCH 2021

Table of Contents

LIST OF FIGURES iv
LIST OF TABLES v
ACKNOWLEDGMENTS vi
ABBREVIATIONS ix
THESIS ABSTRACT xi
CHAPTER I
BACKGROUND AND SIGNIFICANCE 1
The Anatomy and Function of the Human and Mouse Prostate 1
Benign and Malignant Prostate Disease 3
Investigation of Normal Prostate Progenitor Cells in Development and the Adult 9
In Vitro Models of Prostate Regeneration 17
Data Gathered in this Thesis 20
CHAPTER II
SINGLE CELL RNA-SEQ ANALYSIS IDENTIFIES A PUTATIVE PROGENITOR POPUALTION IN HUMAN PROSTATE SAMPLES *IN VITRO* 22
ABSTRACT 22
CONTRIBUTION BY AUTHORS 23
INTRODUCTION 23
MATERIALS AND METHODS 25
Primary Prostate Epithelial Cells 25
Monolayer and Organoid Culture 26
10x Genomics Single Cell Separation, Library Prep & Sequencing 28
Single Cell RNA-Seq Analysis 30
RT-qPCR Gene Expression 33
RESULTS 33
Organoid Cultures Contain More Populations of Epithelial Cells than Monolayer Cultures 33
Identification of Epithelial Populations 34
Stem and Progenitor Populations Found in Both Monolayer and Organoid Conditions 37
KRT13+ Cells are Quiescent and Exhibit Similar Expression as Prostate Progenitor Cells 38

DISCUSSION 43
CHAPTER III
SINGLE CELL RNA-SEQ ANALYSIS OF THE MOUSE PROSTATE IDENTIFIES FACTORS NECESSARY FOR THE REGENERATIVE PHENOTYPE OF PROSTATE CELLS *IN VITRO* 50
ABSTRACT 50
CONTRIBUTION OF COLLABORATORS 51
INTRODUCTION 51
MATERIALS AND METHODS 53
Single Cell RNA-Seq Sample Prep & Analysis 53
IF Imaging of Mouse Tissue Sections and Organoids 54
Flow Sorting of Dissociated Mouse Prostates 55
Mouse and Human Organoid Culture and Colony Forming Unit Assays 55
Statistical Analyses 56
RESULTS 58
scRNA-Seq Analysis of Intact and Castrate Mouse Prostates 58
Identifying Luminal Progenitor Cells 64
Immunofluorescence Microscopy and Flow Cytometry Validation of Luminal Progenitor Cell Biomarkers 66
Pathway Analysis of the Luminal Progenitor Cell Population 68
Treatment with Small Molecule Inhibitors Targeting Candidate Factors Leads to an Ablation of Normal Mouse Prostate Regeneration *In Vitro* 69
Small Molecule Inhibition of Candidate Factors also Ablates Human Prostate Regeneration *In Vitro* 73
DISCUSSION 75
CHAPTER IV
DISCUSSION, CONCLUSIONS, AND FUTURE DIRECTIONS 84
REFERENCES 94

LIST OF FIGURES

Fig 1: Rough Anatomy of the Human and Mouse Prostate 4

Fig 2: The Study of Hormone-Dependent Regeneration 14

Fig 3: Characterization of Organoid Culture Conditions 16

Fig 4: Identification of Prostate Epithelial Subpopulations *In Vitro* 39

Fig 5: Individual tSNE Plots and RT-qPCR Validation of Monolayer and Organoid Samples 40

Fig 6: Gene Expression of the 10 Clusters Identified in the Combined scRNA-Seq Dataset 42

Fig 7: Presence of the KRT13+ Population in Tissue, Monolayer Cells, and Organoids44

Fig 8: KRT13+ Subpopulation is Quiescent 47

Fig 9: scRNA-Seq Data from the Intact and Castrate Mouse Prostate 63

Fig 10: scRNA-Seq UMAPs with Populations Identified 65

Fig 11: Expression Patterns Observed among Populations in scRNA-Seq Data 67

Fig 12: Immunofluorescence and Flow Cytometry Validation of LPC Biomarker Expression 70

Fig 13: Pathway Analysis of LPC Expression Profile 72

Fig 14: Inhibition of Candidate Factors in the Mouse Organoid Context 77

Fig 15: Inhibition of Successful Candidate Factors from Mouse Organoid Assays Leads to Successful Ablation of Human Prostate Regeneration *In Vitro* 79

LIST OF TABLES

Table 1: Primary Cell Patient Characteristics 27

Table 2: Quality Metrics for Single Cell Solutions and 10x Genomics Sequencing Output 29

Table 3: Canonically Expressed Factors for Prostate Epithelial Populations 32

Table 4: Primers used for Quantitative Real-Time PCR 36

Table 5: Antibodies used for Immunofluorescence and Flow Cytometry 57

Table 6: Quality Control Metrics for Mouse Prostate Samples and scRNA-Seq Analyses 59

Table 7: Candidate Factors and Small Molecule Inhibitors Targeting Them 74

ACKNOWLEDGMENTS

I would like to express my sincerest gratitude to my thesis mentor, Dr. Donald Vander Griend. His constant efforts to put me into a position to succeed as a young scientist are greatly appreciated. I would also like to express gratitude to my pro-forma campus liaison Dr. Ilaria Rebay, whose organizational efforts and advice allowed me to navigate the difficulties of pursuing research off-campus while still completing my degree requirements at the University of Chicago.

I would like to acknowledge past members of the Vander Griend lab who supported and mentor me as I completed my rotation and early training in prostate research. These members include Hannah Brechka, Raj Bhanvadia, Mark Gillard, Lari de Wet, Sophia Lamperis, and Anthony Williams. A very special thank you must be made to Erin McAuley, who was my immediate superior and mentor during my training in the Vander Griend Lab and directly taught me many of the techniques I employed in my dissertation. Additionally, thank you to Calvin Van Opstall for patiently helping me with my experiments and lending a degree of sanity and clarity during our lab's moving process.

I would also like to acknowledge the current members of the Vander Griend Lab who have contributed to my thesis research. Thank you to Dr. Srikanth Perikh for his invaluable help with animal protocols and surgeries during these experiments. Thank you to Ryan Brown for his never-ending efforts to organize and collate our lab. Thank you to Alex Burr for his tireless work aiding me in my project as part of his volunteer work. Additionally, I want to add a note of appreciation to the recently added scientists in our lab, including Dr. Jordan Vellky, Heddy Williams, and Lisa Gutgesell. Although

they will not be directly continuing this specific project in the future, these women will be the future of the Vander Griend lab and have all the makings of excellent contributors to both the lab environment and data output.

I am grateful for the support provided by my thesis committee: Dr. Jill de Jong, Dr. Xioayang Wu, and Dr. Victoria Prince. Their guidance and patience throughout my candidacy are deeply appreciated.

I am thankful for the expertise and advice provided by numerous core facilities, including the University of Chicago Flow Cytometry Core and Human Tissue Resource Center as well as the University of Illinois at Chicago Flow Cytometry Core and Research Histology Core. I would also like to thank the University of Chicago Cell and Molecular Biology Cluster Office and the Office of Graduate and Postdoctoral Affairs. I would also like to thank the MCB Training Grant administrators Benjamin Glick and Phoebe Rice both for the financial support of the grant as well as the training environment they created for awardees. Additionally, I would like to thank UChicagoGRAD and the MyCHOICE programs and their staff.

I would like to thank my rugby team, Lincoln Park RFC, for providing a necessary escape from the doldrums of academia and a welcoming environment for me to vent my frustrations throughout the graduate school process. May Bacchus smile upon all of you degenerates, now and into the future.

An eternal thanks to my parents Scott and Jayne for encouraging me to pursue my education as far as it would take me as well as providing a firm bit of motivation whenever I allowed myself to fall behind. Also, I would like to thank my sister Margaret

and her husband Matts, who have spent countless hours exploring Chicago with me as I stumbled my way through both my undergraduate and graduate tenure.

Finally, I wish to express my gratitude to my wife and best friend Anna. Her love and support were invaluable to me throughout this process, and it cannot be stated enough that my graduation would have been impossible without her help.

ABBREVIATIONS

AR (Androgen Receptor)
Bcl-2 (Bcl2 Apoptosis Regulator)
BPH (Benign Prostatic Hyperplasia)
CARNs (Castration-Resistant Nkx3.1-Positive Cells)
Ccl6 (C-C Motif Chemokine Ligand 6)
CD24 (Cytodifferentiation Factor 24)
CD26 (Cytodifferentiation Factor 26)
Cytodifferentiation Factor 44 (CD44)
CD49f (Cytodifferentiation Factor 49f)
CFA (Colony Forming Assay)
ChrA (Chromogranin A)
Claudin 5 (Cldn5)
CRPC (Castration-Resistant Prostate Cancer)
CTNNB1 (Catenin Beta 1), Dcn (Decorin)
DHT (Dihydrotestosterone)
DKK1 (Dickkopf Wnt Signaling Pathway Inhibitor 1)
E17 (Embryonic Day 17)
ERG (ETS Related Gene)
FBS (Fetal Bovine Serum)
Fgf2 (Fibroblast Growth Factor 2)
Fgf7 (Fibroblast Growth Factor 7)
Fgf10 (Fibroblast Growth Factor 10)
FST (Follistatin), Growth Arrest Specific 5 (Gas5)
GLI1 (Gli Family Zinc Finger 1)
HIF1A (Hypoxia Inducible Factor 1 Subunit Alpha)
IGFBP2 (Insulin-Like Growth Factor Binding Protein 2)
IGFBP3 (Insulin-Like Growth Factor Binding Protein 3)
INHBA (Inhibin A)
IPA (Ingenuity Pathway Analysis)
Klf4 (Kruppel-Like Factor 4)
Krt5 (Keratin 5)
Krt8 (Keratin 8)
Keratin 13 (Krt13)
Krt14 (Keratin 14)
Krt18 (Keratin 18)
LPC (Luminal Progenitor Cell)
Lgr5 (Leucine-Rich Repeat Containing G Protein-Coupled Receptor 5)
Igf1 (Insulin-Like Growth Factor 1)
LUTS (Lower Urinary Tract Symptoms)
Ly6d (Lymphocyte Antigen 6D)
LYPD3 (LY6/PLAUR Domain Containing 3)
Matrix Metalloprotease 9 (MMP9)
Nkx3.1 (Nk3 Homeobox 1)
Nf-kB (Nuclear Factor Kappa Beta)

Notch1 (Notch Receptor 1)
p38 MapK (p38 MAP Kinase)
Pbsn (Probasin)
PCa (Prostate Cancer)
Proliferating Cell Nuclear Antigen (Pcna)
PSA (Prostate Specific Antigen)
Pdpn (Podoplanin)
PrE (Prostate Epithelial)
Psca (Prostate Stem Cell Antigen)
Quality Control (QC)
RT-qPCR (Real-Time Quantitative PCR)
Sca-1 (Stem Cell Antigen 1)
scRNA-Seq (Single-Cell RNA-Seq)
SERPINB1 (Serpin Family B Member 1)
SFRP1 (Secreted Frizzled-Related Protein 1)
Shh (Sonic Hedgehog)
Smo (Smoothened)
Sox2 (SRY-Box Transcription Factor 2)
Syn (Synaptophysin)
TIMP3 (TIMP Metallopeptidase Inhibitor 3)
Trop2 (Tumor-Associated Calcium Signal Transducer 2)
Tumor Protein p63 (p63)
Transurethral Resection of the Prostate (TURP)
UGSM (Urogenital Sinus Mesenchyme)
Yes-Associated Protein 1 (Yap1)

THESIS ABSTRACT

The human prostate is a significant source of disease burden for adult males. In the malignant context, prostate cancer is the most common non-cutaneous cancer in males. Benign prostatic hyperplasia is also common, affecting a majority of males over the age of 60. This high disease burden has been a focus of study for many years, but an answer to the ultimate question of what predisposes the prostate to such a high level of disease has eluded researchers. One possible explanation for the disease burden of the prostate may lie in the capacity of the prostate for hormone-dependent regeneration. This is a process by which the prostate shrinks in the absence of androgen signaling, and regenerates to its original size when androgen is reintroduced to the system. The study of hormone-dependent regeneration has allowed researchers to analyze the progenitor cell populations of the prostate.

In this thesis, single cell RNA-Seq approaches were used to investigate the progenitor cell populations of the prostate. First, I investigated cells harvested from monolayer and organoid culture conditions to better understand the progenitor populations present in these models and differences between the models overall. This yielded evidence that prostate progenitor cells expressing Keratin 13 were preserved in both monolayer and organoid conditions. This presence of prostate progenitor cells was validated using immunofluorescence microscopy targeting Keratin 13 protein. In comparing the single cell RNA-Seq data from the two culture conditions, we were able to observe an enrichment of proliferating populations in the monolayer sample and an enrichment of intermediate cells in the organoid sample. Further comparison of these *in vitro* samples with *in vivo* prostate data gathered by another lab provided evidence that

the *in vitro* samples were enriched for proliferating cells while the *in vivo* sample contained terminally differentiated cell populations that were not observed *in vitro*. These data provide an in-depth validation of the preservation of prostate progenitor cells in commonly used *in vitro* models, as well as providing insights into the different cell populations selected for in monolayer and organoid culture conditions respectively.

Application of single cell RNA-Seq approaches to *in vivo* mouse prostate led to the identification of a luminal progenitor cell population in both the intact and castrate mouse prostate. These cells expressed luminal keratins as well as multiple putative progenitor cell markers. The presence of luminal progenitor cells in the mouse prostate was also validated using both immunofluorescence microscopy and flow cytometry. Pathway analysis of the expression data from luminal progenitor cells allowed for the selection of candidate factors likely to contribute to the prostate progenitor cell phenotype. Small molecule inhibitor treatment targeting two of these factors, Yap1 and Bcl-2, caused a significant decrease in *in vitro* regeneration of organoids derived from both mouse and human cells. These results provide in-depth expression data for luminal progenitor cells and also identify factors necessary for the prostate progenitor cell phenotype. These factors can be leveraged to better understand luminal progenitor cells and possibly be used to treat prostate disease in the future.

CHAPTER 1

BACKGROUND AND SIGNIFICANCE

The Anatomy and Function of the Human and Mouse Prostate

The human prostate is a walnut-shaped organ present in the urogenital assembly of most mammals and is responsible for the secretion of prostatic fluid (C. H. Lee, Akin-Olugbade, and Kirschenbaum 2011). This fluid, consisting mostly of nutrients like citrate, contributes to fertility by sustaining the survival of sperm cells within the ejaculate (C. H. Lee, Akin-Olugbade, and Kirschenbaum 2011). Internally, the prostate has a branching ductal architecture made up of numerous epithelial glands surrounded by a large stromal compartment (Cunha et al. 1987). These epithelial glands are made up of luminal epithelial cells responsible for the secretion of prostatic fluid as well as basal epithelial and neuroendocrine cells (Oliveira et al. 2016). The surrounding prostatic stroma contains a diverse population of cells, including endothelial cells, fibroblasts, immune cells, and smooth muscle cells that are responsible for the contraction of the prostate during ejaculation (Levesque and Nelson 2018).

The established histological guidelines of the prostate epithelium enable the reliable identification of cell types using validated protein markers. Luminal epithelial cells are marked by Keratin 8 (Krt8) and Keratin 18 (Krt18) as well as Prostate Specific Antigen (PSA) and Androgen Receptor (AR) (Ittmann 2018). In flow cytometry applications, luminal cells are often sorted using Cytodifferentiation Factor 24 (CD24) as well as Cytodifferentiation Factor 26 (CD26) (Karthaus et al. 2014; Crowell, Fox, et al. 2019). The basal compartment of the prostate epithelium is marked by Keratin 5 (Krt5), Keratin 14 (Krt14), and Tumor Protein 63 (p63) (Ittmann 2018). The predominant flow

marker for basal cells is Cytodifferentiation Factor 49f (CD49f) (Choi et al. 2012). Neuroendocrine cells of the prostate are marked histologically by Chromogranin A (CHRA) and Synaptophysin (SYN) (Cohen et al. 1993; Di Sant'Agnese 1998). Although neuroendocrine cells are present in the prostate epithelium, it is important to note that little is known about their function in the prostate and that this thesis will contain very little discussion of the neuroendocrine cell population.

The murine prostate is a common model system used in prostate experimentation, especially in the study of hormone-dependent prostate regeneration. Importantly, there are some observable anatomical differences between the murine prostate and that of a human. Firstly, the murine prostate is separated into histologically distinct lobes, while the human prostate is a single continuous tissue divided into histological zones according to proximity to nearby organs (**Fig. 1**) (Ittmann 2018; Toivanen, Mohan, and Shen 2016). Second, the basal compartment of the murine epithelium is semi-continuous, while the human prostate epithelium contains a continuous basal layer (Ittmann 2018). Third, the luminal compartment of the murine prostate has been proven to be self-sustaining in regeneration studies, while the same behavior has yet to be observed in the human context (Choi et al. 2012; Moad et al. 2017). This discrepancy between species may be due in part to the inability to apply hormone-dependent regenerative experimental approaches to human patients due to ethical constraints.

Aside from secretory activity, the prostate exhibits another scientifically interesting behavior through its capacity for hormone-dependent regeneration. In short, the prostate undergoes a wave of apoptosis in the absence of androgen signaling,

shrinking to approximately a tenth of its original size (**Fig 2A**) (Cunha et al. 1987; Sugimura, Cunha, and Donjacour 1986b). Upon the reintroduction of androgen signaling, the prostate can regenerate to its original size, recapitulating its original architecture and regaining its secretory function. This process is thought to be common among animals that engage in seasonal breeding, but it is important to note that humans and other animals that lack breeding seasons also have prostates capable of hormone-dependent regeneration (Li Xin et al. 2003). This process has been harnessed scientifically to create an experimental regimen that uses surgical castration in mice to initially remove androgen signaling and the subsequent subcutaneous implantation of a silane testosterone pellet to reintroduce androgen signaling and induce the regeneration of the involuted prostate. The testosterone pellet can be removed and re-implanted up to thirty times, with each oscillation of androgen signaling leading to a stereotyped regeneration response (Sugimura, Cunha, and Donjacour 1986b; Tsujimura et al. 2002). This experimental approach to the study of hormone-dependent regeneration has been used successfully to identify numerous markers and behaviors of the stem and progenitor cell populations necessary for prostate regeneration.

Benign and Malignant Prostate Disease

Prostate disease is often classified in two broad categories: benign and malignant. Benign prostatic hyperplasia (BPH) is a condition in which the prostate increases significantly in size in adult men (Ramsey 2000; Aaron, Franco, and Hayward 2016). BPH is a common disease, with a majority of men over the age of 50 diagnosed

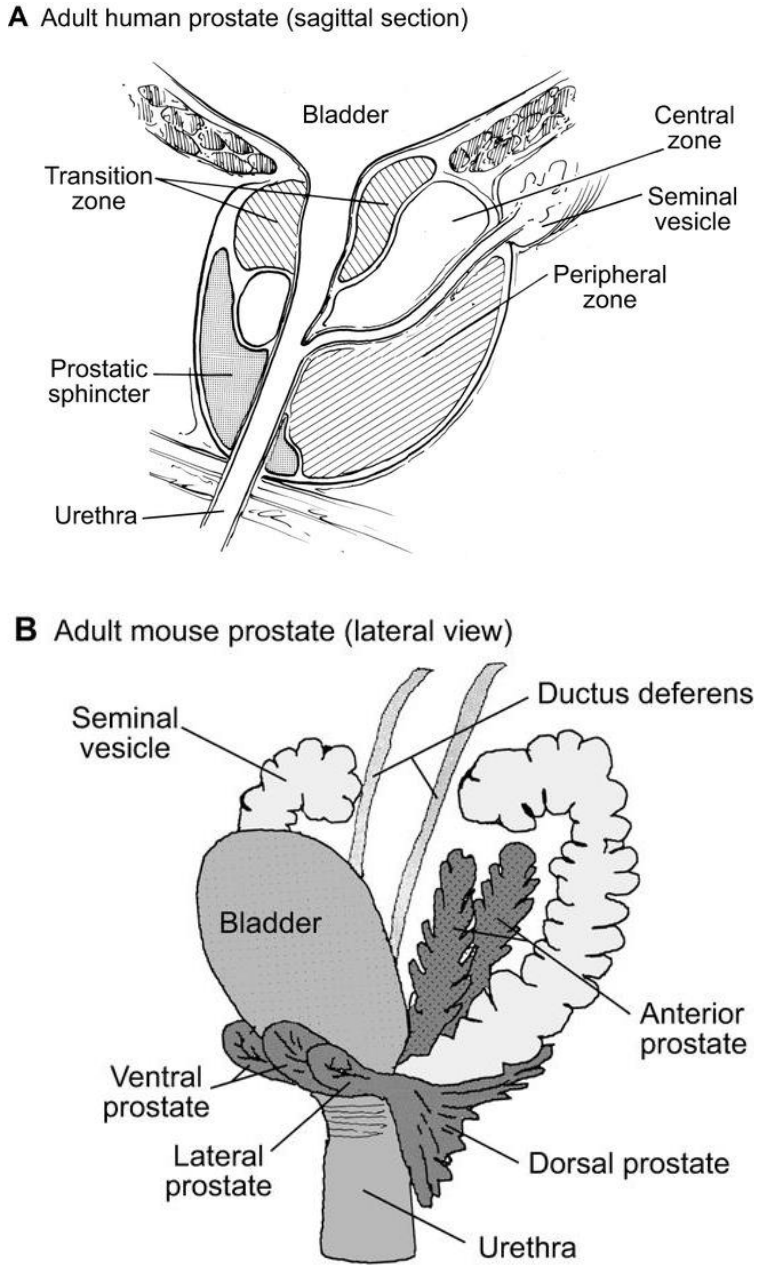

Fig. 1: Rough Anatomy of the Human and Mouse Prostate. A. Drawing depicting the human prostate (Toivanen and Shen 2017). The organ is continuous and subdivided into histological zones, with the Transition Zone closest to the bladder, the Peripheral Zone furthest away from the bladder, and the Central Zone located between the Transition Zone and Peripheral Zone. B. A drawing depicting the mouse prostate. The mouse prostate consists of distinct histological lobes (Anterior, Ventral, Dorsal, and Lateral), marked in dark grey in the image (Toivanen and Shen 2017).

(Lim 2017; Ramsey 2000; Wei, Calhoun, and Jacobsen 2005; Black et al. 2006). This prostatic growth eventually impinges on the prostatic urethra, leading to Lower Urinary Tract Symptoms (LUTS) including reduced bladder voiding, frequent urination, and painful urination (Lepor 2005). Pathologically, BPH can exhibit a clear phenotype in which epithelial cells “stack” on top of themselves, producing crowded glands that expand the tissue (Aaron, Franco, and Hayward 2016). Other pathologies of BPH exist, including stromal varieties, but this thesis will focus on epithelial hyperplasia of the prostate. Treatments currently available for BPH include Alpha Adrenergic Antagonists (Alpha Blockers), 5-alpha-reductase inhibitors, and Tadalafil (Aaron, Franco, and Hayward 2016). Alpha Blockers cause the relaxation of smooth muscle surrounding the bladder neck and urethra, relieving the symptoms of urinary constriction consistent with BPH (Lepor 2007). 5-alpha-reductase inhibitors work on the hormonal axis, causing a partial inhibition of androgen signaling that can lead to prostate shrinkage over time (E. H. Kim, Brockman, and Andriole 2018). Lastly, Tadalafil is an erectile dysfunction medication that has been shown to cause a reduction in prostate size as a side effect in some patients (Hatzimouratidis 2014). Tadalafil achieves this effect by inhibiting PDE5, leading to an accumulation of cyclic GMP that reduces the effects of erectile dysfunction and leads to a relaxation of smooth muscle in the prostate, reducing its size (Hatzimouratidis 2014). Extreme cases of BPH that lead to a significant blockage of the urethra or other dangerous symptoms are treated with a minimally invasive surgical prostate removal called a transurethral resection of the prostate (TURP) (Rocco et al. 2011). BPH is a chronic disease, meaning that patients must maintain their treatment regimen treatment indefinitely to alleviate their symptoms long-term. This has created a

sizeable material drain on the American medical system, as BPH is pervasive in older men and lacks a permanent treatment option (Black et al. 2006). A treatment approach through which the regenerative or proliferative activity of the prostate is permanently ablated would be advantageous in treating BPH and would also provide a superior alternative to current treatments that can only temporarily alleviate symptoms.

Prostate cancer (PCa) is characterized by the outgrowth of malignant tissue within the prostate (Rawla 2019). Much like BPH, PCa is a common disease in men. In fact, PCa is the most common non-cutaneous cancer in men constituting 20% of new cancers in men in the year 2019 (Rawla 2019; American Cancer Society 2020). Malignant outgrowth is commonly observed histologically in the luminal compartment of the prostate epithelium, although rarer neuroendocrine and basal cancers also exist (Conteduca et al. 2019; van der Kwast et al. 2003). The prognosis of prostate cancer is often related using a histologically determined Gleason Grade, where cancerous regions of tissue samples are given a numeric grade between 7 and 10, with 7 being low-risk and 10 being extremely high-risk, undifferentiated tissue (Grignon 2018).

The commonality of prostate cancer has engendered a serious interest in discovering effective treatments for many decades. In the early 1940s, Charles Huggins made one of the first breakthroughs in prostate cancer treatment, discovering that castration could effectively inhibit cancerous outgrowth by starving the neoplastic tissue of its needed androgen signals (Huggins and Hodges 1941). Even today, the majority of prostate cancer cases are treated using chemical blockade of androgen signaling after prostatectomy or radiation therapy to induce a castrate state within the prostate (Jayadevappa et al. 2017). This, along with other recent advancements in treatment,

has yielded a 10-year survival rate of 95% for prostate cancer patients (American Cancer Society 2020). Although this survival rate is encouraging, the pervasive nature of prostate cancer means that the 5% of patients who succumb to the disease before the 10-year mark still constitutes a large number of individuals. Additionally, patients who are successfully treated with castration or prostatectomy do not remain in permanent remission. More advanced prostate cancer cases that escape initial treatment regimens are often refractory to androgen deprivation therapy, commonly referred to as Castration-Resistant Prostate Cancer (CRPC) (Rawla 2019). This variety of prostate cancer is currently considered incurable and is much more aggressive than the early-stage cancers that respond to androgen deprivation therapy (Chandrasekar et al. 2015).

CRPC is first and foremost marked by its lack of androgen dependence, but it also displays numerous additional behaviors shared with undifferentiated cells in the prostate epithelium (Chandrasekar et al. 2015). One common process through which prostate cancers achieve castration resistance is the aberrant upregulation of AR signaling targets involved in cell proliferation and survival independent of ligand binding. This can occur through amplification of the AR gene leading to hypersensitivity to AR signaling. This can lead to cells responding to the low, persisting levels of AR in the castrate state (Chandrasekar et al. 2015). Other mechanisms of CRPC include mutations of the AR gene that allow the AR protein to escape normal regulatory pathways, and expression of AR splice variants (AR variants 1-7) that achieve similar androgen independence as AR mutants (Visakorpi et al. 1995; W. Liu et al. 2008; Hara et al. 2005; Guo et al. 2009). One of the chief genetic causes of prostate cancer that is

also a significant contributor to CRPC is the TMPRSS2-ERG gene fusion, which allows for the constitutive overexpression of the ETS related gene (ERG) (Yu et al. 2010). ERG is an important regulator during vascular development, and its expression marks both early prostate cancers as well as CRPC (Birdsey et al. 2015; Adamo and Ladomery 2016). This mutation also shares some similarities with an additional route to castration resistance; the activation of growth factor pathways that induce developmental proliferation and survival programs that allow cells to persist and multiply in the absence of androgen signaling (Nadiminty et al. 2013; Vlaeminck-Guillem, Gillet, and Rimokh 2014; Wen et al. 2000). Additionally, CRPC cells show an increased propensity for lineage plasticity. Cells observed in castration resistant cancerous growths can also express numerous lineage markers outside the typical luminal markers expressed by early stage cancers, including basal markers like KRT5 and neuroendocrine markers like SYN (Beltran et al. 2019). This behavior is thought to be a method through which cancerous cells can “escape” conventional treatments by assuming lineage identities that are refractory to those treatments (Beltran et al. 2019). Altogether, these molecular mechanisms paint a picture of cancerous cells assuming many of the behaviors of epithelial progenitor cells, including low proliferation rates, high lineage plasticity, and the activation of cell survival programs. The field surrounding prostate disease is working to better understand how the pathways underlying these stem-like behaviors are activated, and which pathways can be successfully targeted in diseases to establish more efficacious and permanent treatments for BPH and PCa. To aid in this effort, many groups have worked to gain a deeper understanding of normal prostate epithelial stem cells.

Investigation of Normal Prostate Progenitor Cells in Development and the Adult

Most knowledge of prostate development has been acquired using mouse models due to the ease of genetic engineering and tissue processing in this model system. Mouse prostate development begins at E6.5 with the formation of prostatic buds on the surface of the embryonic urogenital sinus (Timms, Mohs, and Didio 1994; Cunha et al. 1987; Aaron, Franco, and Hayward 2016). The mouse prostate is nascent at birth, consisting mainly of prostate buds that have yet to undergo the outgrowth and epithelial organization necessary to resemble the adult prostate (Timms, Mohs, and Didio 1994). As the mouse matures and reaches 15 days of age, the prostate grows and begins to develop the branching architecture observed in the adult (Timms, Mohs, and Didio 1994; Sugimura et al. 1986; Sugimura, Cunha, and Donjacour 1986a). Between 6 and 8 weeks of age, the mouse prostate undergoes canalization. This process involves the differentiation and organization of the prostate epithelium (Keil et al. 2012). Using histology, one can observe the shift from largely undifferentiated prostate basal cells expressing the cytokeratin markers of both the basal and luminal lineages to the terminally differentiated and distinct basal and luminal epithelial cell lineages observed in the adult mouse prostate (Toivanen and Shen 2017; Keil et al. 2012). At 8 weeks of age, the mouse has completed puberty and prostate development, meaning that the prostate has assumed the full size, architecture, and secretory function of the adult organ (Cunha et al. 1987; Toivanen and Shen 2017; Castillo-Martin et al. 2010).

Prostate development is mainly influenced by androgen signaling, but numerous necessary factors exist downstream of this initial signal. The prostate budding observed

on E17 is initiated by the reception of androgen signals leading to the secretion of numerous morphogenic ligands including Wnt and Sonic Hedgehog (Shh) (Schneider et al. 2000). Downstream of these ligands are transcription factors including Nk3 Homeobox 1 (Nkx3.1), a factor that is necessary for prostate budding at E17 and postnatal prostate growth (Schneider et al. 2000). Other developmental factors present in the developing prostate mesenchyme include Fibroblast Growth Factors 7 and 10 (Fgf7, Fgf10) and Insulin-Like Growth Factor 1 (Igf1) (Thomson and Cunha 1999; Sugimura et al. 2003). These factors are capable of inducing prostatic growth in organ culture conditions, and their genetic disruption leads to a significant reduction in prostate size and number of branch points (Thomson and Cunha 1999; Sugimura et al. 2003).

Epithelial stem and progenitor cells are most often characterized in the two contexts of embryonic/neonatal development as well as in the adult. Prostate development begins at embryonic day 6.5 with the nascent urogenital sinus. This tissue gives rise to the prostate, seminal vesicles, and urethra in males while it gives rise to the uterus and vagina in females. In males, the urogenital sinus is exposed to androgen signaling at E6.5, leading to the activation of Wnt signaling and its downstream target Nkx3.1. Nkx3.1 is a necessary factor in prostate budding, the process by which the tissue that will eventually become the ducts of the prostate buds out of the urogenital sinus. Buds will continue to form and grow out until E18, when the raw tissue of the prostate is complete. Next, the prostate undergoes a process called canalization, where the tissue of the nascent prostate organizes into epithelial glands capable of secreting prostate fluid. This is marked histologically by the bifurcation of the basal lineage, which

at this point expresses both p63 basal markers and Krt18 luminal markers, into the separate basal and luminal lineages seen in the adult prostate. Canalization continues until the end of puberty at 8 weeks of age, meaning that the prostate is often considered “adult” at that age.

The adult prostate is largely quiescent in the presence of normal androgen signaling, only undergoing limited amounts of tissue turnover through anoikis and subsequent stem cell activity to replace the lost cells. Due to the lack of stem cell activity in the intact prostate, researchers have used hormone-dependent regeneration to activate the stem cell phenotype (**Fig. 2A**).(Sugimura, Cunha, and Donjacour 1986b) One of the initial assays showing evidence of stem cell activity in the prostate used BrDU pulse-chase coupled with hormone-dependent regeneration. A rare population of cells was able to retain BrDU through 11 cycles of hormone-dependent regeneration, yielding evidence that a persistent population of slow-cycling cells existed in the prostate and contributed to regeneration (Tsujimura et al. 2002). This approach of hormone-dependent regeneration has typically been coupled with lineage tracing, indelibly marking cells that express candidate stem cell factors and assaying their dynamics throughout an androgen cycle. Cells that survive castration, evidenced by the persistence of the indelible mark in the involuted prostate, and contribute to regeneration, evidenced by the clonal outgrowth of the indelibly marked cells post-regeneration, are considered to exhibit stem or progenitor characteristics.

Putative prostate epithelial stem cell markers including Tumor-Associated Calcium Signal Transducer 2 (Trop2), Stem Cell Antigen 1 (Sca-1), Leucine-Rich Repeat Containing G Protein-Coupled Receptor 5 (Lgr5), and SRY-Box Transcription

Factor 2 (Sox2) were discovered using this approach (Goldstein et al. 2008; Burger et al. 2005; B. Wang et al. 2015; E. McAuley et al. 2019). In addition to the straightforward discovery of biomarkers, broader discoveries about the nature of prostate epithelial stem cells were made using these methods. At the inception of the field, researchers believed that epithelial stem cells resided solely in the basal compartment of the prostate epithelium, and that luminal cells were almost exclusively descended from basal stem cells during prostate regeneration. This belief was influenced by evidence from prostate development as well as the understanding of epithelial regeneration in other organs and early data showing the existence of stem cells within the basal lineage. Later investigations spearheaded by the lab of Michael Shen yielded evidence that rare cells within the luminal lineage were also capable of persisting through castration and contributing to regeneration. Initially identified as castration-resistant Nkx3.1-positive cells (CARNs), these luminal progenitor cells exhibited unipotency *in vivo* but were capable of bipotency in organoid culture conditions (**Fig. 2B**) (X. Wang et al. 2009). Further investigation by the Shen lab also yielded evidence that the luminal lineage of the mouse prostate is self-sufficient during regeneration, and that most of the luminal cells produced during regeneration are derived from cells already residing within the luminal lineage (Choi et al. 2012). Altogether, these data helped create the current model of murine prostate regeneration, which involves the contribution of castration-resistant progenitor cells residing in both the basal and luminal lineages.

Although the practice of analyzing hormone-dependent regeneration using lineage tracing has yielded important advances in the identification of prostate progenitor cells, there are some limitations to the approach. First, lineage tracing has a

limited number of markers that can be tracked at any one time (Wuidart et al. 2016). Due to this limitation, it can be difficult to investigate the overlap in expression of different stem markers among cell populations present in the prostate epithelium. Second, although cells are observed to survive castration and contribute to regeneration, the markers used to observe these behaviors are rarely causal. Although some putative epithelial stem markers, such as Lgr5, are necessary for maximal prostate regeneration, the majority of markers used are not mechanistic contributors to the stem cell phenotype (B. Wang et al. 2015; Li and Shen 2019). These limitations have led to the validation of numerous markers but a distinct lack of knowledge regarding the overlap of markers in progenitor cell populations and the necessary mechanistic contributors underlying the prostate progenitor cell phenotype.

Recently, researchers have applied single cell RNA-Seq workflows to prostate stem cell investigations with the express goal of overcoming some of the limitations inherent to lineage tracing systems. One of the first of these applications was an investigation of healthy human prostate samples performed by the lab of Douglas Strand. This led to the identification of a stem-like population of cells in the prostate epithelium, referred to by the Strand lab as Club/Hillock cells, that were largely marked by an expression of Keratin 13 (Krt13) (Henry et al. 2018). This study is among the first to show definitive evidence identifying normal stem cells in the human context while also setting a new histological guideline for the identification of this population in the context of neoplastic disease. Another investigation using scRNA-Seq was undertaken by the Goldstein lab at UCLA, this time using the aging mouse prostate as a model.

A.

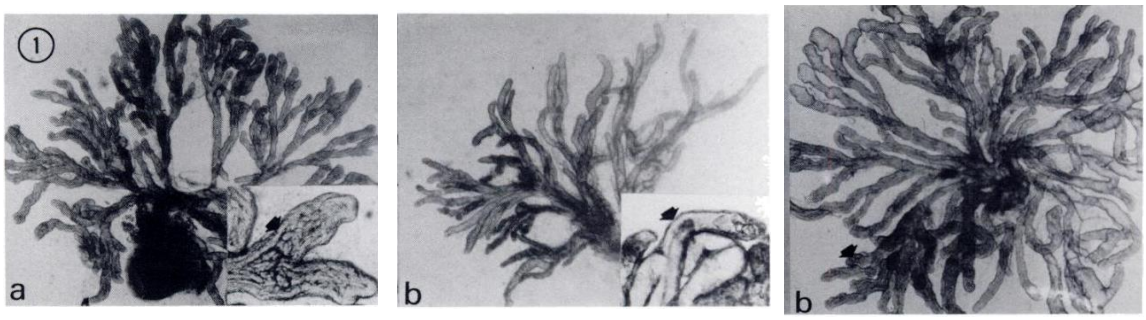

B.

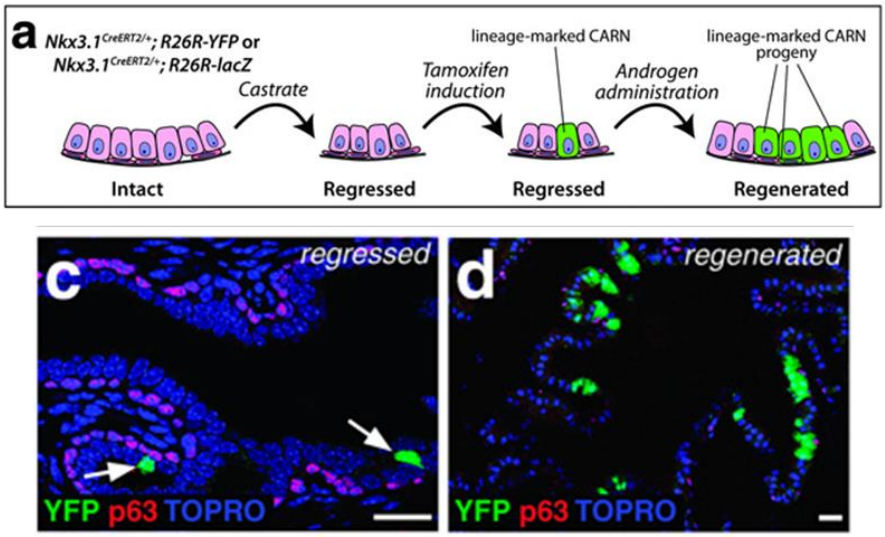

Fig 2: The Study of Hormone-Dependent Regeneration. A. Representative image depicting hormone dependent regeneration of the mouse prostate (Sugimura, Cunha, and Donjacour 1986b). In the middle subpanel, the castrate prostate is reduced to a fraction of its original size in the presence of androgen signaling, which is depicted in the far-left subpanel. The far-right subpanel shows a regenerated prostate, which has been exposed to androgen signaling after a period of castration. B. Figure showing an example of the application of lineage tracing to the mouse prostate. In this study, it was found that Nkx3.1-expressing luminal cells could persist through castration and contribute to prostate regeneration after the reintroduction of androgen, thus exhibiting a prostate progenitor cell phenotype (X. Wang et al. 2009). Subpanel a depicts the experimental design of treatment and genetic engineering that allowed researchers to indelibly mark $Nkx3.1^{+}$ cells with a YFP lineage marker and track them through regeneration. Subpanel c depicts the rare $Nkx3.1^{+}$ cells in the regressed condition, while subpanel d depicts $Nkx3.1^{+}$ cells after regeneration, providing evidence that these cells contributed to regeneration due to the presence of YFP-marked clonal bands in the prostate epithelium.

This investigation identified both basal and luminal progenitor cells and found that the aging mouse prostate contained more of these cells than the prostates of younger mice (Crowell, Fox, et al. 2019). More specifically, this study yielded evidence that tissue taken from the prostates of older mice was more capable of regeneration on average than tissue taken from the prostates of younger mice (Crowell, Fox, et al. 2019).

Further investigation of the mouse prostate stroma by the Xin lab found that the stromal populations could be roughly subdivided yielding a specific pair of signaling stromal populations that, when co-cultured with epithelial cells in organoid culture conditions, could influence the identity of daughter cells during *in vitro* regeneration (Kwon et al. 2019). This population of stromal cells, referred to as R1 cells, was ultimately marked by the expression of multiple signaling molecules including Wnt and Bone Morphogenic Protein (Bmp) ligands as well as Steroid 5 Alpha-Reductase 2 (Srd5a2), an enzyme necessary for the synthesis of testosterone (Kwon et al. 2019; Toivanen and Shen 2017). Altogether, this expression profile implied R1 cells were responsible for the secretion of morphogenic and hormonal signals that are important to epithelial cell differentiation and survival. A more thorough and holistic investigation of stem populations using scRNA-Seq was performed by the Sawyers lab. This group captured samples at multiple timepoints during the process of prostate involution and regeneration, cataloguing the changes in the prostate stem cell population throughout the process (Karthaus et al. 2020). By analyzing these data, the group was able to conclude that many of the ostensibly differentiated cells in the luminal lineage are able to adopt elements of the stem cell phenotype in the hormone-deprived mouse prostate

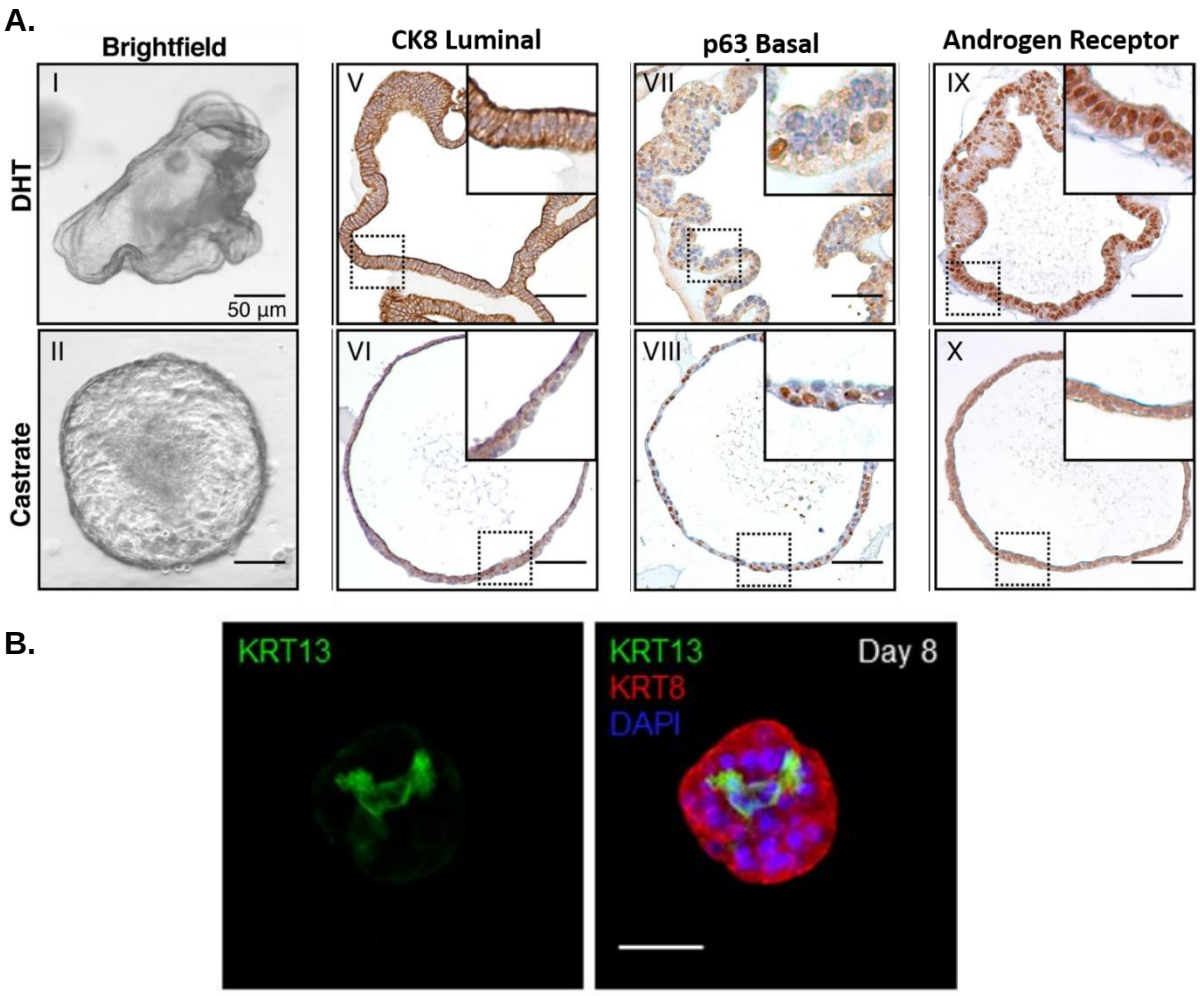

Fig. 3: Characterization of Organoid Culture Conditions. A. Images depicting the cell types and architecture of human prostate organoids. CK8+ luminal cells as well as p63+ basal cells are clearly visible. Organoids exhibit a clear downregulation of CK8 and AR when deprived of androgen signaling (depicted in subpanels VI, VIII, and X) (Karthaus et al. 2014). B. Images showing the expression of KRT13 (green), a putative marker of prostate progenitor cells, expressed in human prostate organoids at day 8 (McCray, Moline, et al. 2019). The left image shows solely the green channel, while the right image shows an overlay giving context for the expression of KRT13. The expression of KRT13 provides evidence of progenitor cells persisting in the organoid culture conditions.

(Karthaus et al. 2020). Although these investigations into the prostate stem compartment using scRNA-Seq have been informative, they are largely descriptive and do not test necessary factors for the survival and regenerative phenotypes of prostate epithelial progenitor cells. An exciting next step for the prostate progenitor cell field would be to distill the available expression data describing the basal and luminal progenitor populations of the prostate into actionable, biologically relevant lists of candidate factors that are necessary for the process of prostate regeneration.

In vitro Models of Prostate Regeneration:

Although the study of prostate regeneration using the androgen cycle approach has yielded considerable results in the study of the mouse prostate, similar approaches are impossible in human patients for ethical reasons. Study of prostate progenitor cell behaviors in human models usually involves either studying these cells in human disease models like xenografts or using extremely creative methods like the mitochondrial DNA mutation rate approach pioneered by Moad et al. in 2017 (Moad et al. 2017; Li and Shen 2019). Additionally, although hormone-dependent regeneration allows for the reliable testing of the regenerative potential of the prostate tissue and the cells therein, it does prevent the study of any cell-intrinsic elements of the prostate progenitor cell phenotype, meaning that it can be difficult to decouple the regenerative potential of particular prostate cells from the environmental and signaling changes induced by hormone modulation. To that end, researchers have developed multiple applications that allow for the expedient and efficient investigation of murine and human regeneration phenotypes using cultured tissue samples.

The first of these approaches, and the one considered the “gold standard” for transplantation studies of prostate progenitor cells, is the urogenital sinus mesenchyme recombination. This procedure, first pioneered by the lab of Gerald R. Cunha, involves the implantation of single mouse prostate epithelial cells along with fetal rat urogenital sinus cells into the renal capsule of a nude mouse (Li Xin et al. 2003). After a period of incubation, researchers can observe the renal capsule of the recipient nude mouse for ectopic prostate tissue, and the amount of ectopic tissue can be used as a readout for an assay comparing regenerative phenotypes of different treatment conditions or biomarker profiles. Rat tissue is differentiated from mouse tissue using histology that detects the variant centromere antigens between the two species (Li Xin et al. 2003). Although this approach is considered the most scientifically rigorous of the tests for intrinsic regenerative capabilities of prostate progenitor cells, it does not lend itself well to quantitation due to the time- and technique-intensive nature of the experiment causing logistical difficulty with producing multiple technical and biological replicates. Additionally, the turnaround between cell implantation and observable tissue growth can be protracted, with many experiments requiring a wait time of up to six months before the experimental endpoint is reached.

In an effort to create an approach with a faster experimental turnaround that still analyzes the regenerative capacity of prostate cells, researchers have pioneered 3D culture techniques for prostate cells. These 3D culture techniques borrow heavily from the intestinal organoid cultures pioneered over the course of the last two decades and involve plating single prostate cells in Matrigel bubbles supplemented with growth factors that are known to induce the outgrowth of prostate tissue (Wallach and Bayrer

2017; Drost et al. 2016). This leads to the growth of spheroids consisting of differentiated prostate tissue and persisting prostate progenitors. IHC analysis of these spheroids led to the observation that the organoids were organized similarly to a prostate epithelial gland, with the basal cells located externally and the luminal cells facing inward toward the lumen of the organoid (Karthaus et al. 2014). The removal of testosterone from the system also leads to the loss of AR expression as well as a quantitative and morphological shrinkage of the luminal compartment of the organoids (**Fig 3A**) (Karthaus et al. 2014). Putative prostate progenitor cells have been observed in both human and mouse-derived organoids (**Fig 3B**) (Crowell, Fox, et al. 2019; McCray, Moline, et al. 2019). Additionally, organoid culture approaches allow for easy quantitative assays testing the regenerative capacity of cells in the form of a colony forming assay. This approach involves plating a known number of single cells in each individual Matrigel bubble and counting the number of organoids resulting from those plated cells after an incubation period (Crowell, Giafaglione, et al. 2019). Colony forming assays (CFA) allow for fast, quantitative experimentation measuring the regenerative potential of cells in multiple treatment conditions. A similar colony forming assay approach has been used repeatedly for preclinical drug discovery in a diverse group of cancers (Katz et al. 2008). Altogether, organoid culture yields a quantitative and fast alternative to test the regenerative capacity of prostate progenitor cells in a controlled environment where these cells can grow multicellular spheroids that exhibit some of the behaviors of physiological prostate tissue.

Data Gathered in this Thesis

scRNA-Seq investigation of *in vitro* samples yielded granular expression data for the diverse populations present in the monolayer and organoid model systems. These data were used to identify progenitor cell populations that were preserved in the monolayer and organoid culture conditions. These cells, expressing KRT13, were later observed using immunofluorescence microscopy as a secondary method of validation. Direct comparison of the monolayer and organoid culture conditions led to the observation that proliferating epithelial cells were enriched in the monolayer condition while undifferentiated intermediate cells were enriched in the organoid culture condition. Subsequent comparison of *in vitro* samples with publicly available *in vivo* data led to the observation that the *in vitro* samples were enriched for proliferating epithelial cells while the *in vivo* sample was enriched for terminally differentiated cells and stromal populations.

Applying a similar approach to *in vivo* mouse prostate samples led to the identification of luminal progenitor cells in both the intact and castrate hormone conditions. These luminal progenitor cells were observed to express Krt8, Krt18, Psca, Sox2, and Trop2. Further investigation of these luminal progenitor cells validated their presence in prostate using immunofluorescence microscopy and flow cytometry. Ingenuity Pathway Analysis produced evidence that genes associated with cell survival and urogenital development were significantly enriched in the expression profile for luminal progenitor cells provided by our scRNA-Seq investigation. Using this pathway analysis, we were able to select candidate factors that may be necessary for the regenerative phenotype of luminal progenitor cells. Testing of small molecule inhibitors

targeting two of these candidates, Yap1 and Bcl-2, led to a significant reduction in regenerative potential of organoids derived from both mouse and human tissue samples.

CHAPTER II

SINGLE CELL RNA-SEQ ANALYSIS IDENTIFIES A PUTATIVE PROGENITOR POPULATION IN HUMAN PROSTATE SAMPLES *IN VITRO*

ABSTRACT

Human primary prostate epithelial (PrE) cells represent patient-derived *in vitro* models and are traditionally grown as a monolayer in two-dimensional culture. Recently, it has been demonstrated that expansion of primary cells into three-dimensional prostatic organoids better mimics prostate epithelial glands by recapitulating epithelial differentiation and cell polarity. Here, we sought to identify cell populations present in monolayer PrE cells and organoid culture, grown from the same patient, using single-cell RNA-sequencing. Single-cell RNA-sequencing is a powerful tool to analyze transcriptome profiles of thousands of individual cells simultaneously, creating an in-depth atlas of cell populations within a sample. Organoids consisted of six distinct cell clusters (populations) of intermediate differentiation compared to only three clusters in the monolayer prostate epithelial cells. Integrated analysis of the datasets allowed for direct comparison of the monolayer and organoid samples and identified 10 clusters, including a distinct putative prostate stem cell population that was high in Keratin 13 (*KRT13*), Lymphocyte Antigen 6D (*LY6D*), and Prostate Stem Cell Antigen (*PSCA*). Many of the genes within the clusters were validated through RT-qPCR and immunofluorescence in PrE samples from 5 additional patients. KRT13+ cells were observed in discrete areas of the parent tissue and organoids. Pathway analyses and lack of EdU incorporation corroborated a stem-like phenotype based on the gene expression and quiescent state of the KRT13+ cluster. Other clusters within the

samples were similar to epithelial populations reported within patient prostate tissues. In summary, these data show that the epithelial stem population is preserved in PrE cultures, with organoids uniquely expanding intermediate cell types not observed in monolayer culture.

CONTRIBUTION BY AUTHORS

The work presented in this chapter has previously appeared in “Single-cell analysis identifies a putative epithelial stem cell population in primary prostate cells in monolayer and organoid conditions”, published in the American Journal of Clinical and Experimental Urology in 2019 (McCray, Moline, et al. 2019). Dr. Tara McCray served as a coequal first author on this publication and contributed equally to the 10x scRNA-Seq library preparation workflow as well as the subsequent analysis. She also performed the immunofluorescence microscopy presented in Fig. 7. Daniel Moline, author of this thesis, also contributed to the process of scRNA-Seq library prep and analysis as well as performing the RT-qPCR presented in Figs. 5 and 7. Writing of the manuscript was divided equally between the two authors.

INTRODUCTION

The prostate epithelium has a high incidence of neoplastic disease with prostate cancer being the second most common epithelial cancer in men (Siegel, Miller, and Jemal 2017; Lim 2017). *In vitro* culture models have produced valuable insights into the biology of the prostate, however, the limited number of cell lines from early and intermediate stages of disease presents a significant obstacle to acquiring data with clinically relevant findings that account for patient heterogeneity (Sobel and Sadar

2005a; 2005b). An alternative strategy is patient-derived primary cell culture, which preserves patient heterogeneity while also providing a tractable *in vitro* model (D. M. Peehl and Stamey 1986; Donna M. Peehl 2003; Niranjan et al. 2013; D. M. Peehl, Wong, and Stamey 1988). Primary prostate cell culture can be a valuable tool for studying “normal” cells, but the culture conditions can select for a homogeneous, transit-amplifying phenotype and against the luminal differentiation of prostate epithelium observed *in vivo* (Uzgare, Xu, and Isaacs 2004; Donna M. Peehl 2004; Bühler et al. 2010; Litvinov et al. 2006). To circumvent this lack of cell diversity, many researchers have turned to organoid culture approaches. Organoids are three-dimensional (3D) structures grown in extracellular matrix that recapitulate many facets of prostate epithelial tissue morphology including structure and cell polarity (Karthaus et al. 2014; Drost et al. 2016; Clevers 2016). Compared to their traditional two-dimensional (2D) monolayer counterparts, organoids can grow from a single stem or progenitor cell in the presence of charcoal stripped fetal bovine serum (FBS) and androgen to differentiate into both basal and luminal epithelial populations (Karthaus et al. 2014; Drost et al. 2016; Chua et al. 2014).

The human prostate consists of stratified epithelial secretory glands surrounded by a fibromuscular stroma. The epithelial glands are composed of a basal layer, a secretory luminal layer, and a rare neuroendendocrine population (Long et al. 2005; Toivanen and Shen 2017). Recently, single-cell RNA-Seq analysis of prostate tissue revealed two additional cell populations within the human prostate epithelium that exhibit stem cell characteristics (Henry et al. 2018). Single-cell RNA-Seq (scRNA-Seq) is a method that lends itself to the identification of cryptic sub-populations within a

heterogeneous sample using an unbiased analysis of individual expression profiles of cells (Wu et al. 2014). This approach involves the isolation of single cells into microfluidic droplets containing oligonucleotide-covered gel beads that capture and barcode the transcripts. Transcripts are converted to cDNA, sequenced, and aligned by barcode using computational analysis to create an individual transcriptome library for each cell. Libraries are then clustered into distinct cell populations using dimensional reduction analysis (Butler et al. 2018; Macosko et al. 2015; Satija et al. 2015).

Here we use scRNA-Seq to compare the subpopulations present within primary prostate cells and organoids from the same patient specimen and identify previously unknown subpopulations of epithelial cells grown *in vitro*. Cell populations were validated in additional patient samples by RT-qPCR and immunofluorescence microscopy.

MATERIALS AND METHODS

Primary Prostate Epithelial Cells

Human primary prostate cells were isolated and established from fresh male radical prostatectomy tissues. Radical prostatectomy patients consented prior to surgery and prostate tissue samples from benign regions of the peripheral zone were collected according to UIC Internal Review Board-approved protocol #2007-0694. A portion of tissue was reserved for histologic inspection by a board-certified pathologist to verify the region as benign. Tissue samples were collected, formalin-fixed, paraffin-embedded, and 5 µm sections were stained with hematoxylin and eosin. Remaining tissue was digested in collagenase/trypsin to produce a single cell suspension. Cells

were grown in Prostate Cell Growth Media (Lonza, Basel, Switzerland) to select for epithelial cells. When ~70% confluent, cells were trypsinized to single cells, counted and cryopreserved into multiple aliquots. Epithelial purity was authenticated with RT-qPCR, confirming the expression of epithelial markers KRT5, KRT8, KRT18 and TP63, and the lack of stromal marker TIMP Metallopeptidase Inhibitor 3 (TIMP3). Patient information is listed within **Table 1**.

Monolayer and Organoid Culture

For standard monolayer culture, prostate epithelial (PrE) cells were thawed from primary passage into a collagen-coated dish and maintained in PrEGM (Lonza; Basal, Switzerland). For organoid culture, a separate aliquot of the same PrE cells was thawed and plated sparsely (500-5,000 cells per well) in a flat-bottom 96-well microplate into 33% growth factor reduced phenol red-free Matrigel (Corning Inc., Corning NY) on top of a solidified base layer of 50% Matrigel in media. 100 µL of organoids suspended in 33% Matrigel were maintained in keratinocyte serum-free media (Gibco, Thermo Fisher Scientific, Waltham, MA) supplemented with 5% charcoal-stripped fetal bovine serum and 10 nM dihydrotestosterone (DHT) as previously described by the Nonn lab at UIC (McCray, Richards, et al. 2019). Media was refreshed every 2-3 days for all cultures. Monolayer cells were collected at ~70% confluent for endpoints and organoids were grown for 8-14 days as detailed in the figure legends. Brightfield images of organoids were captured at 10x and 20x magnification using the Evos FL Auto 2 imaging System (Thermo Fisher Scientific, Waltham, MA).

TABLE 1					
Primary Cell Patient Characteristics					
PrE ID	Pathology	Age	Race	Prostate Region of Origin	Endpoints
PrE1	Benign, Moderate Chronic Inflammation	58	AA	PZ, L5 left posterior (scRNA-Seq) PZ, L2 left posterior (FFPE)	scRNA-Seq
PrE2	Benign	68	AA	PZ, L3 (whole mount and RNA) PZ, L5 (FFPE)	RT-qPCR, IHC and tissue staining
PrE3	Benign, Mild Chronic Inflammation, Atrophy	63	EA	PZ, L1 Left Anterior	RT-qPCR, IHC and tissue staining
PrE4	Benign, Mild Chronic Inflammation, Focal Atrophy	58	AA	PZ, L3 Left Posterior	RT-qPCR, IHC and tissue staining
PrE5	Benign	71	AA	PZ, L5 Left Anterior (whole mount and RNA) PZ, L3 Right Anterior (FFPE Block)	IHC and tissue staining
PrE6	Benign	60	AA	PZ, L4 Left Anterior	IHC and tissue staining

Table 1: Primary Cell Patient Characteristics. Abbreviations: AA = African American, EA = European American, PZ = Peripheral Zone

10x Genomics Single Cell Separation, Library Prep, and Sequencing

Patient-matched epithelial cells were grown in monolayer and organoid culture as described above. Monolayer cells were collected by TrypLE (Gibco, Thermo Fisher Scientific, Waltham, MA) dissociation. Organoids were harvested at day 8 by Dispase (STEMCELL Technologies, Vancouver, Canada) dissociation followed by a second dissociation to single cells using TrypLE. Cell number and viability were determined by a Trypan Blue exclusion assay quantified on a Cellometer Automated Cell Counter (Nexcelom, Lawrence MA). Both samples consisted of > 80% viable cells (**Table 2**) prior to proceeding with the 10x Genomics (Pleasanton, CA) protocol for 3' Transcript Capture and Single Cell Library Prep. Cell samples were loaded at a concentration to yield approximately 5,000 total captured cells on a 10x Chip A. GEM generation, RT, cleanup, cDNA amplification, fragmenting, end repair & A-tail prep, and sample index tagging were performed using the Chromium Single Cell 3' Library and Gel Bead Kit v2 per manufacturer's instructions. Libraries were labeled with a sample index and pooled for sequencing at a concentration of 10 nM. Sample quantification and quality control were performed using Qubit Fluorometer (Thermo Fisher Scientific, Waltham, MA) and TapeStation Bioanalyzer (Agilent Technologies, Santa Clara, CA). Sequencing was run on the HiSeq 4000 (Illumina, San Diego, CA) at the University of Illinois at Urbana Champaign (UIUC) DNA services. Samples were sequenced across 3 lanes of the HiSeq 4000, generating 100 base pair paired-end reads at a depth of 45,000 reads per cell. Leftover cells not used for scRNA-Seq were collected into TRIzol Reagent (Thermo Fisher, Waltham MA) and reserved for validation of the sequencing.

TABLE 2

Quality Metrics for Single Cell Solutions and 10x Genomics Sequencing Output

Readout	Monolayer	Organoid
Viability at collection	85.60% live cells	81% live cells
Aimed Recovery	5,000 total cells	5,000 total cells
TapeStation Yield	173,000 pmol/L	121,000 pmol/L
Concentration	44 ng/uL	31.4 ng/uL
Qubit Yield	88 ng/uL	82 ng/uL
Achieved Cell Recovery	5,194 total cells	7,422 total cells
Mean Reads Per Cell	31,629 reads/cell	41,116 reads/cell
Mean Genes Per Cell	3,569 genes/cell	3,783 genes/cell
Reads Mapped Confidently to Genome	87.10% of total reads	86.90% of total reads
Number of Cells Remaining after Seurat QC	3,687 cells	5,322 cells

Single Cell RNA-Seq Analysis

For initial read alignment and quality control, Single-cell RNA sequencing samples were processed and aligned to Ensembl genome GRCh38 using the Cell Ranger 3.0.0 pipeline by UIUC DNA Services. The Cell Ranger output was loaded into Seurat pre-release v3.0 for clustering (Butler et al. 2018). Cells with high mitochondrial features (> 8% of total mapped reads) were struck from the analysis to remove the influence of dead cells. A small number of cells with unusually high or low numbers of mapped reads were also removed from the dataset, as these outliers could be doublets or poorly captured cells (Butler et al. 2018; Macosko et al. 2015; Satija et al. 2015). Cells removed in QC totaled 29% of the initial input, see **Table 2** for full QC. Individual genes related to the cell cycle or with uniquely low unique molecular identifier (UMI) counts within the context of the dataset had their variance regressed out to minimize their influence on variance-based clustering.

A JackStraw resampling method was used to select statistically significant ($p < 0.05$) principal components (Butler et al. 2018). These components were used to identify the distance between cells for a k-nearest neighbors calculation and construction of a shared nearest neighbor graph. Modularity (M) was used as a quantitative measure of the independence of individual networks in the t-SNE plot, using $M > 0.8$ as a cut-off to ensure reproducibility (Newman 2006). Principal components used for the analysis of monolayer and organoid culture conditions totaled 27 and 40 respectively. The integrated dataset was analyzed using 30 principal components to produce the t-SNE plots shown.

Canonical correlative analysis was performed in Seurat to integrate the separate datasets and allow for direct comparison of populations between the monolayer and organoid samples (Butler et al. 2018). Clusters were assigned identities based on their expression of previously reported epithelial markers listed in **Table 3**. Heat maps and dot plots were generated in Seurat. Highly expressed genes in each cluster are provided in **Table 4**.

Pseudotime analysis was performed in Monocle version 2.10 (Trapnell et al. 2014). Cell Ranger output was uploaded into Monocle and data was subset to exclude cells with low and high numbers of mRNAs, removing dead cells and doublets (cells with < 9000 or > 45000 captured transcripts). Clustering of cells was performed unguided without the influence of marker genes, using 27 principal components. Monocle performed unsupervised selection of genes that define progress, performing dimensional reduction to produce a plot ordering cells in pseudotime.

Our integrated tissue analysis used canonical correlative analysis was used to integrate the monolayer, organoid and a publicly available human prostate tissue data set (D17_FACS_filtered GSE_117403) to allow for direct comparison of populations between the *in vitro* samples and *in vivo* tissue (Henry et al. 2018). 30 principal components were used to yield a t-SNE with M > 0.95 (**Fig. 8**). Clusters were assigned identities based on their expression of previously reported epithelial markers listed in **Table 3**. A dot plot was generated in Seurat for genes highly expressed by each cluster. Highly expressed genes in each cluster are provided in Table S1.

TABLE 3					
Canonically Expressed Factors for Prostate Epithelial Populations					
Publication	Pan-Epithelial	Luminal	Basal	Intermediate	Stem
Henry et al. 2018	CD326, CD324, **TACSTD2, ITGA6**	DPP4, **KRT8, KRT18,** KLK3, MSMB, ACPP, KLK4, PLAG2A, MT1E, KLK2, SMC, SOCS2, TSPAN8	**PDPN, KRT5,** TP63, CD104, CD271, RGCC, **KRT14,** DST, NOTCH4, LTBP2, **DKK1, KRT15**	KRT19, **KRT18,** KRT14	SCGB1A1, **PSCA, KRT13, LCN2, LYPD3, SERPINB1,** SCGB3A1, PIGR, WFDC2, FCGBP, **CSTB,** APOBEC3A
Zhang et al. 2016	**TACSTD2**	AR, KLK3, ALOX15B, ACPP, TOX3, FOLH1, OSTADPP4, CKK4, PLA2G2A, MB, CWH43, TRPV6, ELOVL2, CPNE4, ANO7, POTEM, MUC2, LMAN1L, DNAJC12, ASRGL1, DLL4, DOCK11, GPR98, SYT7, INHB8, TBXAS1, SERHL2, NPTX2, GFTP2, PTPRN2, CSGALNACT1, ST8SIA1, VNN3, C2, TRPM8, RAMP1PDE8B, SPDEF, LTB, HLA-DMB, LAC286002, FGF13, DCDC2, KRT20, FBP1, SLC2A12, TSPAN8	TP63, **KRT5, KRT14, KRT6A,** BNC1, KRT34, FAT3, SYNE1, TNC, FGFR3, DKK3, COL17A1, CSMD2, CDH13, FIX1, MUM1L1, MMP3, DLK2, FLRT2, IL33, GIMAP8, **PDPN,** FHL1, VSNL1, NRG, IGFBP7, ERG, HMGA2, IL1A, NOTCH3, THBS2, TAGLNSPARC, FOXI1, MSRB3, NGFR, NIPAL4, ANXABL2, COL4A6, KCNQ, JAG2, WNT7A, KCNMA1, LTBP2, JAM3, SH2D5, MRC2, **SERPINB13,** CNTAP3B, ARH, AEBP1, DEC1, SERPINF1, C16, KIRREL		
Hu et al. 2017					**KRT13,** IGF2, CCL2, CARM1, LDH1A2, ALDH8A1, LIFRCAC15, **PSCA,** NANOG, SOX2, PCAT1, VEGFC, NESTIN, FOXA1, APRAC1
Moad et al. 2018					SCNN1A, **CENPF,** PPL, DDIT4, **KLK11,** DLK1
Wang et al. 2001	**KRT8, KRT18**	KRT19, GST, KRT5, TP63, KRT14	KRT19		
Schmelz et al. 2005		TPI1, KLK3	KRT5	KRT19	**KRT6A**

TABLE 3: Canonically Expressed Factors for Prostate Epithelial Populations: Bold text indicates factors detected in scRNA-Seq analysis of *in vitro* culture samples.

RT-qPCR Gene Expression

Multiple patient-derived epithelial cell cultures (**Table 1**) were grown as matched monolayer and organoid cultures as described above. Cells were stored in TRIzol reagent before RNA isolation. Samples were homogenized by chloroform and RNA collected by alcohol precipitation and rehydration. RNA quantity and quality were determined by OD 260/280 and 260/230 on the NanoDrop Spectrophotometer (ThermoFisher Scientific, Waltham MA). cDNA was synthesized with the High-Capacity cDNA Reverse Transcription Kit (Applied Biosystems, Beverly Hills CA) and qPCR run on LightCycler (Roche Applied Science, Penzberg, Germany). RQ was calculated from ΔΔCT to the reference gene RPL13A, primers are listed in **Table 4** (Livak and Schmittgen 2001).

RESULTS

Organoid Cultures Contain More Populations of Epithelial Cells than Monolayer Cultures:

Patient-derived PrE cells can be grown in monolayer or organoid culture conditions as *in vitro* models of prostate cell biology and as useful tools for mechanistic studies. Here we compared the cell populations within these patient-derived models using scRNA-Seq analysis on monolayer epithelial cells and organoids from a single patient (**Fig. 4A**). Seurat was used for clustering and analysis of the individual datasets separately, identifying 6 clusters in the organoids and only 3 within the monolayer cells (**Fig. 5A-B**) (Butler et al. 2018). Integration of the monolayer and organoid datasets together increased the number of cells to allow for higher-granularity clustering with the

same modularity cutoff, thus permitting greater separation of intermediate cell types and subpopulations (Butler et al. 2018). Additionally, this integration allowed for the direct comparison of the two samples on the same t-SNE plot to observe common cell populations across both culture conditions. Together, these factors informed our decision to use an integrated dataset. The resulting 10 clusters are shown on a t-SNE plot (**Fig. 4B**) and the contribution of monolayer and organoid cells to each cluster is shown by bar graph (**Fig. 4C**). Each cluster had varying representation of cells from both culture conditions, but clusters 1, 3, 8 and 9 were enriched in the organoid sample while cluster 2, 4 and 5 were enriched in the monolayer sample. Genes highly expressed by monolayer (Follistatin (FST), Insulin-Like Growth Factor Binding Protein 2 (IGFBP2), Secreted Frizzled-Related Protein 1 (SFRP1)) or organoid (Inhibin A (INHBA), Insulin-Like Growth Factor Binding Protein 3 (IGFBP3), Serpin Family B Member 1 (SERPINB1)) cells were also tested by RT-qPCR in pooled sample of leftover scRNA-Seq RNA as a secondary validation to our data (**Fig. 5C**). This was supported using 3 additional patient samples, corroborating the trends established by our integrated scRNA-Seq comparison of the two culture conditions.

Identification of Epithelial Populations

The 10 integrated populations each expressed a unique set of biomarkers with some degree of overlap (**Fig. 6A**). The cell type identity of each cluster was determined by cross-reference with previously reported gene expression profiles (Table 3) and is shown by dot plot (**Fig. 6B**). Cluster 0 was identified as a group of quiescent cells expressing high levels of the basal marker Dickkopf Wnt Signaling Pathway Inhibitor 1 (DKK1), moderate levels of luminal markers KRT8 and KRT18, as well as Matrix

Metalloprotease 9 (MMP9), a factor shown to be highly expressed by PC3 prostasphere cells compared to PC3 monolayer cells (Henry et al. 2018; Portillo-Lara and Alvarez 2015).

Cluster 1 is marked by the expression of KRT6A and SERPINB13, denoting its members as a previously described glandular epithelial cell with possible stem characteristics (Schmelz et al. 2005). Cluster 2 contained cells expressing the basal marker Podoplanin (PDPN) as well as proliferation markers, indicating that this cluster contains proliferating basal cells (Henry et al. 2018). Cluster 3 exhibited high levels of cell cycle arrest gene Growth Arrest Specific 5 (GAS5) as well as low expression of cell cycle progression genes including Cytodifferentiation Factor 44 (CD44) and Proliferating Cell Nuclear Antigen (PCNA), denoting its possible identity as a population of quiescent cells. This population was also notable for its low expression of epithelial markers, which could signify that these cells are in a relatively undifferentiated state. Cluster 4 constituted another proliferating basal population, marked by its expression of MKI67 as well as the basal marker DKK1. Cluster 5 was also identified as a proliferating population, with high levels of the luminal marker KRT18. Cluster 6 exhibited high expression of numerous putative prostate epithelial stem cell markers including KRT13, SERPINB1, LY6D, PSCA, Kallikrein-Related Peptidase 11 (KLK11) and Cystatin B (CSTB) (Moad et al. 2017; Henry et al. 2018; Hu et al. 2017). These markers were also expressed by Cluster 7, with Clusters 6 and 7 differing by their expression levels of basal and luminal markers. Clusters 8 and 9 were difficult to identify as they both contain a very small number of cells. Cluster 8 highly expressed CTNNB1 and Cluster 9 was enriched for cells expressing IFI27 and IFI6, markers typically expressed by

Table 4			
Primers Used for Quantitative Real-Time PCR			
Target Gene	**Primer sequence (5'-3')**	**PCR Product Size (bp)**	**Exons**
RPL13A	F-GGAGCAAGGAAAGGGTCTTAG		8
	R-GGTTGCTCTTCCTATTGGTCATA		
LYPD3	F-GATGCTCCCCGAACAAGATGA	104	2/3
	R-CAGCGAGAATTGTCCGTGGAT		
	PrimerBank ID: 93004087C1		
LY6D	F-GCTCCCAGACGACATCAGAG	168	1/2
	R-TGTTCGTGGTCTTGCAGAAG		
KRT13	F-AGGTGAAGATCCGTGACTGG	134	1/2
	R-GATGACCCGGTTGTTTTCAA		
PSCA	F-TGCTGCTTGCCCTGTTGAT	216	1/3
	R-CCTGTGAGTCATCCACGCA		
	PrimerBank ID: 5031995A1		
LCN2	F-ACAAAGACCCGCAAAAGATG	128	2/3
	R-GCAACCTGGAACAAAAGTCC		
S100P	F-AAGGTGCTGATGGAGAAGGA	163	1/2
	R-ACTTGTGACAGGCAGACGTG		
SERPINB1	F-CTGGCGTTGAGTGAGAACAA	143	2/3
	R-TCAACCGTGTTGAAATGGAA		
INHBA	F-GGAGGGCAGAAATGAATGAA	95	2/3
	R-AATCTCGAAGTGCAGCGTCT		
IGFBP3	F-GTCAACGCTAGTGCCGTCAG	107	1/2
	R-CGGTCTTCCTCCGACTCAC		
FST	F-TCTGCCAGTTCATGGAGGAC	106	1/2
	R-TCCTTGCTCAGTTCGGTCTT		
SFRP1	F-CTACTGGCCCGAGATGCTTA	169	1/2
	R-GCTGGCACAGAGATGTTCAA		
IGFBP2	F-CCTCTACTCCCTGCACATCC	79	3/4
	R-CCCGTTCAGAGACATCTTGC		
AR	F-CCAGGGACCATGTTTTGCC		1/2
	R-CGAAGACGACAAGATGGACAA		
KRT8	F-GCTGGTGGAGGACTTCAAGA	66	2/3
	R-TCGTTCTCCATCTCTGTACGC		
KRT18	F-CACAGTCTGCTGAGGTTGGA	110	6/7
	R-CAAGCTGGCCTTCAGATTTC		
KRT5	F-ATCGCCACTTACCGCAAGC	110	7/9
	R-CCATATCCAGAGGAAACACTGC		

endothelial cells (Henry et al. 2018). These markers indicate that Cluster 8 and Cluster 9 may be persisting stromal contaminants, however they also express PDPN and MMP9 which are basal and PC3 prostasphere markers respectively (Henry et al. 2018; Krämer et al. 2014).

We observed that the organoid culture condition was enriched for several cell populations when compared to the monolayer condition, such as clusters 1, 3, 7, 8 and 9 (**Fig. 4C**). Cells in clusters 1 and 7 were identified as progenitor populations according to their suite of expressed biomarkers (**Fig. 6B**). Clusters 8 and 9, although very small, were present in the organoid condition (**Fig. 4C**) and expressed some stromal genes (**Fig. 6B**), although whether these cells are surviving stroma from the patient or represent epithelial-mesenchymal transition could not be determined from our study. These findings indicate that organoid culture conditions are conducive to the survival and proliferation of cell populations that are underrepresented from samples cultured in monolayer conditions.

Stem and Progenitor Populations Found in Both Monolayer and Organoid Conditions

Cluster 6 was of considerable interest as it contained markers of a previously reported putative prostate epithelial stem cell population: SERPINB1, KRT13, LYPD3, PSCA, LY6D, CSTB, and Lipocalin 2 (LCN2) (Henry et al. 2018; Hu et al. 2017). It also was marked by low expression of cell cycle genes and high expression of the cycle-arrest gene GAS5, implying that the cells are quiescent. Cluster 6 was also the only cluster to express PSCA. This expression profile is similar to that of the KRT13 label-retaining prostate stem cell described by Hu et al (Hu et al. 2017). RT-qPCR for LY6D, KRT13, PSCA, and LCN2 validated their expression in both monolayer and organoid

samples derived from multiple patients (**Fig. 7A**), corroborating the presence of populations observed via scRNA-Seq.

To visualize the stem cell population and confirm protein expression, we stained the original parent tissue, 2D cells and 3D cells for the marker KRT13 (**Fig. 7B-F**). Tissue expression of KRT13 in the patient sample used for the scRNA-Seq allowed us to observe rare islets of KRT13 expression similar to the pattern previously described (**Fig. 7B**) (Henry et al. 2018). This phenomenon was also observed in 2D cells (**Fig. 7C**). At day 8, and in some cases at day 14, the organoids showed one or few KRT13 positive cells (**Fig. 7D**), consistent with the idea that an organoid is maintained by a single resident stem cell. At day 8, the time point used for scRNA-seq, 3D cells showed KRT13 expressed by a small population of cells (**Fig. 7D**), confirming our scRNA-Seq population size. When staining was performed on day 14, we observed that the KRT13+ cells were located on the interior of the spheroid structure (**Fig. 7E**) which may correlate to these stem cells generating the inner luminal cells. There were also instances of multiple clustered KRT13+ cells that may represent different stages of stem/progenitor hierarchy (**Fig. 7F**).

KRT13+ Cells are Quiescent and Exhibit Similar Gene Expression as Prostate Progenitor Cells

Stem cells are known to rarely proliferate in tissue and undergo asymmetric division in culture to maintain their quiescent state (Hu et al. 2017). To visualize cellular state, Monocle was used to create a differentiation trajectory of the organoid sample in pseudotime based upon gene expression patterns within the sample. Pseudotime analysis provided evidence that KRT13-expressing cells were in a different state than

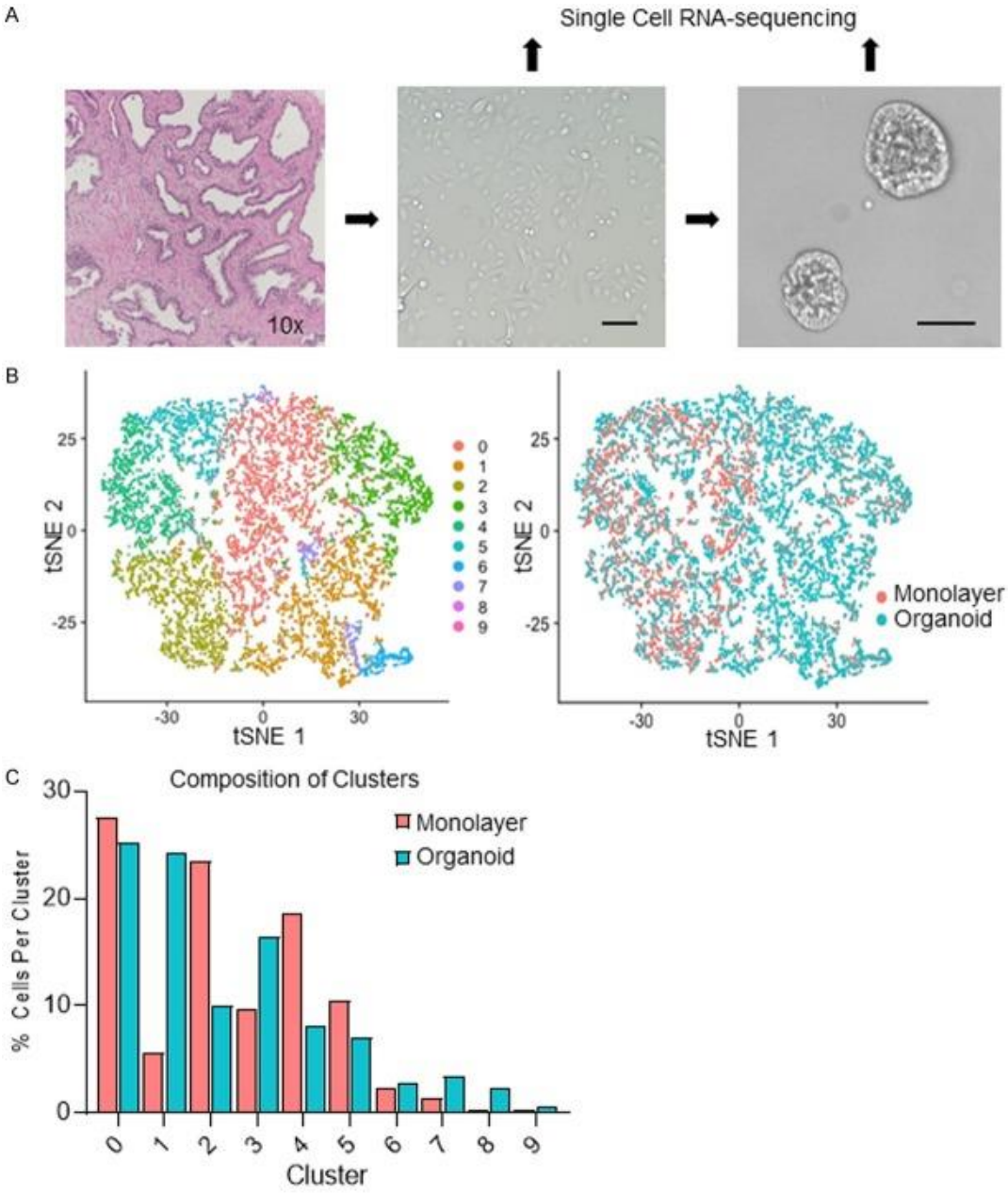

Fig. 4: Identification of Prostate Epithelial Subpopulations *In Vitro*. A. Experimental design and workflow. H&E of prostate tissue from originating patient (left), bright field images of the passage 2 monolayer cells (middle) and day 8 organoids (right) at time of collection for single cell sequencing (scale bar = 100 µm). B. T-distributed Stochastic Neighbor Embedding (t-SNE) plots of integrated data for monolayer and organoid cells (left) and t-SNE showing identity of monolayer (pink) and organoid (blue) cells (right), M > 0.80. C. Bar chart depicting the contributions of monolayer (pink) and organoid (blue) cells to each cluster, the ratio of cells per cluster to the total number of cells for that sample is shown.

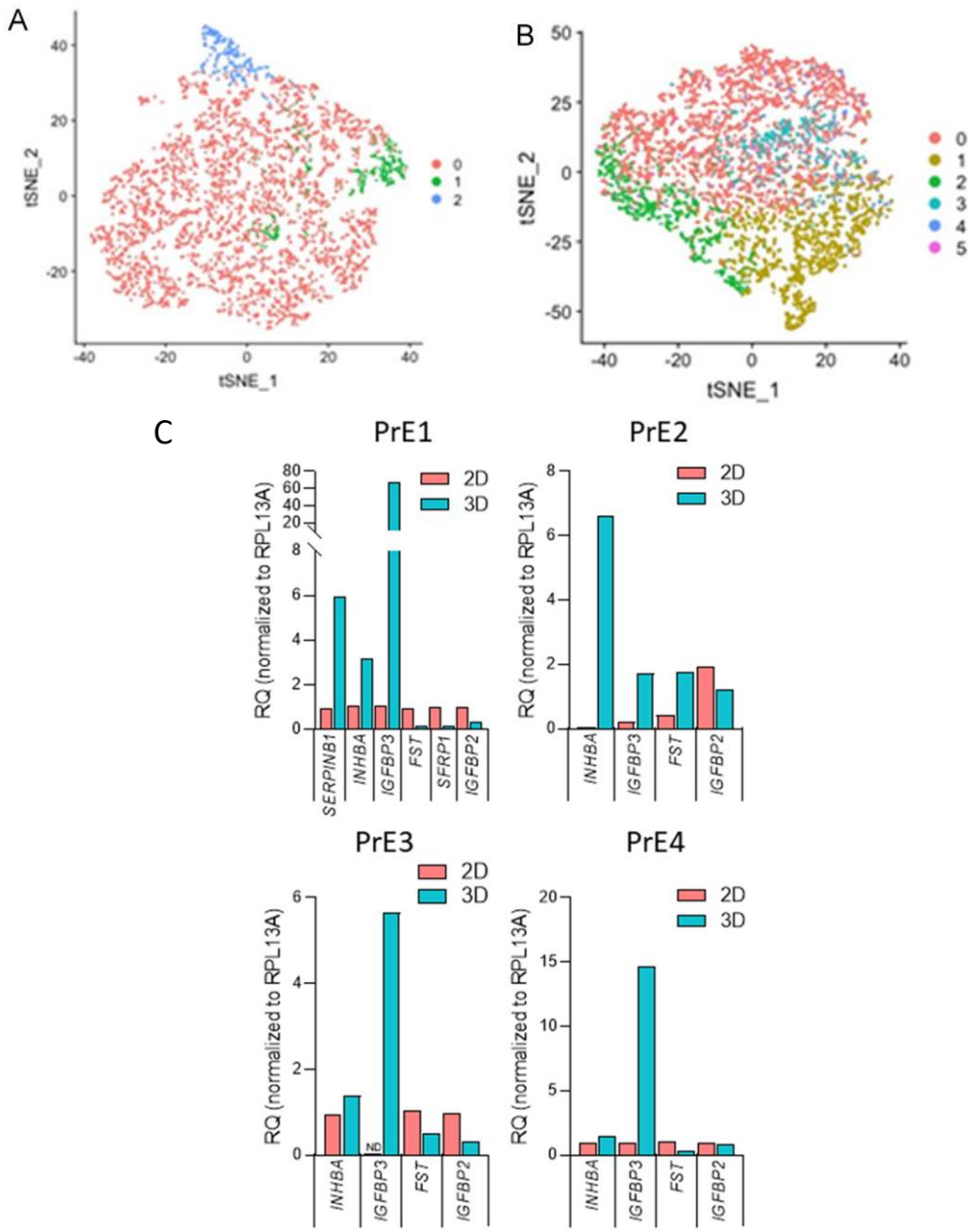

Fig. 5: Individual tSNE Plots and RT-qPCR Validation of Monolayer and Organoid Samples. A. tSNE plot for the monolayer sample showing three different populations identifiable in the sample. B. tSNE plot for the organoid sample showing six different populations identifiable in the sample. C. RT-qPCR data showing the upregulation of specific factors, including IGFBP3 and INHBA in the organoid condition relative to the monolayer condition.

MKI67-positive cells (**Fig. 8A**). To validate this, we performed an EdU incorporation assay on fully-formed organoids Organoids were pulsed with EdU overnight to mark actively-dividing cells followed by fixation and staining for KRT13. As expected, KRT13+ cells were EdU-negative, indicating that they proliferate slowly (**Fig. 8B**). It has been shown that knockdown of KRT13 in undifferentiated prostasphere culture leads to diminished sphere formation and self-renewal (Hu et al. 2017). Our findings provide further support for KRT13 as a quiescent prostate stem marker in the *in vitro* context and agree with the previously characterized role of KRT13+ cells in stem cell maintenance.

Recently, Henry et al. identified a KRT13+ “hillock” epithelial cell population within prostate tissue which may harbor stem characteristics *in vivo* (Henry et al. 2018). Our monolayer and organoid data were integrated and compared with a publicly available human prostate single cell data set (GSE117403) from this study (**Fig. 8C**). The KRT13+ hillock population was present in all three samples, supporting our identification of Cluster 6 in our monolayer and organoid integrated analysis. Of note, there was enrichment for this cluster in the organoid sample to comparable levels as what is observed in tissue. Additionally, integrated analysis with the prostate tissue supported that clusters 8 and 9 were stromal cell types.

To understand what regulatory pathways may be active in the KRT13+ cells, we performed Ingenuity Pathway Analysis (IPA) on genes highly expressed by this cluster. IPA Canonical Pathways that were significantly enriched and activated (positive z-score) or inactivated (negative z-score) are shown (**Fig. 8D**). Of note, p53 signaling was

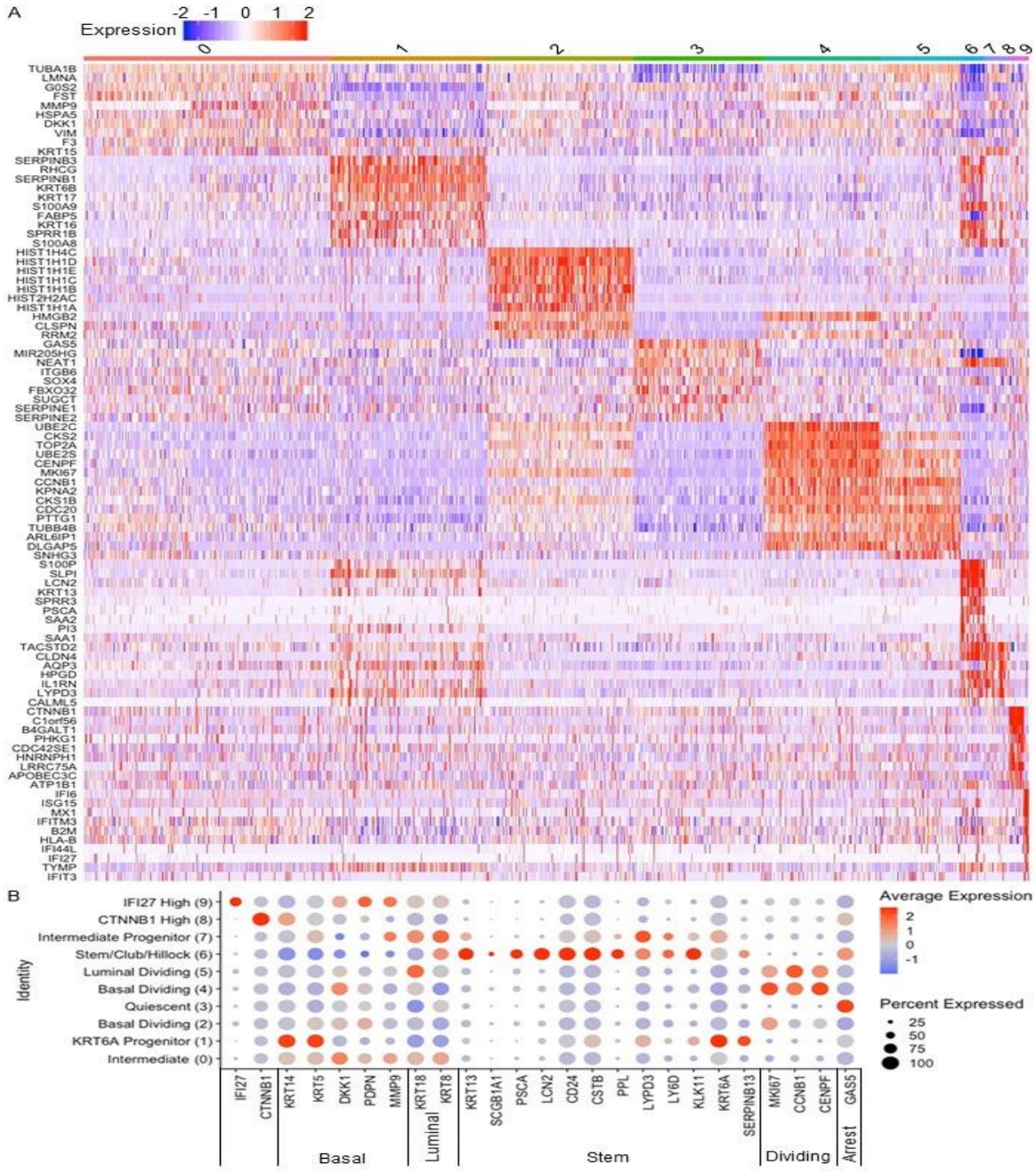

Fig. 6: Gene Expression of the 10 Clusters Identified in the Combined scRNA-Seq Dataset. A. Heat map for top 10 genes expressed by each of the 10 clusters found in the integrated dataset. B. Naming assignments for the clusters and genes of interest shown by dot plot. Red is highly expressed and blue is lowly expressed, the size of the dot indicates the percentage of cells in that cluster that are expressing the gene.

predicted to be activated (z-score = 1.00) while cyclins were predicted to be inactivated (z-score = -1.00). Canonical pathways for the KRT13+ cells are shown in Fig. 8D. IPA Upstream Regulator Analysis was used to identify the transcriptional regulators and nuclear receptors predicted to be active in Cluster 6 based upon genes upregulated in the cluster. Kruppel-Like Factor 4 (KLF4) was projected to be active, which has recently been reported to regulate prostate stem cell homeostasis in mice and has been implicated with KRT13 expression (Xiong et al. 2018). Similarly, Gli Family Zinc Finger 1 (GLI1) and Catenin Beta 1 (CTNNB1) also exhibited positive z-scores in this analysis, implying the activity of the Shh and Wnt morphogenic pathways; both pathways have been reported as significant contributors to prostate tissue regeneration in the murine context (S. H. Lee et al. 2015; Peng and Joyner 2015).

DISCUSSION

To investigate prostate function and disease experimentally, researchers often utilize cell lines, primary cells and organoid culture for *in vitro* modeling. While it is nown that monolayer cultures contain rare populations of stem and progenitor cells, most 2D cells observed consist of transit-amplifying epithelial phenotypes (Uzgare, Xu, and Isaacs 2004; Donna M. Peehl 2004; Bühler et al. 2010; Litvinov et al. 2006). Prostate epithelial organoids grow out from a single cell and differentiate into basal and luminal cell types while maintaining a resident stem/progenitor cell that originated the organoid (Karthaus et al. 2014; Drost et al. 2016; Chua et al. 2014; Hu et al. 2017). While these basic profiles of *in vitro* epithelial cells are known, recent utilization of scRNA-Seq analysis has identified potentially novel populations of prostate epithelial cells from human prostate tissues (Henry et al. 2018). To our knowledge, scRNA-Seq analysis of

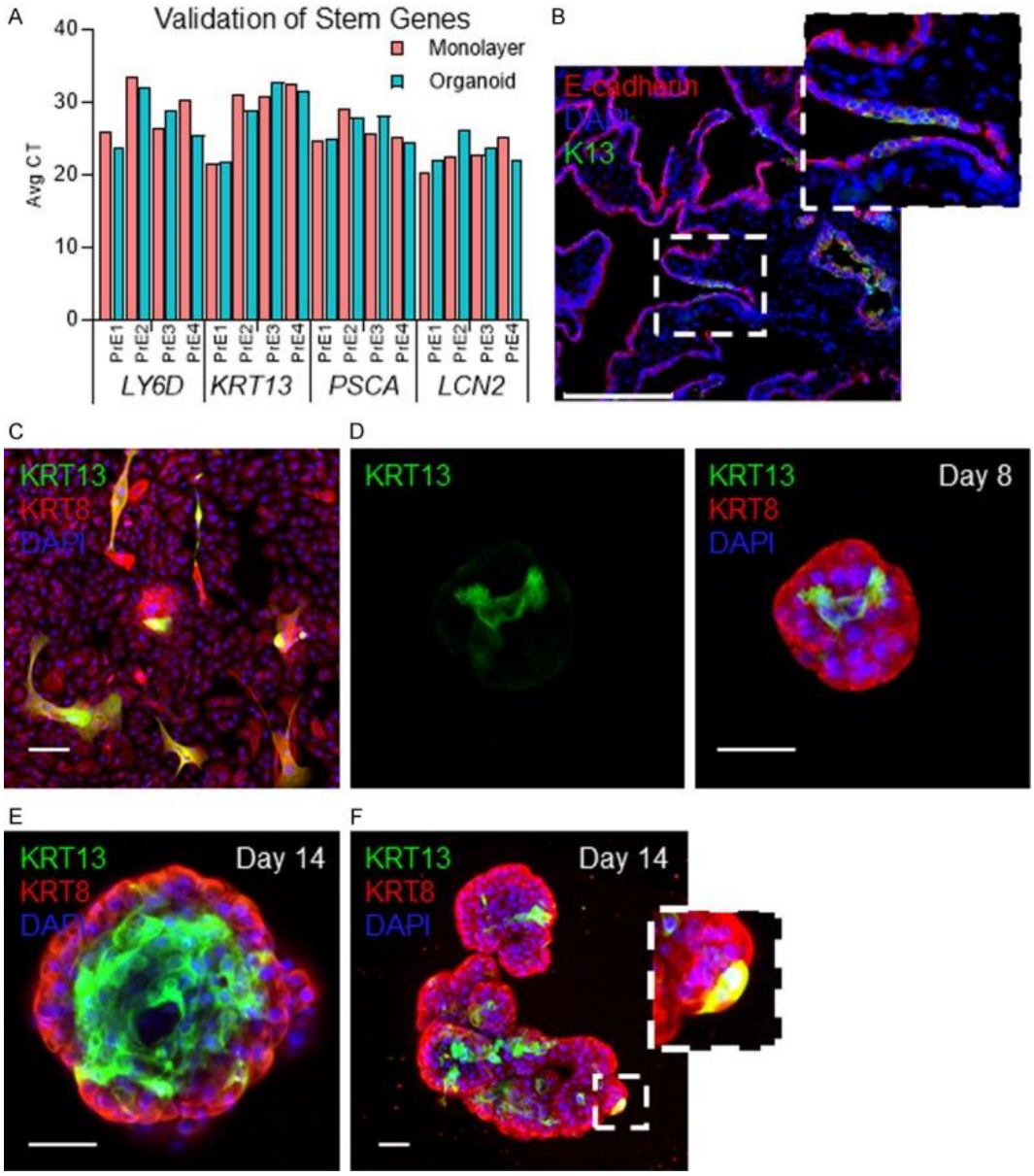

Fig. 7: Presence of the KRT13+ Population in Tissue, Monolayer Cells and Organoids. A. RT-qPCR analysis for stem cell markers in whole RNA extracts of monolayer and organoid samples derived from 4 patients. B. Immunofluorescent staining for KRT13, DAPI and E-cadherin on the scRNA-Seq patient tissue (scale bar = 200 µm). C. Immunocytochemistry of monolayer cells derived from patient PrE2 stained for KRT13, KRT8, and DAPI (scale bar = 50 µm). D. Whole-mount immunocytochemistry of day 8 organoid cells derived from patient PrE2 stained for KRT13, KRT8 and DAPI (scale bar = 50 µm). E, F. Whole-mount immunocytochemistry of day 14 organoid cells derived from patient PrE2 stained for KRT13, KRT8, and DAPI, inset (right) shows KRT8+/KRT13+ cell (scale bar = 50 µm).

human primary prostate organoid models has not been performed. Using an integrated analysis, we identified 10 cell populations in monolayer and organoid culture, thus identifying more cell types than previously reported *in vitro*. Our analyses revealed populations of cells at varying levels of differentiation along the basal and luminal lineages. More specifically, KRT13+ putative stem cell populations were identified in both monolayer and organoid conditions and had expression profiles similar to those previously reported for KRT13+ cells in tissue (Henry et al. 2018). We identified three putative stem and progenitor populations by high KRT13 or KRT6A expression, which have been previously described to mark regenerative cells in tissue and prostasphere culture (Henry et al. 2018; Schmelz et al. 2005; Hu et al. 2017). The three populations also showed expression of LY6D, LY6/PLAUR Domain Containing 3 (LYPD3), and CSTB and one specific cluster of the three had high expression of PSCA. PSCA and KRT13 were previously described by Henry et al. to mark two previously unknown clusters of epithelial cells, termed “club” and “hillock”, based upon their similarity to immunomodulatory and progenitor-like cells found in the mouse lung, respectively (Henry et al. 2018). In contrast to the tissue-isolated cells in that study, which had distinct populations that were either PSCA+ (club) or KRT13+ (hillock), the *in vitro* cells had one PSCA High/KRT13 High cluster and one PSCA Low/KRT13 High cluster. KRT13 protein expression did vary greatly between organoid samples at day 8 and day 14, with day 14 organoids displaying multiple KRT13+ cells (**Fig. 7F**). The two PSCA Low clusters, 1 and 7, expressed stem markers LY6D, LYPD3, KLK11, and CSTB while also co-expressing basal and luminal markers. These cells may be more committed basal and luminal progenitors that reside below the KRT13 High/PSCA High cells on the

stem-hierarchy. The degree of KRT13 expression has been shown to positively correlate with the level of stemness in other contexts, where differentiated daughters show less expression as they divide and differentiate (Hu et al. 2017). This was observed in some organoids that showed double positive KRT8/KRT13 cells (**Fig. 7F**) and is likely the explanation for the heterogeneity of KRT13 expression seen in the day 14 organoids (**Fig. 7F**).

KRT13+ hillock cells of the human prostate were named so because of their similarities to cells in the mouse lung that show a progenitor-like phenotype (Henry et al. 2018; Montoro et al. 2018). In the organoids we observed some evidence of KRT13+ hillock cells exhibiting a capacity for branching morphogenesis due to their localization to the interior of branching organoids (**Fig. 7F**) which may be similar to a “hillock” region seen in patient tissue. This morphological similarity provides additional evidence that KRT13+ cells observed in this study are similar to those characterized by Henry et al.

Recently, FACS-sorted mouse prostate epithelial cells that were analyzed using Fluidigm qPCR showed LY6D expression in a population of organoid-forming cells found in both the luminal and basal compartment (Barros-Silva et al. 2018). The LY6D+ cells formed solid, acinar or translucent organoids, similar to the organoid morphologies that we observed in our culture (**Figs. 7E, 7F**). Human DLK1+ prostate basal cells have also been shown to form solid spheroids, spheroids with lumens and spheroids with tubules. LY6D and KRT13 were co-expressed in population 6 and 7 in our 3D cells and had similar expression profiles to the reported DLK1+ cells (Moad et al. 2017). PPL was highly expressed in cluster 6 and KLK11 was highly expressed in clusters 1 and 6. These genes were published as being expressed by the proximal niches that maintain

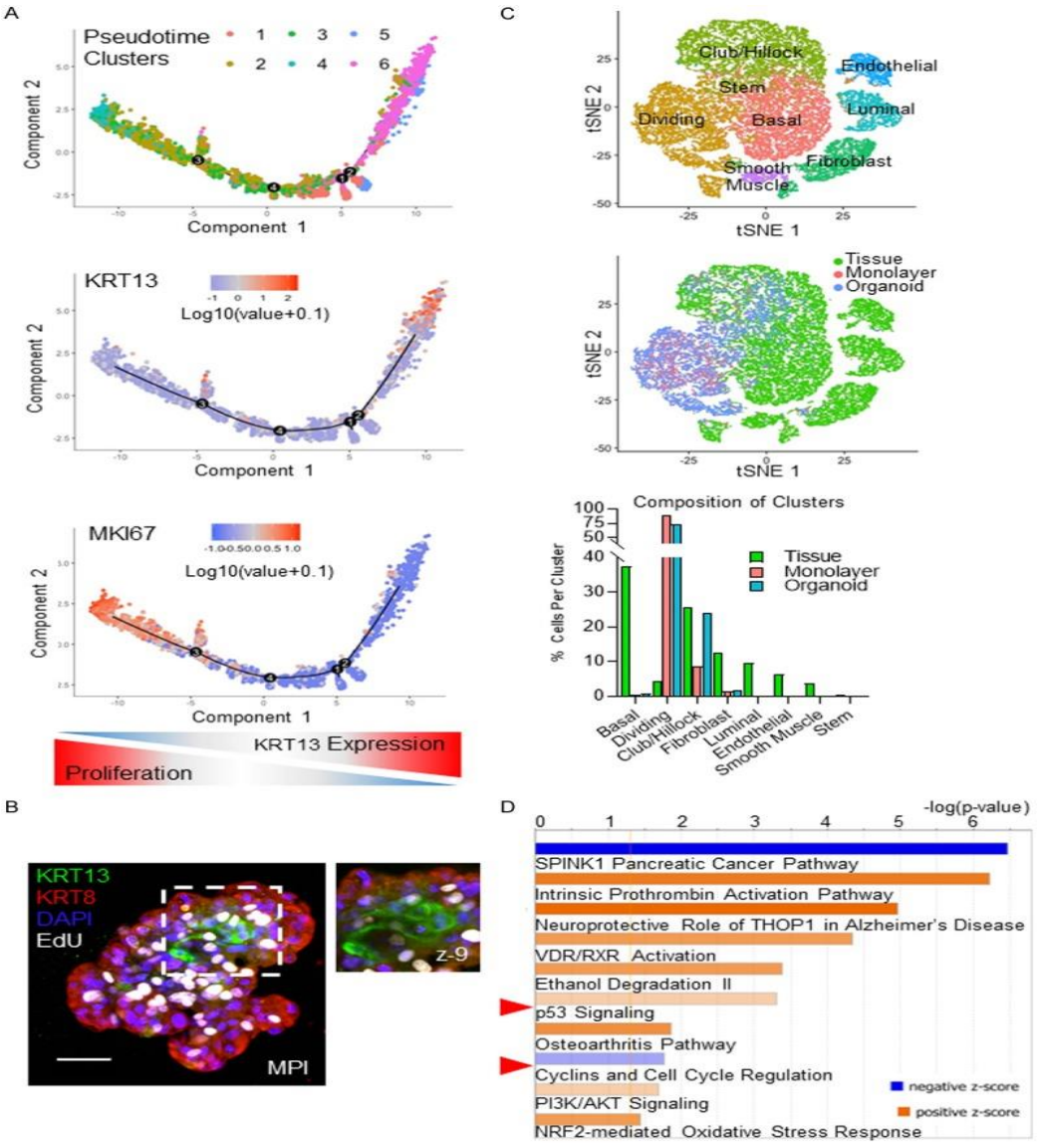

Fig. 8: KRT13+ Subpopulation is Quiescent. A. Pseudotime plots of organoid cell clusters (top), KRT13 expression (middle) and MKI67 expression (bottom). B. EdU incorporation and whole-mount immunocytochemistry of day 14 organoid cells derived from patient PrE3 stained for KRT13, KRT8 and DAPI (scale bar = 50 µm). C. T-SNE plot of integrated data sets shows 8 cluster identities (top), sample identities (middle), bar chart depicting the contribution of sample to each cluster (bottom). D. Ingenuity pathway analysis of genes highly expressed by cluster 6.

epithelial flow in human prostate and contain possible DLK1+ prostate stem cells (Moad et al. 2017). Taken together, these reports provide substantial support for the notion that KRT13+ cells are a stem cell population in organoid culture and indicate that this model system would be useful for studying hillock biology and proximal niches *in vitro*. It is important to note that the monolayer culture condition yielded numerous KRT13+ cells that exhibited a stretched morphology typical to terminally differentiated cells and notably different from other KRT13+ cell shapes (**Fig. 7C**). These data introduce the possibility that KRT13 may be an excellent stem cell marker when used in combination with secondary markers like LY6D and PSCA, but on its own it could mark a broad population that contains epithelial stem cells along with a small population of unhealthy squamous cells or differentiated daughter cells in this context.

The lack of expression of luminal markers AR and KLK3 in the organoids by scRNA-Seq should be interpreted with caution. A limitation of all single cell sequencing technologies is that it captures only 10-20% of transcripts per cell (the 10x Chromium Single Cell 3' v2 Kit used here has a capture rate of 14-15%), thus absence of the gene in the analysis is not conclusive evidence that it is not expressed. We did detect low AR expression by RT-qPCR of whole organoids (**Fig. 5C**). Growth of fully differentiated luminal cells with robust AR remains a challenge in the field of human prostate organoids.

Overall, we observed that both monolayer and organoid culture are capable of cultivating a rare population of putative stem-like cells that are marked by high expression of KRT13, LY6D, LYPD3, and PSCA. These cells are similar to cells found in the basal and luminal compartments of mouse prostate and human club/hillock

regions, implying that we are describing the *in vitro* isolation and culture of a population of stem-like cells that reside in tissue. There were populations of intermediate cells that were overrepresented in the organoid condition, as well as a KRT6A+ progenitor population that was enriched in 3D. Our catalog of unique populations in these two *in vitro* models shows the preservation of a specific stem-like cell population as well as provides an in-depth atlas of the populations present in both monolayer and organoid models. This can serve as a valuable resource to the field, allowing for a deeper understanding of which cells are present in benign model systems and how they may change between *in vitro* and *in vivo* conditions.

CHAPTER III

SINGLE CELL RNA-SEQ ANALYSIS OF THE MOUSE PROSTATE IDENTIFIES FACTORS NECESSARY FOR THE REGENERATIVE PHENOTYPE OF PROSTATE CELLS *IN VITRO*

ABSTRACT:

The human prostate presents a significant rate of disease in aging males, as both prostate cancer and benign prostate hyperplasia are very common diseases. A possible explanation for this high disease burden is the activity of stem cells within the prostate, and their innate capability for regeneration going awry over time. Using murine models of prostate behavior and scRNA-Seq analysis, we were able to identify numerous cell populations within the prostate. Among these populations was a group of cells expressing luminal markers as well as multiple putative progenitor cell markers, which we designated as Luminal Progenitor Cells. The expression data gathered from these cells were distilled to a list of candidate factors necessary for the Luminal Progenitor Cell regenerative phenotype using Ingenuity Pathway Analysis. Subsequent testing of inhibitors targeting these factors led to the inhibition of *in vitro* regeneration in organoids derived from both mice and human patient samples. Specifically, inhibition of Bcl2 Apoptosis Regulator (Bcl-2) regulation of apoptosis and Yes-Associated Protein 1 (Yap1) signaling produced promising results in both contexts and warrant continued analysis for their role in normal prostate regeneration. Altogether, this study outlines a new set of druggable targets for normal prostate regeneration as well as serving as a proof of concept for using scRNA-Seq to identify druggable targets for prostate diseases in the future.

CONTRIBUTION OF COLLABORATORS:

The lab of Dr. Larisa Nonn provided patient samples for our human organoid studies as well as providing training in human organoid culture techniques.

INTRODUCTION:

The prostate is an accessory sex organ located beneath the bladder that is responsible for the secretion of prostatic fluid (C. H. Lee, Akin-Olugbade, and Kirschenbaum 2011; Ittmann 2018; Aaron, Franco, and Hayward 2016). In addition to these normal secretory functions, the prostate has a high rate of neoplastic and hyperplastic disease (Ramsey 2000; Rawla 2019). Prostate cancer is among the most common cancers in men and benign prostate hyperplasia (BPH) affects a majority of men over the age of 60 (American Cancer Society 2020; Wei, Calhoun, and Jacobsen 2005). It is believed that aberrant prostate epithelial progenitor activity plays a role in the high rate of prostate disease (X. Wang et al. 2009; Tokar et al. 2005; L Xin 2013). Further investigation of epithelial progenitors, both their biomarkers and the pathways necessary for their regenerative phenotype, may therefore provide significant insight and pharmacologic strategies to understand and target the initiation and progression of prostate disease.

Mice provide a tractable model system for studying prostate epithelial progenitors due to their capacity for hormone-dependent regeneration. After castration, the mouse prostate undergoes a wave of apoptosis shrinking to approximately a tenth of its original size (Sugimura, Cunha, and Donjacour 1986b; Cunha and Lung 1978). The reintroduction of androgen, often through surgical implantation of a testosterone pellet,

leads to the regeneration of the prostate and recapitulation of its original ductal architecture and secretory function (Sugimura, Cunha, and Donjacour 1986b; Cunha and Lung 1978). This hormonal modulation of progenitor cell regenerative activity allows for the direct investigation of cells in the prostate epithelium which exhibit the regenerative phenotype necessary for regeneration, allowing for the possible identification of factors optimal for targeted treatment. Using this hormonal regeneration model, researchers have found that mouse prostate regeneration is in part dependent upon the regenerative activity of cells located proximal to the urethral ducts and referred to as prostate epithelial progenitor cells (Moad et al. 2017; Tsujimura et al. 2002; Burger et al. 2005, 1; Goldstein et al. 2008). Originally thought to only belong to the basal epithelial lineage, cells exhibiting regenerative capacity *in vivo* were also discovered in the luminal compartment of the prostate epithelium (Karthaus et al. 2014; X. Wang et al. 2009; Y. A. Yoo et al. 2016, 1). A rare subset of luminal epithelial cells was also found to be bipotent when cultured as organoids *in vitro* (X. Wang et al. 2009; Chua et al. 2014). Additionally, these luminal prostate progenitor cells have been studied using single-cell transcriptomics, finding numerous biomarkers for the luminal progenitor cell population (Crowell, Fox, et al. 2019; Joseph et al. 2020; Crowley et al. 2020). Although single-cell transcriptomics have been used to identify luminal progenitor populations in the prostate epithelium, these approaches can also be used to identify candidate pathways and factors necessary for the regenerative phenotype in an unbiased way.

Here, we use single-cell RNA-Seq data to analyze the intact and castrate prostate, quantifying the change in biomarkers after the loss of androgen as well as identifying candidate pathways for progenitor cell ablation. These candidate pathways

were chemically perturbed in *in vitro* organoid cultures derived from both mouse and human tissue samples, showing the necessity of our candidate factors in both contexts. These data provide new information on the behavior of prostate progenitor cells as well as unique candidate avenues for future treatment of prostate progenitor cells in disease states.

MATERIALS AND METHODS

Single Cell RNA-Seq Sample Prep and Analysis:

Mice were castrated according to institutional guidelines at 8 weeks of age. A cohort of castrated mice were subcutaneously implanted with a 1.5cm silastic implant packed with powdered R1881 (Steraloids, Newport, RI) and sealed with silicone adhesive, making these mice the ‘hormone normal’ condition. Another cohort of mice were left without a testosterone implant, making these mice the ‘castrate’ condition. After 3 weeks, mice were euthanized according to institutional guidelines before removal and dissections of their prostates. Dissected prostate lobes were then dissociated enzymatically using Type I Collagenase (Sigma-Aldrich, St. Louis, MO) and Dispase (STEMCELL Technologies, Vancouver, Canada). The resulting single-cell solution was then counted using a Nexcelom Cellometer (Nexcelom, Lawrence, MA), setting a necessary threshold for cell viability in the sample at 70% viable. Samples at 70% viability were then processed using the 10X 3’ scRNA-Seq V2 protocol as we previously reported (McCray, Moline, et al. 2019). In short, cells were separated into individual microfluidic droplets along with an oligonucleotide-covered gel bead using the 10X Chromium Controller (10X Genomics, Pleasanton, CA). Cells were then lysed in the presence of their respective beads, capturing their transcripts. Captured transcripts

were then converted to cDNA and eventually into an Illumina-compatible sequencing library according to the 10X protocol. The resulting library was sequenced at the University of Illinois at Urbana-Champagne on an Illumina NovaSeq (Illumina, San Diego, CA) at 100bp Paired-End read depth. Reads were then aligned to the mm10 annotated reference genome using CellRanger v3.0.1 (10X Genomics, Pleasanton, CA). QC and clustering were performed in the R Package Seurat (Satija Lab, New York, NY) (Satija et al. 2015). Downstream pathway analysis was performed in Ingenuity Pathway Analysis (IPA) (Qiagen, Hilden, Germany).

IF Imaging of Mouse Tissue Sections and Organoids:

C57BL/6J mice were obtained from Harlan/Envigo (Indianopolis, IN).Prostates from both castrate and hormone normal 11 week old mice were dissected and cryoembedded in OCT. Cryoembedded prostates were cut and placed on slides by the University of Illinois at Chicago Research Histology and Tissue Imaging Core (UIC, Chicago, IL). Sections were then stained using primary and secondary antibodies at concentrations detailed in Table 5. Stained slides were then imaged on a Keyence BZ-X800 benchtop microscope (Keyence, Osaka, Japan). Images were analyzed using the accompanying Keyence Image Analysis software as well as FIJI. Images were adjusted for exposure and haze reduction using the corresponding functions in the Keyence Image Analysis software and subsequently counted using a cell counting macro in FIJI. Three biological replicates were used for each staining, with 4 technical replicates within each biological replicate. Images provided in figures are representative of fluorescent staining observed in all biological replicates.

Flow Sorting of Dissociated Mouse Prostates:

Prostates from three mice 8-12 weeks of age were dissociated using collagenase and dispase. The resulting single-cell solution was then stained with conjugated antibodies targeting CD26 (APC) and TSPAN8 (PE) (**Table 5**). Samples were sorted on a MoFlo Astrios (Beckman Coulter Life Sciences, Indianapolis, IN) at the University of Illinois at Chicago Flow Cytometry Core.

Mouse and Human Organoid Culture and Colony Forming Unit Assays:

Prostates from three intact mice 8-12 weeks of age were enzymatically dissociated using Type II Collagenase (Manufacturer, Location) and Dispase (STEMCELL Technologies, Vancouver, Canada). The resulting single-cell solution was resuspended in 50% Growth Factor Reduced, Phenol Red-free Matrigel (Corning, Corning, NY) and plated in serum-free Advanced DMEM (Thermo Fisher Scientific, Waltham, MA) containing A83-01 (A.G. Scientific, San Diego, CA), y-27632 (STEMCELL Technologies, Vancouver, Canada), R-Spondin (Peprotech, Rocky Hill, NJ), and Noggin (Peprotech, Rocky Hill, NJ) at the same concentrations detailed in Drost et al. 2016 (Drost et al. 2016). Mouse organoids were plated into six technical replicates per each treatment condition, per each biological replicate. Small molecule inhibitors were administered upon plating of the organoids (**Table 7**), and treatment courses proceeded for 72hrs before imaging of the wells on the Keyence BZ-X800. Wells were imaged at 4x magnification, acquiring a three-dimensional Z-Stack of the entire well. Max projection images were then created from the Z-stacks, allowing for the viewing of all organoids in one two-dimensional image. These stitched images were counted using the automated cell counting function in the Keyence Image Analysis

software (Keyence, Osaka, Japan). To ensure that organoids were counted specifically and not individual cells or small cell clumps, a size threshold was instituted, only including individuals with a perimeter of 200um or greater in the analysis. This threshold was chosen because it yielded counting results that most closely mirrored preliminary hand-counted results, calibrating the software to adhere to the researcher's definition of an organoid according to size and circularity. Organoid counts from individual wells were then divided by the total number of cells plated in that well, yielding a percentage of colony forming units which could be used as a rough measurement of regenerative capacity. %CFU data was then compared using a two-tailed student's t-test with a significance threshold of $t < 0.05$. Human organoid culture was performed using a protocol similar to the one detailed in McCray et al. 2019.16 In short, biopsies from healthy regions of human prostates were dissociated into single cells and cultured as PrECs in 2D before being transferred to 3D culture in 33% Matrigel and fed using KSFM media (Thermo Fisher Scientific, Waltham, MA). These human organoids were treated with drugs upon plating and imaged using the Evos FL Auto 2 imaging System (Thermo Fisher Scientific, Waltham, MA). Images were stitched using FIJI and subsequently counted using the Celleste image analysis software (Thermo Fisher Scientific, Waltham, MA). Colony forming units were also found and compared between treatment conditions in the same manner as the mouse organoid assays.

Statistical Analyses:

Statistical analyses for this study were performed in R. Statistical tests for our scRNA-Seq dataset were performed using the Seurat add-on for R, and any p-values reported in this paper referring to scRNA-Seq expression trends are adjusted p-values

Table 5

Antibodies Used for Immunofluorescence and Flow Cytometry

Target Protein	Host Organism	Manufacturer	Dilution
Cd26	Rat	Biolegend	1ug/million cells
Psca	Rabbit	Lifespan Biosciences	1:100 (Tissue) 1:100 (Organoids)
Tspan8	Rat	R&D Biosystems	1:50 (Tissue) 1:100 (Organoids)
Tspan8 (PE Conjugated)	Rat	R&D Biosystems	10uL/million cells
Krt5	Chicken	Biolegend	1:1000 (Tissue) 1:100 (Organoids)

that account for multiple sampling errors. These adjusted p-values are supplied by the program's clustering algorithm, which is thoroughly explained in Butler et al.17 In our organoid drug treatment experiments, conditions were compared to one another using a two-tailed student's t-test with a threshold of $t < 0.05$. This analysis was performed using each of the six technical replicates as the dataset for the specific experimental condition, and the analysis was performed within each biological replicate for that particular drug experiment. Biological replicates were not compared directly to one another in an effort to avoid the confounding effects of stochastic differences in regenerative potential between the individual replicates, which can be observed in the box-and-whisker plots provided in Figs. 14 and 15. A similar approach was undertaken with the human organoid drug treatment conditions, with each drug treatment compared to the vehicle condition using a two-tailed t-test with a threshold of $t < 0.05$.

RESULTS

scRNA-Seq Analyses of Intact and Castrate Mouse Prostates

We initially sought to investigate the unique populations of the mouse prostate in an effort to catalog their biomarkers and potential critical signaling pathways. To achieve this goal, we employed single-cell RNA-Seq analysis, using cells from both the intact and castrate prostates of mice 8-12 weeks of age (see **Table 6** for cell sample and sequencing output quality metrics) (**Fig. 9A**). The raw expression matrices from these data were then subjected to a quality control workflow in Seurat, an R add-on used for dimensional reduction-based analysis of scRNA-Seq datasets (Butler et al. 2018; Macosko et al. 2015; Satija et al. 2015). Our quality control workflow allowed for

Table 6

Quality Control Metrics for Mouse Prostate Samples and scRNA-Seq Analyses

Readout	Intact	Castrate
Viability at Collection	80.2%	74.2%
Sample Density	5.12e6 cells/mL	2.59e5 cells/mL
Average Features Per Cell	989.78	1401.37
Number of Principle Components	43	43
Modularity of Generated UMAP	0.8412	0.8902

the removal of cells from the dataset that had too few reads (indicating they were poorly captured), too many reads (indicating a doublet or multiplet of cells was captured), or a percentage of mitochondrial reads above 10% (indicating the cells were dead or dying). This curated dataset was then analyzed via a dimensional reduction analysis, producing 18 clusters in the intact and 19 clusters in the castrate condition (**Fig. 9B-C**).

In the intact condition, a cluster of cells was identified expressing markers consistent with differentiated luminal cells. Statistically significant biomarkers included Krt8, Krt18, and Probasin (Pbsn) (**Fig. 10A**). These Differentiated Luminal Cells were observed to be 61% of the total cells in the Intact Prostate, constituting a majority of the cells in the sample (**Fig 11C**). In addition to these Differentiated Luminal Cells, we also identified a group of luminal cells expressing high Nkx3.1 (**Fig 10A**). Designated as $Nkx3.1^{Hi}$ Luminal Cells, this population of cells expressed a high level of Nkx3.1 as well as the normal luminal cell markers Krt8 and Krt18 (**Fig 11A**). A Proliferating Luminal Cell population was also identified in the Intact Prostate, expressing Ki-67 (Ki67) as well as Krt8 and Krt18 (**Fig 10A**). Although the prostate is largely considered to be quiescent in the hormone normal state, there is a limited rate of epithelial turnover that could account for by the proliferating luminal cell population observed here (Toivanen, Mohan, and Shen 2016). Another cluster of cells expressed Krt8 and Krt18 as well as putative progenitor cell markers including Sox2, Trop2, and Psca (**Fig 10A**) (E. McAuley et al. 2019; Goldstein et al. 2008, 2; Henry et al. 2018). These cells were subsequently identified as Luminal Progenitor Cells. Three clusters were identified due to their expression of stromal fibroblast markers. First, a cluster of cells expressing stromal marker Decorin (Dcn) as well as signaling ligand Fibroblast Growth Factor 2 (Fgf2) were

identified as Fgf Signaling Fibroblasts (**Fig 10A**) (Henke et al. 2012). Another signaling fibroblast cluster of cells was identified in the dataset, this one expressing Dcn as well as Wnt2 (**Fig 10A**). Both Fgf and Wnt signaling factors are known to play a role in prostate development and epithelial regeneration (Kwon et al. 2019; Kato et al. 2013; S. H. Lee et al. 2015). Additionally, a group of cells expressing Dcn as well as Ki67 were identified as proliferating fibroblasts (**Fig. 10A**). Other elements of the prostate stroma were also identified, including cluster of cells was identified that expressed numerous immune cell markers like C-C Motif Chemokine Receptor 6 (Ccl6), a marker of T-cells (Coelho et al. 2007). Endothelial Cells were also present among the stromal populations identified in the intact condition, marked by their expression of Claudin 5 (Cldn5) (**Fig. 10A**) (Escudero-Esparza, Jiang, and Martin 2012). Lastly, Basal Epithelial cells were identified in the Intact Prostate, expressing Krt5, Krt14, and progenitor cell markers including Sox2 and Trop2 (**Fig. 10A**). Other basal populations that were ostensibly more differentiated and did not express these progenitor cell markers were not resolved in this dataset, likely owing to the underrepresentation of the cell type after tissue digestion. For relative expression levels of biomarkers as well as the relative size of each population as a percentage of total cells, see Fig. 11.

Investigation of the castrate prostate led to the identification of numerous similar populations to those found in the Intact Prostate, while also uncovering new populations observed only in the castrate prostate. Differentiated Luminal Cells were identified once again, expressing Krt8, Krt18, and Pbsn (**Fig. 10B**). The persistence of Differentiated Luminal Cells in the castrate prostate is interesting, as these cells are androgen dependent. Differentiated Luminal Cells are a much smaller percentage of total cells in

the Castrate Prostate (6.8%) when compared to the Intact Prostate (61.1%), showing some adherence to predicted androgen dependence of these cells (**Fig. 11D**). The small population of surviving Differentiated Luminal Cells in the castrate prostate may be expressing a survival program that allows them to persist in the absence of androgen, but more experimentation is necessary to find more conclusive evidence of this. Nkx3.1^{Hi} Luminal Cells were also identified in the Castrate Prostate, again expressing Krt8, Krt18, and Nkx3.1 (**Fig 10B**). An additional luminal population observed exclusively in the Castrate condition expressed Krt8, Krt18, and Trop2. Interestingly, this population did not express the other putative progenitor markers Psca and Sox2 that were observed in the Luminal Progenitor Cell population in the intact condition. This led to the identification of this cluster as Intermediate Luminal Cells, although their relationship to the Luminal Progenitor Cell population requires further investigation. Luminal Progenitor Cells were also identified in the castrate condition, once again expressing Krt8, Krt18, Sox2, Psca, and Trop2 (**Fig 10B**). Basal Epithelial Cells were observed in the castrate prostate, expressing Krt5, Krt14, Sox2, and Trop2 much like their counterparts in the intact condition (**Fig 10B**). Immune Cells and Endothelial Cells were also observed in the castrate prostate, expressing markers similar to those observed in the same populations in the intact condition (**Fig 10B**). These Immune Cells constituted a higher proportion of total cells in the castrate condition (32.5%) than the intact condition (8.8%) (**Fig 11D**). This difference between hormonal states may be due to the significant reduction in luminal cells in the tissue, or it may be due to an activation of the immune cells of the prostate stroma in the absence of androgen signaling. Further investigation may be able to differentiate between these

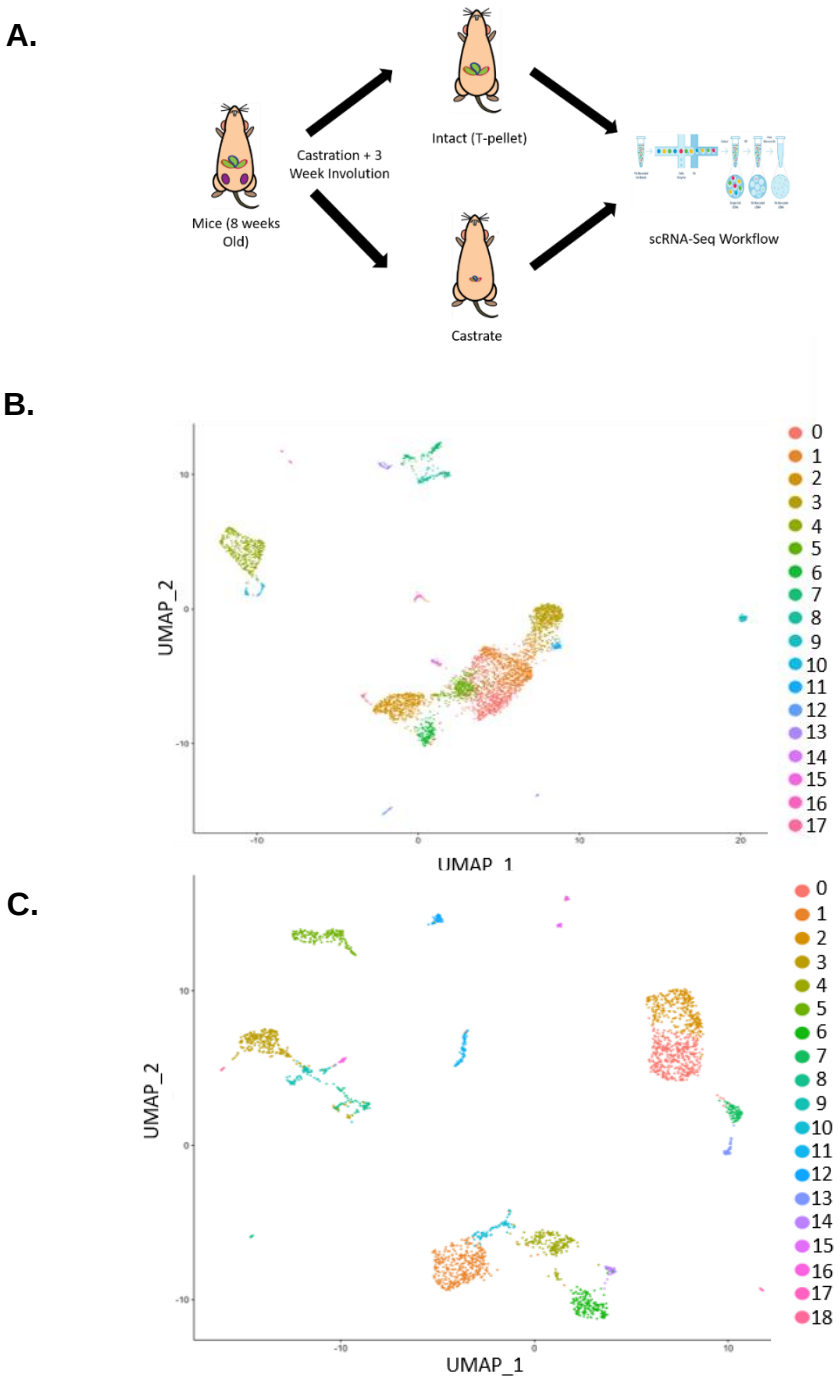

Fig. 9: scRNA-Seq Data from the Intact and Castrate Mouse Prostate. A. Experimental design for scRNA-Seq. In short, mice were castrated at 8 weeks of age and separated into intact and castrate cohorts. These cohorts had their prostates dissected and dissociated after a three-week period. Dissociated prostate samples were then subjected to the 10x scRNA-Seq library prep workflow. B. Unsupervised UMAP depicting clusters identified by scRNA-Seq analysis in the intact mouse prostate sample. C. Unsupervised UMAP depicting clusters identified by scRNA-Seq analysis in the castrate mouse prostate sample.

competing explanations. Signaling fibroblasts were observed in the castrate condition, both the Fgf Signaling Fibroblast and Wnt Signaling Fibroblast populations (**Fig 10B**). Additionally, the Proliferating Luminal Population was notably absent from the castrate condition. The Proliferating Stromal Population was absent from the castrate condition (**Fig 10B**). The lack of proliferating luminal and stromal populations in the castrate condition implies that there is a lower rate of tissue turnover in the absence of androgen signaling.

Identifying and Defining Luminal Progenitor Cells

Luminal Progenitor Cells (LPCs) are of particular interest to us in the context of this study. They are a cell type that can contribute to disease, and there is little knowledge of the mechanistic contributors to their specific phenotype (Tokar et al. 2005; X. Wang et al. 2009; Li and Shen 2019). Using the perspective afforded by these two datasets, we have been able to establish a marker profile for LPCs within the context of this experiment. This profile includes Krt8, Krt18, PSCA, Trop2, and Sox2, as these are the factors clearly expressed by the LPC population in both the intact and castrate hormone conditions. These putative progenitor markers have been independently verified to enrich for progenitor cell phenotypes in the mouse prostate epithelium (Henry et al. 2018; Goldstein et al. 2008; E. McAuley et al. 2019). Although the LPC populations identified in the intact and castrate conditions share numerous similarities, they also have notable differences in their respective expression patterns. The Castrate LPCs do not express AR to a statistically significant degree, possibly owing to a regulatory change in the population due to the loss of AR signaling. Castrate LPCs also express certain factors of note including the morphogen Shh and putative progenitor cell

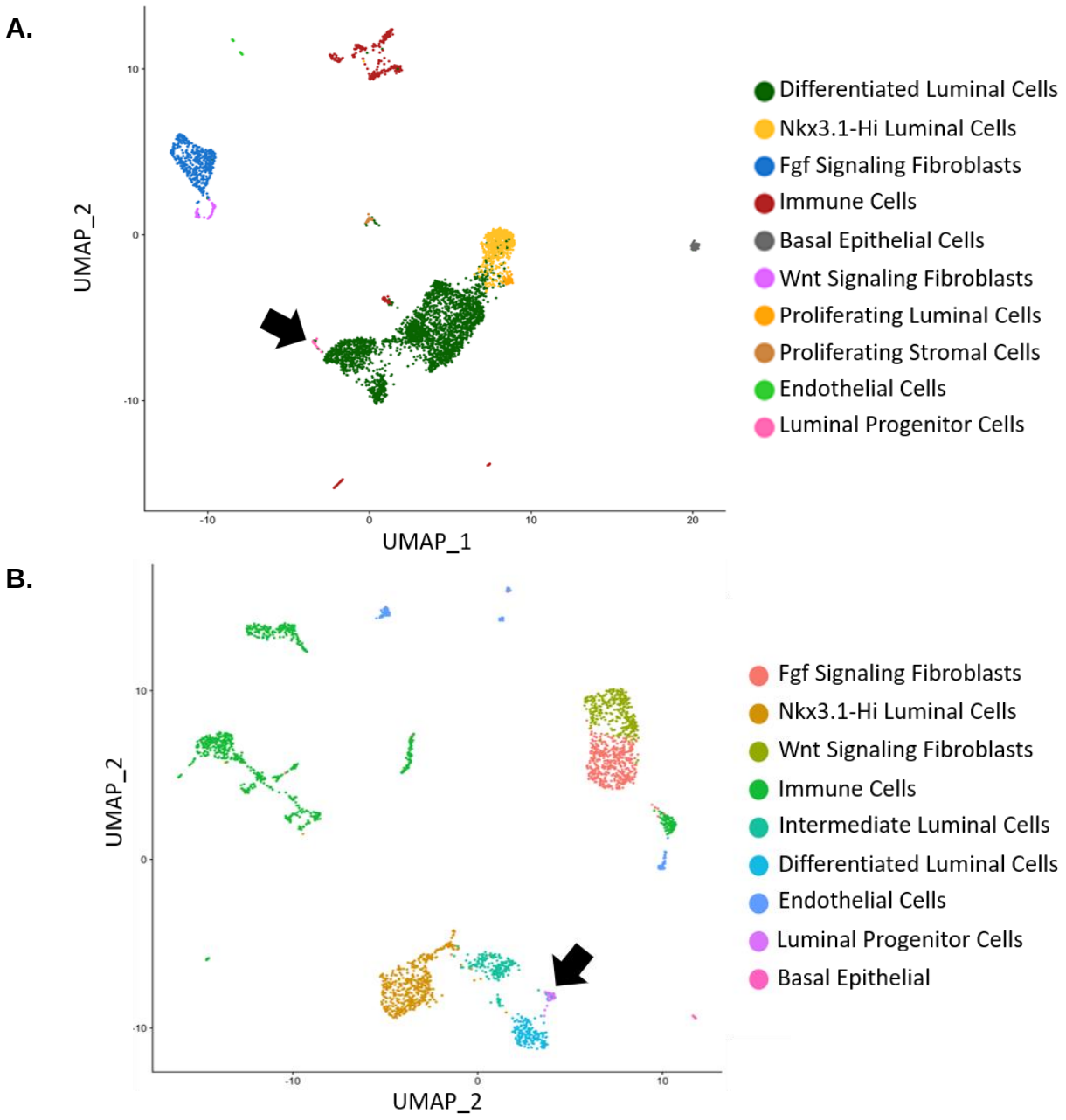

Fig. 10: scRNA-Seq UMAPs With Populations Identified. A. UMAP for intact prostate depicting identified populations. Arrow points toward the luminal progenitor cell population. B. UMAP for castrate prostate depicting identified populations. Luminal Progenitor Cells were identified in both conditions, and the luminal compartment was observed to be more heterogeneous in the castrate condition. Arrow points toward the luminal progenitor cell population.

marker Ly6d (Barros-Silva et al. 2018). Further investigation is required to understand the implications of these differences in expression pattern between hormone states. Additionally, there is a two-fold upregulation in the number of luminal progenitor cells in the castrate condition when compared to the intact condition (0.3% in intact, 0.8% in castrate), in agreement with the observed enrichment of cells with a progenitor phenotype in the castrate prostate (**Fig 11C-D**) (X. Wang et al. 2009; Karthaus et al. 2020). Overall, these data provide evidence that a suite of biomarkers corresponding to the luminal progenitor cell population can be identified using scRNA-Seq analysis, and that these cells can be discerned from more differentiated luminal populations in both the castrate and intact conditions.

Immunofluorescence Microscopy and Flow Cytometry Validation of Luminal Progenitor Cell Biomarkers

We next undertook a validation of our marker suite using orthogonal methods, specifically immunofluorescence microscopy and flow cytometry. Specifically, we were interested in validating the expression patters of the LPC population in the intact and castrate conditions. This population is not only of interest due to a relative lack of study of its mechanistic underpinnings, but also due to its possible role in prostate disease.(X. Wang et al. 2009) IF microscopy on cryo-embedded mouse prostates showed overlap of Psca and Tspan8, two markers that were statistically significant markers for the Luminal Progenitor Cell population in both the intact and castrate condition (**Fig. 12A)**. Flow cytometry targeting CD26+/Tspan8+ cells showed the presence of candidate luminal progenitor cells in the intact prostate at 5.5% of total live cells (**Fig 12B**).

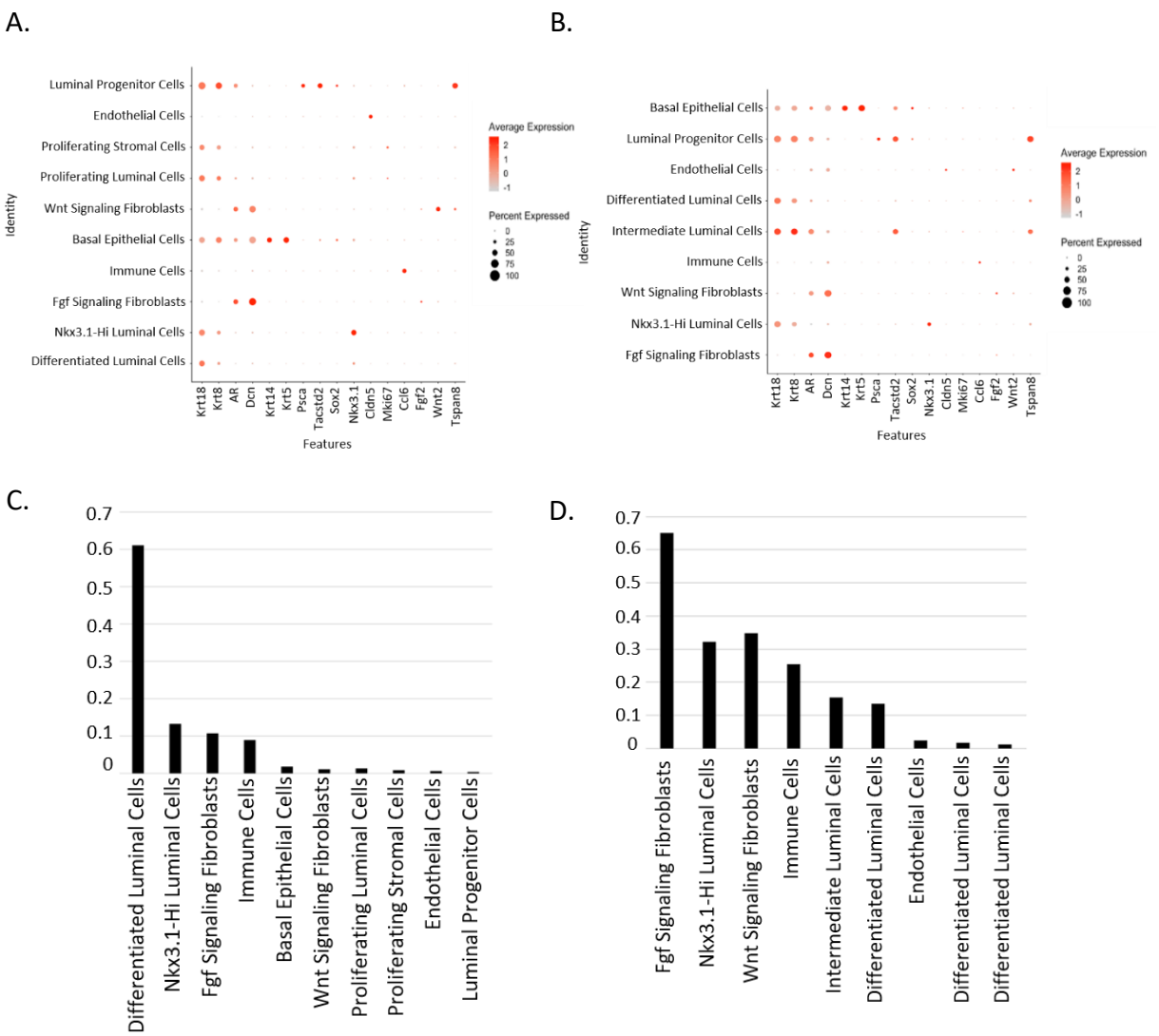

Fig. 11: Expression Patterns Observed Among Populations in scRNA-Seq Data. A. Dotplot depicting the expression of relevant factors in the intact condition. LPCs were observed to express high levels of Krt8, Krt18, Psca, Tacstd2, and Sox2. B. Dotplot depicting the expression of relevant factors in the castrate condition. LPCs were once again observed to express high levels of Krt8, Krt18, Psca, Tacstd2, and Sox2. C. Size of identified populations as a percentage of total cells in the intact sample. D. Size of identified populations as a percentage of total cells in the castrate sample. The castrate condition saw an increase in the size of the Luminal Progenitor Cell population as well as an absence of proliferating populations that were observable in the intact condition.

Although our flow cytometry approach yielded a higher number of LPCs as a percentage of total cells in the dissociated prostate, this may be due to a lack of specificity in our gating approach. Tspan8 transcript expression may be a marker for LPCs according to our scRNA-Seq, but our IF and Flow Cytometry data show that Tspan8 also marks a small population of cells other than LPCs. Future experimentation may require the inclusion of further markers in our IF and flow cytometry panels to avoid impurities in sorted fractions and account for the differences between transcript and protein of Tspan8. Overall, these efforts provide evidence validating the expression pattern of biomarkers used to identify the Luminal Progenitor Cell population in our scRNA-Seq dataset.

Pathway Analysis of the Luminal Progenitor Cell Population

We next sought to understand the factors necessary for the LPC phenotype in an effort to possibly perturb their regenerative phenotype. Ingenuity Pathway Analysis was used to analyze the gene list generated from the luminal progenitor population identified using scRNA-Seq from the intact condition. The gene list was enriched for the upregulation of genes associated with Self Renewal of Cells (z-score = 2.781), Cell Survival (z-score = 3.631), Growth of Organism (z-score = 2.738), Colony Formation (z-score = 2.13), and Colony Formation of Cells (z-score = 2.31) (**Fig. 13A**). De-enriched gene lists with a z-score below -2 included Congenital Malformation of the Urogenital System (z-score = -2.936), Apoptosis of Epithelial Cells (z-score = -2.048), Morbidity or Mortality (z-score = -10.444), Organismal Death (z-score = -10.377), and Apoptosis (z-score = -3.265) (**Fig 13A**). Additionally, Upstream Regulator Analysis revealed a list of factors predicted to have an effect on the phenotype of LPCs. These factors included

Yap1 (z-score = 2.449), a transcription factor in the Hippo Pathway, as well as numerous upstream regulators of Bcl-2, a factor with canonical anti-apoptotic activity (Fig 4B) (Willis et al. 2003). Factors with an established role in regulating Bcl-2 that were identified by Upstream Analysis included regulators IL12 (z-score = 2.00), HIF1A (z-score = 2.027), ARNT (z-score = 2.156), and MAPK9 (z-score = 3.020) (**Fig. 13B**) (J. K. Yoo et al. 2002; Neelam, Brooks, and Cammarata 2013; Maundrell et al. 1997). Altogether, the enrichment of factors associated with the functional outputs reinforces the identification of the cluster as LPCs as well as identifying possible mechanistic contributors for the maintenance of these progenitor cells. In particular, our analysis prioritized multiple factors, including Yap1, Bcl-2, p38 MAP Kinase (p38 MapK), Smoothened (Smo), Notch Receptor 1 (Notch1), and negative control Nuclear Factor Kappa Beta (Nf-kB) (**Table 7**). Preliminary testing of these candidate factors narrowed our investigation down to Yap1, Bcl-2, p38 MAP Kinase, and Nf-kB (data not shown). Although these factors have been investigated in some capacity in prostate cancer, their testing in the context of normal prostate regeneration has been limited or nonexistent depending on the factor (Peng and Joyner 2015; Kwon et al. 2014; Kelly and Strasser 2011; Salem and Hansen 2019). We therefore investigated the necessity of the aforementioned factors to the LPC regenerative phenotype.

Treatment with Small Molecule Inhibitors Targeting Candidate Factors Leads to an Ablation of Normal Mouse Prostate Regeneration *In Vitro*

In an effort to both validate our Ingenuity Pathway Analysis and to identify possible avenues for ablating the prostate's regenerative phenotype, we began testing small molecule inhibitors targeting factors of interest using *in vitro* organoid culture.

A.

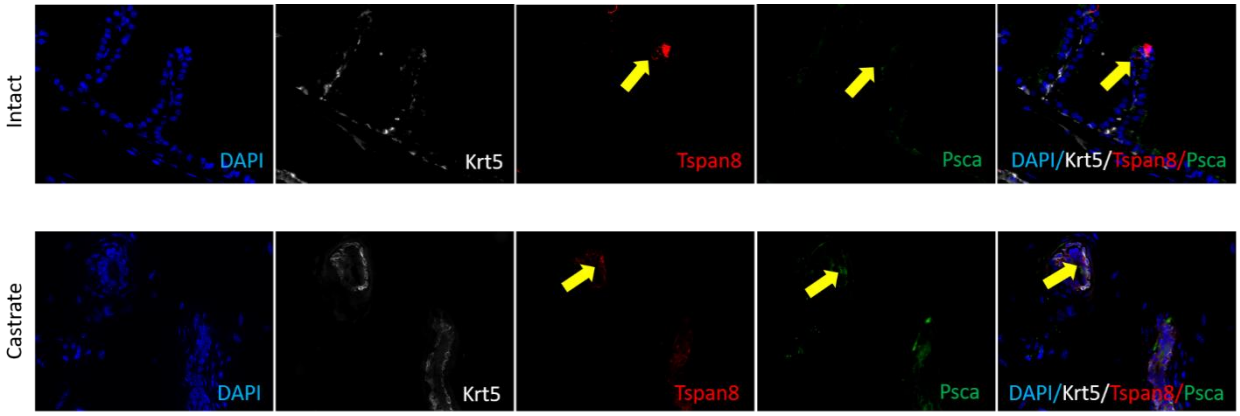

B.

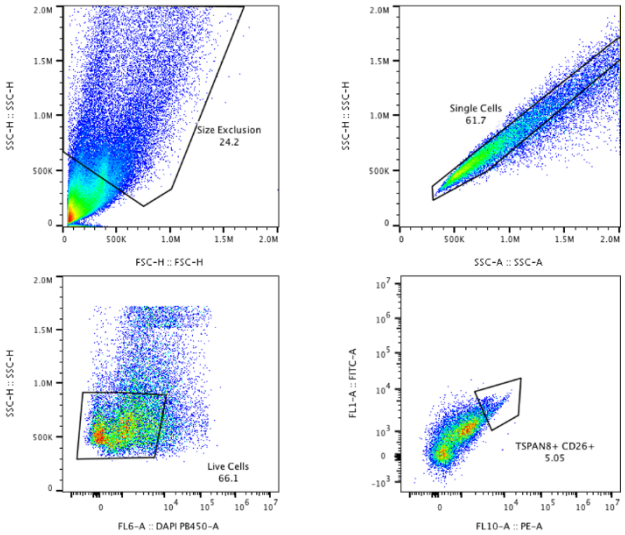

Gate	%Parent	%Total
Size Exclusion	24.20%	24.20%
Single Cells	61.70%	14.90%
Live Cells	66.10%	9.95%
Tspan8+/CD26+	5.05%	0.5%

Fig. 12: Immunofluorescence and Flow Cytometry Validation of LPC Biomarker Expression. A. Immunofluorescence data including luminal cells expressing both Tspan8 and Psca (Arrows). B. Flow Cytometry data marking cells expressing both CD26 and Tspan8 (lower right panel). $CD26^{+}/Tspan8^{+}$ cells constituted 5.05% of live cells according to this analysis.

Mouse organoids were plated at one thousand cells per well in the presence of drug and allowed to grow for 72hrs before being imaged and counted. Treatment with CA3, a small molecule inhibitor targeting Yap1, led to a significant reduction of the regenerative phenotype as evidenced by a reduced percentage of colony-forming units in the CA3-treated condition (p-values = 0.02, 0.004, 0.02) (**Fig. 14A**) (Song et al. 2018). These data implicate the Hippo signaling pathway in the regenerative phenotype of mouse progenitor cells *in vitro*. Inhibition of Bcl-2 using Venetoclax also produced a robust loss of regeneration phenotype (p-values = 0.0004, 0.002, 0.00005) (**Fig. 14B**). This reduction in regenerative phenotype was mirrored in organoids treated with SB203580, an inhibitor of p38 MAPK, an upstream regulator of Bcl-2 (p-values = 0.03, 0.005, 0.0008) (De Chiara et al. 2006) (**Fig 14C**). However, treatment with SC75741, an inhibitor targeting Nf-KB, did not produce a significant reduction in the regenerative phenotype of prostate cells cultured as organoids (**Fig. 14D**). It is important to note that Nf-kB was predicted to be downregulated in Ingenuity Pathway Analysis (**Table 7**). Due to the combination of predicted downregulation by Ingenuity Pathway Analysis as well as Nf-kB's established role in the literature as a canonical activator of Bcl-2 expression, we selected Nf-kB as a negative control for our approach (Catz and Johnson 2001). The lack of regenerative phenotype upon treatment with SC75741 provides evidence that our candidate selection approach was accurate in its predictions of factor activity and could choose both likely and unlikely candidate factors.

A.

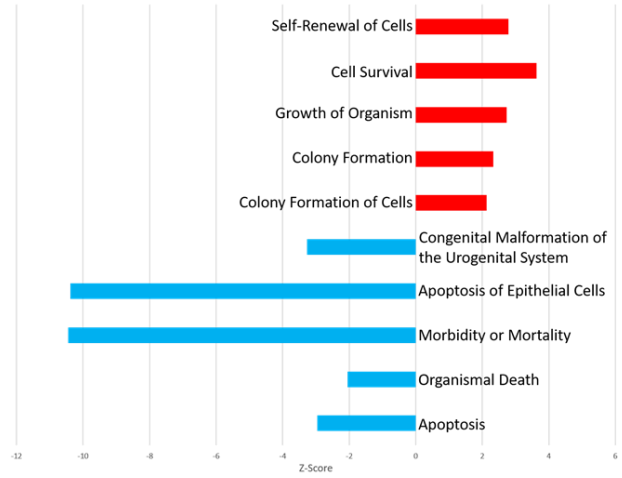

B.

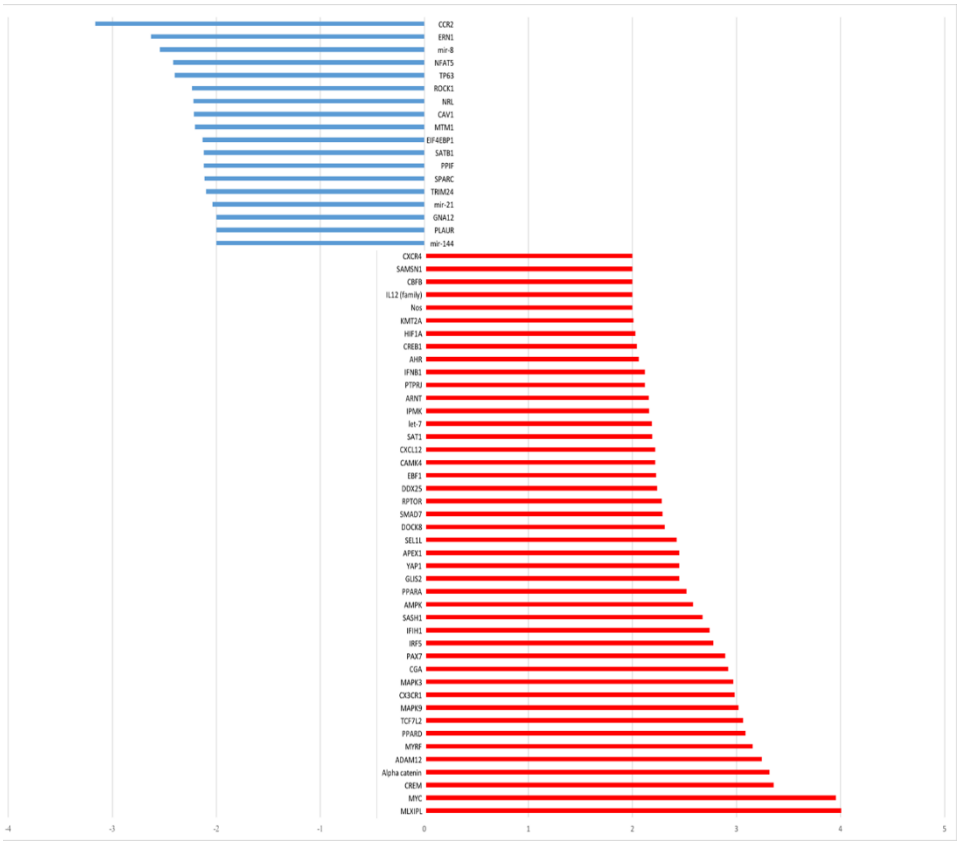

Fig. 13: Pathway Analysis of LPC Expression Profile. A. Top 5 activated and top 5 deactivated diseases and functions according to Z-score generated by IPA Analysis, providing evidence of an enrichment of genes in the LPC expression pattern related to cell survival and urogenital development. B. Upstream Regulator Analysis results relating factors predicted to have an effect in LPCs. Factors of interest in Upstream Analysis include the transcription factor Yap1 and upstream regulators of Bcl-2 including IL12, HIF1A, ARNT, and MAPK9.

Small Molecule Inhibition of Candidate Factors also Ablates Human Prostate Regeneration *In Vitro*

Finally, we wanted to investigate whether these drug treatments also ablated the progenitor cell regeneration phenotype using human model systems. Cells from benign regions of human prostatectomy samples were dissociated and subsequently cultured as organoids using a similar protocol to the one used in McCray et al. 2019 (McCray, Richards, et al. 2019). These organoids were then treated with venetoclax, SB203580, SC75741, or CA3 to test the efficacy of these inhibitors in ablating human progenitor cell regeneration *in vitro*. Treatment with either CA3 (p-value = 2.3e-8) or venetoclax (p-value = 5.8e-5) produced an ablation of the regenerative phenotype *in vitro* similar to the one observed in mouse organoids (**Fig. 15B**). Treatment with negative control SC75741 did not produce significant change in the regenerative phenotype similar to the response observed in the mouse organoid condition. Interestingly, treatment with SB203580 did not produce a significant change in the regenerative phenotype of human cells *in vitro* (**Fig. 15B**). This may be due to a differential requirement for p38 MapK in the human context, or possibly due to a differential dosing requirement in the human organoid culture conditions. This differential response between species requires further experimentation to be fully understood. The reduction in regenerative phenotype was also mirrored in the measurement of average organoid area, providing evidence that the proliferative activity of surviving progenitor cells was also reduced in the presence of CA3 (p-value = 4.8e-5) and Venetoclax (p-value = 5.8e-5) in human organoids (**Fig. 15C**).

Table 7

Candidate Factors Generated from Pathway Analysis and Inhibitors Targeting Them

Factor Name	IPA-Predicted Direction	Drug	Preliminary Testing Result
Yap1	Up	CA3	Reduced Regeneration
Bcl-2	Up	Venetoclax	Reduced Regeneration
p38 MapK	Up	SB203580	Reduced Regeneration
Nf-kB	Down	SC75741	No Change
CTNNB1	Up	XAV-939	Reduced Regeneration
Notch1	Up	FLI-06	Reduced Regeneration
Smo	Up	Vismodegib	No Change

DISCUSSION

This study's approach to the use of scRNA-Seq analysis to identify possible mechanistic contributors to the luminal progenitor cell phenotype has yielded promising results. Firstly, we were able to identify LPCs in both the intact and castrate hormone conditions as expressing the following biomarkers; Krt8, Krt18, Psca, Trop2, Sox2, and Tspan8. LPCs were clearly enriched in the castrate condition according to scRNA-Seq analysis, adding more evidence in support of their possible progenitor cell phenotype. Additionally, our scRNA-Seq analysis identified luminal diversity in the castrate conditions that seems to imply the appearance of intermediate cell populations not observed in the intact condition. Another unique luminal population was found to express Nkx3.1 while not expressing other putative progenitor cell markers, providing evidence that Nkx3.1 marks a population separate from the luminal progenitor population it was originally used to characterize. Our method of leveraging gene lists generated by Seurat for candidate factors necessary for the LPC phenotype was successful, implicating Bcl-2 regulation of apoptosis and the Yap1/Hippo signaling axis in the LPC phenotype. Additionally, further investigation of candidate factors upstream of Bcl-2 implies that the activation state of Bcl-2 is more important than active transcription of the factor. The necessity of both Bcl-2 and Yap1 to *in vitro* regeneration phenotypes were validated in human-derived organoids as well, yielding evidence that the effect of these factors upon prostate regeneration phenotypes is robust across different species and culture conditions.

Although these data are promising, it is important to note that the inhibitors used only test a single factor at a time. This can cause difficulty when trying to emphatically

conclude about the interrelatedness of factors, even factors whose interactions have been clearly and canonically validated in other contexts. Additionally, organoid culture is an *in vitro* facsimile of regeneration, and not the same as the physiological phenomenon. Although the interplay of specific cell signals and interactions is impossible to mimic *in vitro* with perfect fidelity, the organoid context provides a way of inducing and measuring a regenerative response *in vitro*. Additionally, the organoid "tissue" produced in this context exhibits similar epithelial organization to prostate epithelial glands and can undergo a involution in response to the removal of androgen similar to the one observed in the physiological prostate *in vivo* (Drost et al. 2016; Karthaus et al. 2014).

Our scRNA-Seq analysis is also in accordance with recently published scRNA-Seq analyses from other research groups. Crowell et al. observed an increase in the number of luminal progenitor cells in the aging mouse prostate. The genetic markers used in their analysis to denote luminal progenitors have significant overlap with the markers we used, including Trop2, PSCA, and Krt6a (Crowell, Fox, et al. 2019). Although Tspan8 was not described as a genetic marker of prostate luminal progenitors in their study, this may be due to differences in analysis parameters like changes in clustering granularity or number of PCs used in dimensional reduction analysis. Additionally, this study reported an expansion in the number of PSCA+ luminal progenitors in the aging mouse prostate, mirroring our own observation of expansion of the luminal progenitor population in the castrate prostate (Crowell, Fox, et al. 2019). Both of these hormonal contexts are divergent from the hormone-normal environment of the healthy young mouse prostate and are marked by a decrease of androgen signaling

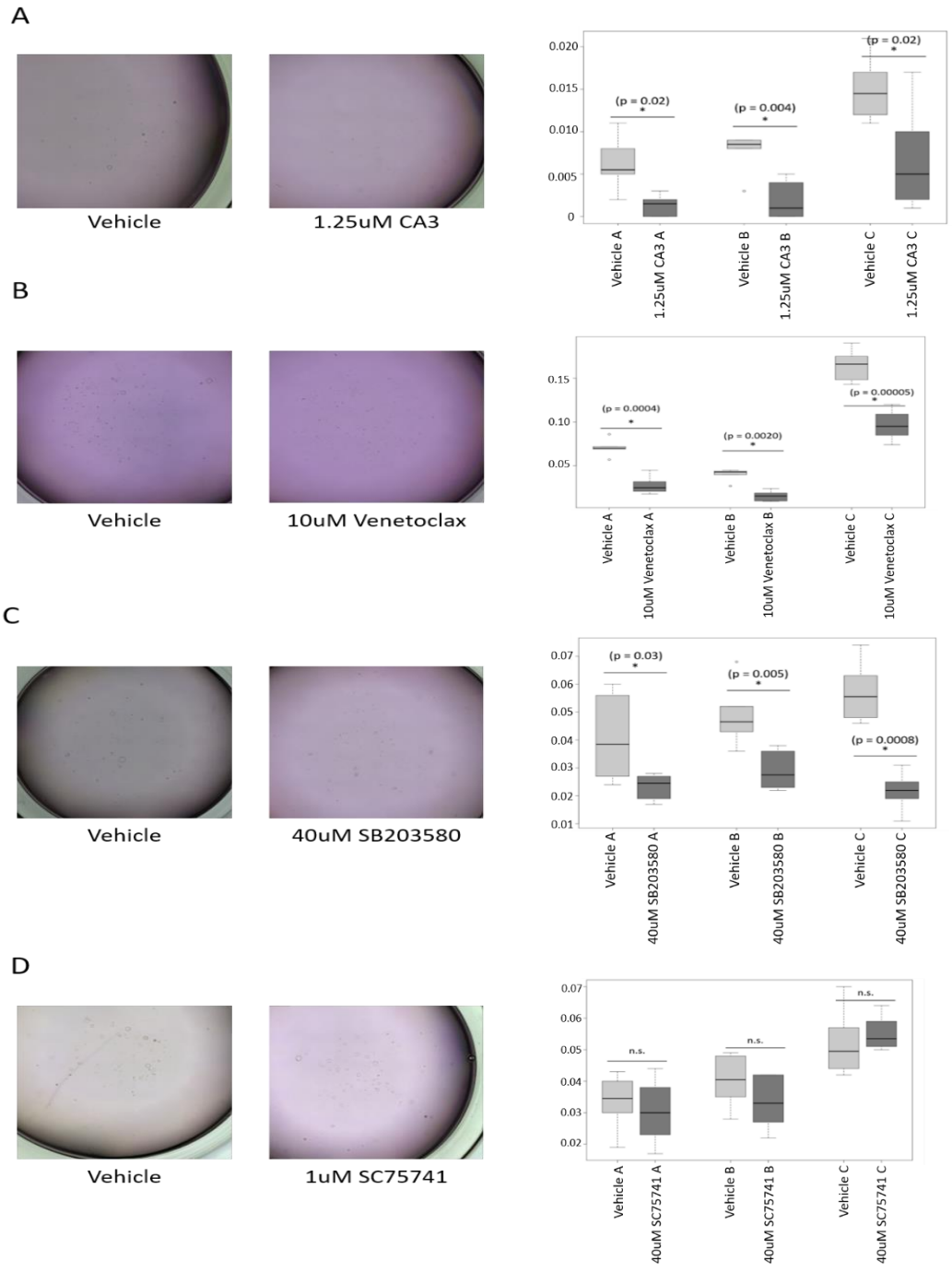

Fig. 14: Inhibition of Candidate Factors Leads to the Inhibition of Normal Mouse Prostate Regeneration *In Vitro*. Representative images and quantitation of results for colony forming assays in organoids treated with CA3 targeting Yap1 (A), venetoclax targeting Bcl-2 (B), SB203580 targeting p38 MapK (C), and SC75741 targeting Nf-kB (D). Treatment with CA3, venetoclax, or SB203580 yielded a significant reduction in % colony forming units in mouse organoids, while treatment with SC75741 did not.

(T. T. Liu et al. 2019; Nicholson and Ricke 2011). Karthaus et al. also observed luminal progenitors in their scRNA-Seq analysis of mouse prostate samples, reporting similar markers to our analysis and that of Crowell et al. including Krt8, Psca, and Trop2 (Karthaus et al. 2020; Crowell, Fox, et al. 2019). Additionally, Karthaus et al. were able to acquire samples from multiple timepoints during prostate involution post-castration and prostate regeneration after the reintroduction of androgen. These data pointed towards an adaptation of stem-like gene expression phenotypes by the luminal cells surviving castration, regardless of their identity before castration (Karthaus et al. 2020). This conclusion from Karthaus et al. provides an explanation for our own observations, as we identified a population of luminal cells expressing Trop2 that was exclusive to the castrate condition. The upregulation of prostate progenitor cell programs in formerly differentiated luminal cells could help explain the appearance of the Intermediate Luminal Cell population in the absence of androgen signaling. Karthaus et al. were also able to increase the organoid-forming potential of cells isolated from mouse prostates through the addition of FGF-10, ERG, and NRG to the culture media (Karthaus et al. 2020). This approach is similar to the one we pursued in our downstream analysis, although we looked to ablate the regeneration of cells *in vitro* with our additions to the organoid media while Karthaus et al. sought to accentuate it. There is some evidence for overlap between the specific factors targeted in this paper and those targeted by Karthaus et al. Fgf signaling has been observed to induce a pro-survival effect in target cells, and can directly upregulate the expression of Bcl family member proteins including Bcl-2 in certain contexts (Agas et al. 2008; Ornitz and Itoh 2015). Additionally, certain modalities of Yap1 activity can lead to increased expression of Fgf ligands

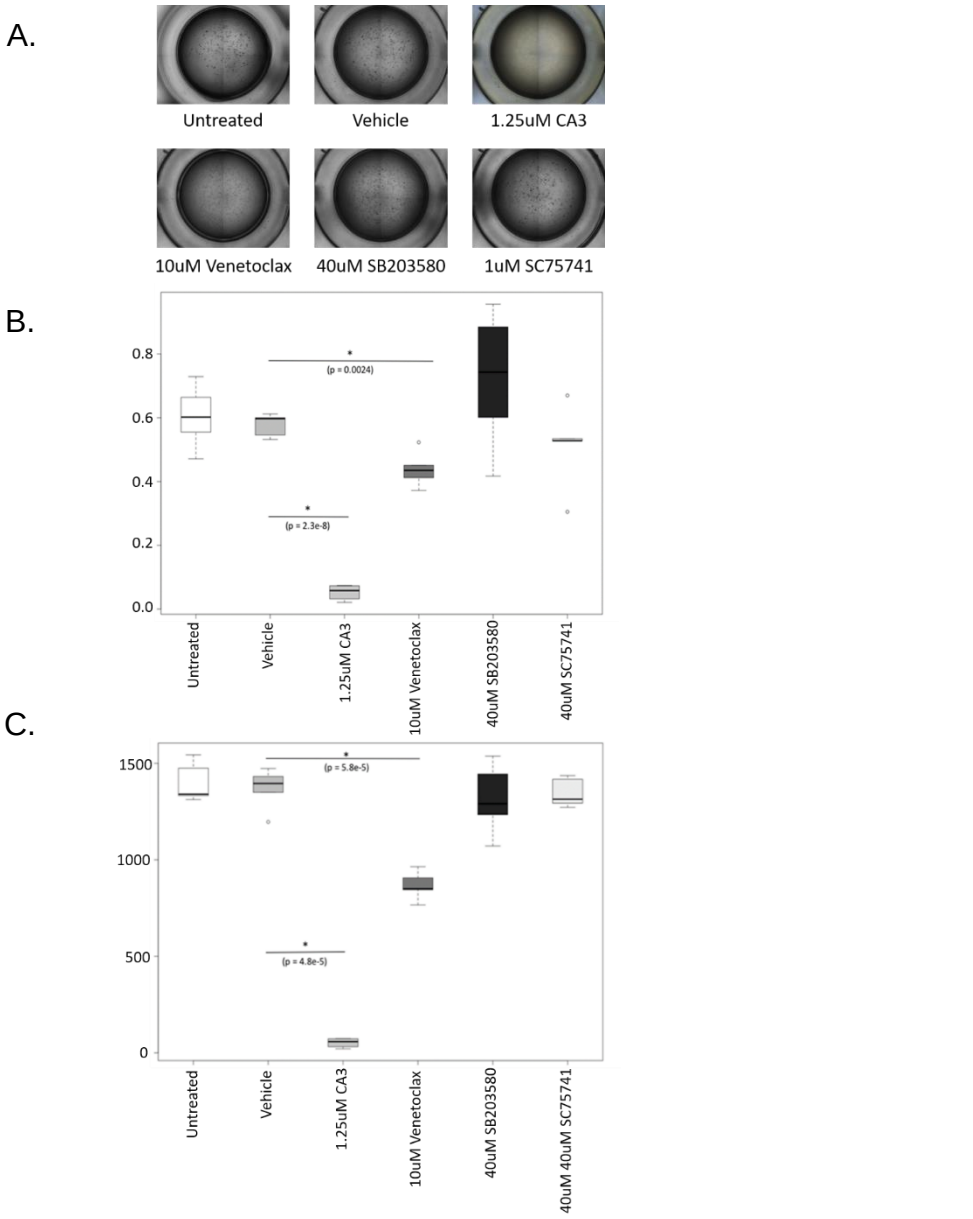

Fig. 15: Inhibition of Successful Factors from Mouse Organoid Assays Leads to Successful Ablation of Human Prostate Regeneration *In vitro*. A. Representative images depicting wells treated with drugs at the specified doses. B. Colony-forming assay data comparing the regenerative phenotype of drug-treated samples to untreated and vehicle-treated controls. Treatment with CA3 targeting Yap1 and venetoclax targeting Bcl-2 yielded a significant reduction in % colony forming units in human-derived organoids relative to the vehicle-treated condition. C. Measurements of average organoid area (in pixels), providing an orthogonal measurement of regenerative response in drug-treated and control conditions. CA3 and venetoclax treatment produced a significant reduction in average organoid area.

(Zhao et al. 2007). Altogether, these data imply that our investigation and the investigation employed by Karthaus et al. could be probing pieces of the same larger network of factors regulating the survival and regeneration phenotypes of prostate epithelial cells. Further investigation is required to understand the full breadth of involved factors and to identify specific contributors that are uniquely necessary for the prostate progenitor phenotype.

Another successful scRNA-Seq investigation of the mouse prostate epithelium was undertaken by Joseph et al. This investigation probed specific locations in the prostate anatomy for a luminal progenitor signal, finding cells that expressed a similar cadre of biomarkers to the ones outlined in our paper including Trop2, Psca, and Krt9 (Joseph et al. 2020). Joseph et al. successfully identified the location of the luminal progenitor cells as the proximal ducts next to the prostatic urethra. Due to the similarity in biomarker profile between our scRNA-Seq analysis and that of Joseph et al., it stands to reason that the luminal progenitors we identified are localized to the same region of the prostate anatomy.

The drugs we used in our organoid studies have been investigated to varying degrees in the prostate context. As of this writing, CA3 has not been used in preliminary studies to treat prostate disease, although the Hippo pathway is a known contributor to prostate cancer progression and Yap1 contributes to cancer cell growth and invasion *in vitro* (Kuser-Abali et al. 2015; Salem and Hansen 2019). Additionally, treatment of TRAMP cancer model mice with verteporfin, a different Yap1 inhibitor, led to a significant reduction in cancer recurrence (Jiang et al. 2017). Overall, verteporfin is a more commonly used inhibitor of Yap1, but CA3 was employed in our study due to its

higher specificity in targeting Yap1 (Song et al. 2018). Verteporfin has a much lower target affinity for Yap1 when compared to CA3, and we chose to use CA3 to avoid the necessity of decoupling the possible undesired off-target effects of Verteporfin from its desired effect on Yap1 (Song et al. 2018). Although research into Yap1's role in prostate cancer has been extensive, little is known about its role in BPH. The identification of Yap1 as a possible necessary factor in the normal prostate regeneration phenotype may potentiate further investigation of Yap1 in the benign disease context.

Modulation of MapK signaling has shown promise as a treatment for PCa, although these pathways have not been investigated as deeply in the context of BPH or normal prostate regeneration. SC203580 has been tested *in vitro* on prostate cancer cells in monolayer culture, yielding a decrease in salinomycin-regulated autophagy in cells treated with LY294002 (K.-Y. Kim et al. 2017). More broadly, p38 MapK signaling has been a subject of interest in the field of prostate disease due to its known dysregulation in prostate cancer as well as data implying possible tumorigenic and tumor suppressor effects of this dysregulation in the prostate cancer context (Koul, Pal, and Koul 2013). As of now, this is the first study to test the effectiveness of SB203580 in ablating normal prostate organoid growth *in vitro*. Similarly, Nf-kB has been a target of interest in the field of prostate disease as well due to its role in interleukin signaling pathways and its observed activation in some prostate cancers (Torrealba et al. 2019; Paule et al. 2007; Nadiminty et al. 2013; Suh and Rabson 2004). SC75741 specifically has not been tested in the context of normal prostate regeneration or prostate disease.

The Bcl-2 axis of apoptosis regulation has been studied extensively in the context of prostate cancer, as this factor has been shown to contribute to the survival of

castration-resistant prostate cancer cells (Kelly and Strasser 2011; J.-H. Kim et al. 2017). Venetoclax has been used as a therapeutic drug for advanced prostate cancer in mouse models and is currently in clinical trials for use in human patients (Suvarna, Singh, and Murahari 2019). Although venetoclax shows promise as a cancer therapeutic, the role of Bcl-2 in BPH and normal prostate regeneration has not been investigated as thoroughly. Overall, the driving public health impetus to treat prostate cancer has led to investigation of factors like Bcl-2, Yap1, and p38 MapK in the cancer context but not in the normal or benign hyperplastic contexts. This has produced a lack of understanding of the contribution of these factors to normal regeneration and benign disease. We hope that these data provided in this study can help advance the study of normal prostate regeneration and spur interest in testing these factors as possible treatment targets in the context of benign disease.

These data raise multiple important questions about their clinical applicability and potential for further investigation of the normal context. First, an important next step in testing the effect of Bcl-2 and Yap1 on normal regeneration is to apply a similar inhibitor-based approach to *in vivo* models of regeneration. This approach could yield data strengthening the association of these factors with regeneration while also providing evidence that the factors can be successfully targeted to ablate normal prostate regeneration in the physiological context. Additionally, the unique luminal diversity of the castrate prostate necessitates further investigation. The biological output of the intermediate luminal population, as well as a deeper understanding of how the more differentiated luminal populations survive in the absence of androgen signaling, could yield important insights into the factors underlying luminal cell survival and their

contribution prostate regeneration. Lastly, the drug testing data here could be leveraged into testing in benign disease models, yielding the validation of possible druggable targets that could provide more permanent or efficacious methods for treating benign prostatic hyperplasia.

CHAPTER IV

DISCUSSION, CONCLUSIONS, AND FUTURE DIRECTIONS

Benign prostate hyperplasia and prostate cancer present a public health issue due to their high rate of occurrence and the fact that they necessitate chronic and expensive treatment (American Cancer Society 2020; Lim 2017; Rawla 2019). Statistically speaking, the average American male will experience some form of either benign or malignant prostate disease in their lifetime (American Cancer Society 2020; Lim 2017). Additionally, many aggressive forms of prostate disease exist that can either cause a significant reduction in quality of life or, in some cases, become refractory to treatment and directly threaten the life of the patient (Teo, Rathkopf, and Kantoff 2019; E. H. Kim, Larson, and Andriole 2016). A concrete explanation for the high disease burden of the prostate has eluded the field for decades, but many researchers have found promising results in investigating the link between normal prostate progenitor cell phenotypes and the development of prostate disease (Tokar et al. 2005; G. Wang et al. 2012; Notara and Ahmed 2012). This research is built upon by the theory that the normal regenerative capacity of rare cells in the prostate epithelium, whether it is cell intrinsic or dependent upon the unique signaling environment of the proximal prostate, is aberrantly activated in diseased prostate epithelial cells due to genetic mutation or disruptions in signaling. Evidence exists for the viability of this theory of prostate disease. There are similarities in phenotype between aggressive forms of prostate cancer and prostate progenitor cells including a slow cycling rate, androgen independence, and lineage plasticity (Chandrasekar et al. 2015; G. Wang et al. 2012). Additionally, experimental increase of estrogen signaling relative to androgen signaling

can induce benign prostate outgrowth in murine models (E. M. McAuley et al. 2017). This finding implies that the modulation of prostate progenitor cell activity through hormone signaling can be achieved outside the normal androgen cycling model and can be caused by the shift in hormone signaling common in aging men that suffer from BPH (Aaron, Franco, and Hayward 2016). Indeed, the aging mouse and human prostates both exhibit an enrichment of prostate epithelial progenitor cells that correlates with the age-induced increase in estrogen signaling in males (Crowell, Fox, et al. 2019). To this end, the investigation of prostate progenitor cells and their mechanistic underpinnings would aid in understanding both benign and malignant prostate disease. This would allow researchers to identify new druggable targets, allowing for the development of new and more efficacious treatments for prostate diseases that have previously been refractory to treatment.

The research presented in this thesis provides insight into the behavior of normal prostate progenitor cells both *in vitro* and *in vivo*. Our investigation of human prostate-derived monolayer and organoid cells using scRNA-Seq analysis yielded data pointing to the persistence of prostate progenitor cells marked by KRT13 in these culture conditions. Additionally, intermediate populations in various states of differentiation were observed using this same method, although these populations were largely exclusive to the organoid condition. The integration of organoid and monolayer datasets with publicly available scRNA-Seq data of healthy human prostate revealed the population differences between *in vitro* and *in vivo* cell types, including the observation of proliferating epithelial populations *in vitro* that are largely not present in the *in vivo* condition. Altogether, these data provide evidence that the organoid culture

environment preserves the prostate progenitor cell populations as well as recapitulating some of their axis of differentiation. Although this facet of organoid culture is advantageous, it does also clearly enrich for behaviors that are non-physiological, including the induction of proliferation that is largely not observed in the *in vivo* context according to our own scRNA-Seq analysis of human prostate samples (McCray, Moline, et al. 2019; Henry et al. 2018). These data not only provide a clearer understanding of the nature of the enrichment of prostate epithelial progenitor cells in the organoid condition, they also provide a tangible output for our scRNA-Seq analysis workflow. The identification of rare intermediate and progenitor cell populations *in vitro*, along with an accompanying orthogonal validation using immunofluorescence microscopy, serves as a proof of concept for the *in vivo* scRNA-Seq investigation presented in this thesis. Additionally, the samples used in our scRNA-Seq analysis of primary prostate epithelial cells were derived from prostatectomy samples. Although these samples were carefully taken from benign regions of the tissue sample, it is important to note that they were derived from a diseased organ. Due to the difficulty in acquiring healthy samples facing the prostate research field, this practice of deriving samples from prostatectomy tissue is common. However common this approach may be, it is important to note that the tissue used in this analysis cannot definitively be described as normal. This may have contributed to a limited degree to the differences observed between the *in vitro* and *in vivo* scRNA-Seq datasets reported in Fig. 8.

Subsequent investigation of the normal prostate yielded further data describing prostate epithelial progenitor cells. First, we were able to establish a biomarker profile for a candidate LPC population. This profile included Krt8, Krt18, Psca, Trop2, Sox2,

and Tspan8. These markers can allow for further experimentation with the luminal progenitor population using secondary methods like flow cytometry. This path is possibly facilitated by the discovery of the expression of cell surface marker Tspan8 in this population. Next, we were able to distill the list of factors generated by our analysis that were uniquely expressed by the LPC population into a list of candidate factors that were expected to be involved in the regenerative phenotype of the LPC population. These candidates included developmental factors like Shh and Yap1 as well as factors involved in cell survival like Bcl-2, p38 MapK, and negative control Nf-kB. Inhibition of these factors yielded promising results, implicating Bcl-2 and Yap1 as necessary factors for the regenerative phenotype of prostate cells *in vitro* in both mouse and human-derived samples. These results outline a group of new druggable targets which could also be leveraged in the future to treat benign prostate disease, but also provides a clear methodological framework for how researchers can use scRNA-Seq approaches to find and test candidate factors necessary for prostate regeneration or contributors to prostate disease. These approaches could allow researchers to identify the rare progenitor-like populations within normal and diseased prostate tissue, and then use the expression profiles generated for these populations to target and treat specific cell populations that may escape treatment normally.

Although these studies have yielded significant results, it is important to state the limitations of our approach. For example, although our identification of prostate progenitor populations in the organoid context in Chapter 2 was validated secondarily using IF microscopy, it is important to state that validation of the quantitative measurement of the number of progenitor cells present in the organoid context requires

an additional secondary method like flow cytometry. This is due to the technically small number of cells that are run in a 10x Genomics workflow, which is usually only slightly higher than the number of cells that are captured and present in the subsequent data analysis. The low number of cells used in scRNA-Seq presents a difficulty in commenting definitively about the quantity of a cell type, especially rare cells, without access to multiple biological replicates or secondary methods of validation.

Although the data attained from our tests of small molecule inhibitors in the organoid context has provided promising results, it is important to state that this methodology is not an exact recapitulation of the physiological context. More specifically, organoid culture conditions do not exactly replicate the physiological signaling environment. For example, FGF is known to be involved in prostate development and regeneration and it is not included the murine and human organoid protocols employed in this thesis (Drost et al. 2016; McCray, Richards, et al. 2019; Kato et al. 2013). The absence of signaling factors, as well as the possible combinatorial interactions of these absent factors with other factors already present in the organoid condition, is a clear source of divergence from the physiological context. Additionally, although organoids exhibit some of the behaviors of the *in vivo* prostate epithelium, the pharmacology of organoids is considerably different than the *in vivo* condition. Organoids are not vascularized, and the treatment of *in vitro* models like organoids with drugs is typically more efficacious and uniform than treating the full organism (Drost and Clevers 2018). Pursuit of *in vivo* validation of the treatment results observed *in vitro* would ameliorate some of the issues presented here, allowing us to make a conclusive

statement about the validity of Bcl-2 and Yap1 as druggable targets necessary for normal prostate regeneration.

The data acquired from the investigations presented in this thesis present numerous interesting avenues for further investigation. Among the questions facing the field of prostate research is the species differences between the human prostate and the murine prostate used as a model system. Although there are visually apparent differences between the human and mouse prostate in both morphology and histology, there are other differences between these species contexts that are of note (Toivanen and Shen 2017). For example, luminal progenitors have yet to be definitively observed in the normal human prostate *in vivo*, and luminal cells that exhibit progenitor-like characteristics are solely observable in the diseased state (Moad et al. 2017; Li and Shen 2019). The normal mouse prostate, on the other hand, has observable luminal progenitor populations *in vivo*. A clear difference between the two tissues is also the observation of proliferating epithelial cells in the mouse prostate that are largely absent from the human prostate condition. Interestingly, the mouse prostate also spontaneously develops prostate disease at a much lower rate than the human prostate, so much so that mouse models of PCa and BPH must be artificially induced using genetic engineering or hormone modulation respectively (Valkenburg and Williams 2011; E. M. McAuley et al. 2017). The presence of proliferating cells has multiple competing explanations, but the most interesting is the possibility that the mouse prostate experiences significantly more tissue turnover than the human prostate. This could provide a possible explanation for the lower rate of prostate disease in the murine prostate, as anoikis resistance and general lack of response to tissue turnover

signals correlate with a higher rate of disease and more aggressive disease subtypes. It is possible to genetically engineer mice with a prostate epithelium less capable of tissue turnover in the luminal compartment, as this has been performed using a genetic construct expressing the Notch intracellular domain downstream of the probasin promoter (Kwon et al. 2014). This led to a loss of normal tissue turnover in the luminal compartment of the prostate epithelium, and a slight overgrowth of the epithelium over the short period of time in which the animals were observed (Kwon et al. 2014). This model could be leveraged even further to investigate if the reduction in tissue turnover rate in the prostate delivers a possible oncogenic effect in the mouse context. This could help answer the question of whether the higher rate of tissue turnover observed in the intact mouse prostate scRNA-Seq data presented in this thesis could possibly explain the lower rate of prostate disease in the model system.

Another possible avenue of interest is the unique luminal cell diversity present in the castrate mouse prostate. This diversity was observed in our scRNA-Seq dataset, specifically in the presence of four unique populations in that condition, identified as LPCs, Intermediate Luminal Cells, Nkx3.1^{Hi} Luminal Cells, and Differentiated Luminal Cells. These data imply a rough path towards differentiation in the luminal compartment of the prostate, starting with LPCs, proceeding to Intermediate Luminal Cells and Nkx3.1^{Hi} Luminal Cells, and ending with Differentiated Luminal Cells. This differentiation axis is largely based on conjecture informed by literature, placing the population expressing the most putative progenitor markers at the least differentiated position, and the population expressing the least progenitor markers at the most differentiated position. Experimental validation of this differentiation axis is necessary to truly

conclude upon its existence, and this could be pursued using scRNA-Seq investigation *in vitro*. Gathering samples over multiple days after the plating of single prostate epithelial cells will allow for a rough quantification of prostate epithelial cell populations during the organoid outgrowth process. By flow sorting LPCs using the markers outlined in this thesis, the initial plating of cells can be highly enriched with LPCs and allow for the tracking of their daughter populations over time in a context that directly induces progenitor cell activity. An accompanying single cell ATAC-Seq solution could also be pursued, allowing for a quantification of changes in the epigenetic landscape of cells over time to accompany the single cell expression data. This can produce a clear picture of how luminal cells differentiate in a controlled condition over time. The conclusions provided by this type of research could be advantageous to the study of prostate disease as they could provide an idea of what factors contribute significantly to the discrete steps in the luminal differentiation process, allowing for the downstream manipulation of those factors to combat prostate cancers that are poorly differentiated.

A final possible future direction prompted by our scRNA-Seq of mouse prostate is looking for a greater understanding of the persisting Differentiated Luminal Cells in the castrate prostate. These cells were observed at a much lower rate in the castrate prostate, but it is important to note that their presence in the absence of androgen signaling implies at least a temporary androgen independence exhibited by these cells in the castrate condition. Expression profiles of differentiated luminal cells in the castrate and intact conditions could be compared to yield a list of factors uniquely expressed by Differentiated Luminal Cells in the castrate condition. These factors could then be distilled down to likely candidate factors contributing to luminal cell survival

using a pathway analysis approach similar to the one employed in Chapter 3 to investigate the LPC population. The resulting list of factors could then be tested for their role in luminal cell survival in the absence of androgen signaling using *in vitro* organoid culture and *in vivo* hormone dependent regeneration models. Conclusions from this investigation could yield significant insight into the pathways and factors underlying androgen independence, which is a key contributor to aggressiveness and treatment resistance in prostate diseases like CRPC.

Altogether, these planned avenues for future investigation will yield significant insight into the mechanistic underpinnings of the prostate progenitor cell phenotype. A deeper understanding of the factors necessary for the prostate progenitor phenotype, specifically in the realms of survival and tissue regeneration, could provide promising druggable targets for the treatment of benign and malignant prostate diseases. BPH presents a unique obstacle for researchers as the underlying causes for the disease are still not known, and factors necessary for the aberrant phenotype of benign prostate overgrowth remain under-studied. The discovery of druggable targets in the normal progenitor cell context can aid in the effort to treat BPH, as it would allow for the discovery of cell-intrinsic factors necessary for the progenitor cell regeneration phenotype that shares multiple similarities with the overgrowth phenotype observed in BPH. PCa provides a different challenge to researchers, as the heterogeneous nature of the disease allows for the numerous subtypes of PCa to escape generalized treatment methods. Adding to the overall catalog of necessary factors in the normal progenitor cell context can provide more druggable targets for the treatment of PCa. Additionally, a greater understanding of the heterogeneity within the normal adult

progenitor cell populations and the downstream intermediate populations can provide a basis for understanding PCa cases that exhibit varying levels of differentiation as well.

REFERENCES

Aaron, LaTayia, Omar Franco, and Simon W. Hayward. 2016. “Review of Prostate Anatomy and Embryology and the Etiology of BPH.” *The Urologic Clinics of North America* 43 (3): 279–88. https://doi.org/10.1016/j.ucl.2016.04.012.

Adamo, P., and M. R. Ladomery. 2016. “The Oncogene ERG: A Key Factor in Prostate Cancer.” *Oncogene* 35 (4): 403–14. https://doi.org/10.1038/onc.2015.109.

Agas, Dimitrios, Luigi Marchetti, Giovanna Menghi, Stefano Materazzi, Giovanni Materazzi, Mariolina Capacchietti, Marja M. Hurley, and Maria Giovanna Sabbieti. 2008. “Anti-Apoptotic Bcl-2 Enhancing Requires FGF-2/FGF Receptor 1 Binding in Mouse Osteoblasts.” *Journal of Cellular Physiology* 214 (1): 145–52. https://doi.org/10.1002/jcp.21170.

American Cancer Society. 2020. “Cancer Facts & Figures 2020.” *American Cancer Society*.

Barros-Silva, João D., Douglas E. Linn, Ivana Steiner, Guoji Guo, Adnan Ali, Hubert Pakula, Garry Ashton, et al. 2018. “Single-Cell Analysis Identifies LY6D as a Marker Linking Castration-Resistant Prostate Luminal Cells to Prostate Progenitors and Cancer.” *Cell Reports* 25 (12): 3504-3518.e6. https://doi.org/10.1016/j.celrep.2018.11.069.

Beltran, Himisha, Andrew Hruszkewycz, Howard I. Scher, Jeffrey Hildesheim, Jennifer Isaacs, Evan Y. Yu, Kathleen Kelly, et al. 2019. “The Role of Lineage Plasticity in Prostate Cancer Therapy Resistance.” *Clinical Cancer Research: An Official Journal of the American Association for Cancer Research* 25 (23): 6916–24. https://doi.org/10.1158/1078-0432.CCR-19-1423.

Birdsey, Graeme M., Aarti V. Shah, Neil Dufton, Louise E. Reynolds, Lourdes Osuna Almagro, Youwen Yang, Irene M. Aspalter, et al. 2015. “The Endothelial Transcription Factor ERG Promotes Vascular Stability and Growth through Wnt/β-Catenin Signaling.” *Developmental Cell* 32 (1): 82–96. https://doi.org/10.1016/j.devcel.2014.11.016.

Black, Libby, Michael James Naslund, Thomas D. Gilbert, E. Anne Davis, and Daniel A. Ollendorf. 2006. “An Examination of Treatment Patterns and Costs of Care among Patients with Benign Prostatic Hyperplasia.” *The American Journal of Managed Care* 12 (4 Suppl): S99–110.

Bühler, Patrick, Philipp Wolf, Arndt Katzenwadel, Wolfgang Schultze-Seemann, Ulrich Wetterauer, Nikolaus Freudenberg, and Ursula Elsässer-Beile. 2010. “Primary Prostate Cancer Cultures Are Models for Androgen-Independent Transit Amplifying Cells.” *Oncology Reports* 23 (2): 465–70.

Burger, Patricia E., Xiaozhong Xiong, Sandra Coetzee, Sarah N. Salm, David Moscatelli, Ken Goto, and E. Lynette Wilson. 2005. “Sca-1 Expression Identifies Stem Cells in the Proximal Region of Prostatic Ducts with High Capacity to Reconstitute Prostatic Tissue.” *Proceedings of the National Academy of Sciences of the United States of America* 102 (20): 7180–85. https://doi.org/10.1073/pnas.0502761102.

Butler, Andrew, Paul Hoffman, Peter Smibert, Efthymia Papalexi, and Rahul Satija. 2018. “Integrating Single-Cell Transcriptomic Data across Different Conditions, Technologies, and Species.” *Nature Biotechnology* 36 (5): 411–20. https://doi.org/10.1038/nbt.4096.

Castillo-Martin, Mireia, Josep Domingo-Domenech, Orit Karni-Schmidt, Tulio Matos, and Carlos Cordon-Cardo. 2010. “Molecular Pathways of Urothelial Development and Bladder Tumorigenesis.” *Urologic Oncology: Seminars and Original Investigations*, The International Bladder Cancer Network - Current Perspectives in Bladder Cancer, 28 (4): 401–8. https://doi.org/10.1016/j.urolonc.2009.04.019.

Catz, Sergio D, and Jennifer L Johnson. 2001. “Transcriptional Regulation of Bcl-2 by Nuclear Factor KB and Its Signifcance in Prostate Cancer.” *Oncotarget* 20 (November): 7342–51.

Chandrasekar, Thenappan, Joy C. Yang, Allen C. Gao, and Christopher P. Evans. 2015. “Mechanisms of Resistance in Castration-Resistant Prostate Cancer (CRPC).” *Translational Andrology and Urology* 4 (3): 365–80. https://doi.org/10.3978/j.issn.2223-4683.2015.05.02.

Choi, Nahyun, Boyu Zhang, Li Zhang, Michael Ittmann, and Li Xin. 2012. “Adult Murine Prostate Basal and Luminal Cells Are Self-Sustained Lineages That Can Both Serve as Targets for Prostate Cancer Initiation.” *Cancer Cell* 21 (2): 253–65. https://doi.org/10.1016/j.ccr.2012.01.005.

Chua, Chee Wai, Maho Shibata, Ming Lei, Roxanne Toivanen, LaMont J. Barlow, Sarah K. Bergren, Ketan K. Badani, et al. 2014. “Single Luminal Epithelial Progenitors Can Generate Prostate Organoids in Culture.” *Nature Cell Biology* 16 (10): 951–61. https://doi.org/10.1038/ncb3047.

Clevers, Hans. 2016. “Modeling Development and Disease with Organoids.” *Cell* 165 (7): 1586–97. https://doi.org/10.1016/j.cell.2016.05.082.

Coelho, Ana L., Matthew A. Schaller, Claudia F. Benjamim, Amos Z. Orlofsky, Cory M. Hogaboam, and Steven L. Kunkel. 2007. “The Chemokine CCL6 Promotes Innate Immunity via Immune Cell Activation and Recruitment.” *The Journal of Immunology* 179 (8): 5474–82. https://doi.org/10.4049/jimmunol.179.8.5474.

Cohen, R. J., G. Glezerson, L. F. Taylor, H. A. Grundle, and J. H. Naudé. 1993. “The Neuroendocrine Cell Population of the Human Prostate Gland.” *The Journal of Urology* 150 (2 Pt 1): 365–68.

Conteduca, Vincenza, Clara Oromendia, Kenneth W. Eng, Rohan Bareja, Michael Sigouros, Ana Molina, Bishoy M. Faltas, et al. 2019. “Clinical Features of Neuroendocrine Prostate Cancer.” *European Journal of Cancer (Oxford, England : 1990)* 121 (November): 7–18. https://doi.org/10.1016/j.ejca.2019.08.011.

Crowell, Preston D., Jonathan J. Fox, Takao Hashimoto, Johnny A. Diaz, Héctor I. Navarro, Gervaise H. Henry, Blake A. Feldmar, et al. 2019. “Expansion of Luminal Progenitor Cells in the Aging Mouse and Human Prostate.” *Cell Reports* 28 (6): 1499-1510.e6. https://doi.org/10.1016/j.celrep.2019.07.007.

Crowell, Preston D., Jenna M. Giafaglione, Takao Hashimoto, Johnny A. Diaz, and Andrew S. Goldstein. 2019. “Evaluating the Differentiation Capacity of Mouse Prostate Epithelial Cells Using Organoid Culture.” *Journal of Visualized Experiments : JoVE*, no. 153 (November). https://doi.org/10.3791/60223.

Crowley, Laura, Francesco Cambuli, Luis Aparicio, Maho Shibata, Brian D Robinson, Shouhong Xuan, Weiping Li, et al. 2020. “A Single-Cell Atlas of the Mouse and Human Prostate Reveals Heterogeneity and Conservation of Epithelial Progenitors.” *ELife* 9 (September). https://doi.org/10.7554/eLife.59465.

Cunha, G. R., A. A. Donjacour, P. S. Cooke, S. Mee, R. M. Bigsby, S. J. Higgins, and Y. Sugimura. 1987. “The Endocrinology and Developmental Biology of the Prostate.” *Endocrine Reviews* 8 (3): 338–62. https://doi.org/10.1210/edrv-8-3-338.

Cunha, G. R., and B. Lung. 1978. “The Possible Influence of Temporal Factors in Androgenic Responsiveness of Urogenital Tissue Recombinants from Wild-Type

and Androgen-Insensitive (Tfm) Mice." *The Journal of Experimental Zoology* 205 (2): 181–93. https://doi.org/10.1002/jez.1402050203.

De Chiara, Giovanna, Maria Elena Marcocci, Maria Torcia, Maria Lucibello, Paolo Rosini, Paolo Bonini, Yukiro Higashimoto, et al. 2006. "Bcl-2 Phosphorylation by P38 MAPK: Identification of Target Sites and Biologic Consequences." *The Journal of Biological Chemistry* 281 (30): 21353–61. https://doi.org/10.1074/jbc.M511052200.

Di Sant'Agnese, P. Anthony. 1998. "Neuroendocrine Cells of the Prostate and Neuroendocrine Differentiation in Prostatic Carcinoma: A Review of Morphologic Aspects." *Urology* 51 (5, Supplement 1): 121–24. https://doi.org/10.1016/S0090-4295(98)00064-8.

Drost, Jarno, and Hans Clevers. 2018. "Organoids in Cancer Research." *Nature Reviews. Cancer* 18 (7): 407–18. https://doi.org/10.1038/s41568-018-0007-6.

Drost, Jarno, Wouter R. Karthaus, Dong Gao, Else Driehuis, Charles L. Sawyers, Yu Chen, and Hans Clevers. 2016. "Organoid Culture Systems for Prostate Epithelial and Cancer Tissue." *Nature Protocols* 11 (2): 347–58. https://doi.org/10.1038/nprot.2016.006.

Escudero-Esparza, Astrid, Wen G. Jiang, and Tracey A. Martin. 2012. "Claudin-5 Participates in the Regulation of Endothelial Cell Motility." *Molecular and Cellular Biochemistry* 362 (1–2): 71–85. https://doi.org/10.1007/s11010-011-1129-2.

Goldstein, Andrew S., Devon A. Lawson, Donghui Cheng, Wenyi Sun, Isla P. Garraway, and Owen N. Witte. 2008. "Trop2 Identifies a Subpopulation of Murine and Human Prostate Basal Cells with Stem Cell Characteristics." *Proceedings of the National Academy of Sciences* 105 (52): 20882–87. https://doi.org/10.1073/pnas.0811411106.

Grignon, David J. 2018. "Prostate Cancer Reporting and Staging: Needle Biopsy and Radical Prostatectomy Specimens." *Modern Pathology* 31 (1): 96–109. https://doi.org/10.1038/modpathol.2017.167.

Guo, Zhiyong, Xi Yang, Feng Sun, Richeng Jiang, Douglas E. Linn, Hege Chen, Hegang Chen, et al. 2009. "A Novel Androgen Receptor Splice Variant Is Up-Regulated during Prostate Cancer Progression and Promotes Androgen Depletion-Resistant Growth." *Cancer Research* 69 (6): 2305–13. https://doi.org/10.1158/0008-5472.CAN-08-3795.

Hara, Takahito, Jin Kouno, Kazuyo Nakamura, Masami Kusaka, and Masuo Yamaoka. 2005. “Possible Role of Adaptive Mutation in Resistance to Antiandrogen in Prostate Cancer Cells.” *The Prostate* 65 (3): 268–75. https://doi.org/10.1002/pros.20282.

Hatzimouratidis, Konstantinos. 2014. “A Review of the Use of Tadalafil in the Treatment of Benign Prostatic Hyperplasia in Men with and without Erectile Dysfunction.” *Therapeutic Advances in Urology* 6 (4): 135–47. https://doi.org/10.1177/1756287214531639.

Henke, Alexander, O. Cathal Grace, George R. Ashley, Grant D. Stewart, Antony C. P. Riddick, Henry Yeun, Marie O’Donnell, Richard A. Anderson, and Axel A. Thomson. 2012. “Stromal Expression of Decorin, Semaphorin6D, SPARC, Sprouty1 and Tsukushi in Developing Prostate and Decreased Levels of Decorin in Prostate Cancer.” *PLOS ONE* 7 (8): e42516. https://doi.org/10.1371/journal.pone.0042516.

Henry, Gervaise H., Alicia Malewska, Diya B. Joseph, Venkat S. Malladi, Jeon Lee, Jose Torrealba, Ryan J. Mauck, et al. 2018. “A Cellular Anatomy of the Normal Adult Human Prostate and Prostatic Urethra.” *Cell Reports* 25 (12): 3530-3542.e5. https://doi.org/10.1016/j.celrep.2018.11.086.

Hu, Wen-Yang, Dan-Ping Hu, Lishi Xie, Ye Li, Shyama Majumdar, Larisa Nonn, Hong Hu, Toshi Shioda, and Gail S. Prins. 2017. “Isolation and Functional Interrogation of Adult Human Prostate Epithelial Stem Cells at Single Cell Resolution.” *Stem Cell Research* 23: 1–12. https://doi.org/10.1016/j.scr.2017.06.009.

Huggins, Charles, and Clarence V. Hodges. 1941. “Studies on Prostatic Cancer. I. The Effect of Castration, of Estrogen and of Androgen Injection on Serum Phosphatases in Metastatic Carcinoma of the Prostate.” *Cancer Research* 1 (4): 293–97.

Ittmann, Michael. 2018. “Anatomy and Histology of the Human and Murine Prostate.” *Cold Spring Harbor Perspectives in Medicine* 8 (5). https://doi.org/10.1101/cshperspect.a030346.

Jayadevappa, Ravishankar, Sumedha Chhatre, Yu-Ning Wong, Marsha N. Wittink, Ratna Cook, Knashawn H. Morales, Neha Vapiwala, et al. 2017. “Comparative Effectiveness of Prostate Cancer Treatments for Patient-Centered Outcomes.” *Medicine* 96 (18). https://doi.org/10.1097/MD.0000000000006790.

Jiang, Ning, Binghu Ke, Kim Hjort-Jensen, Diego Iglesias-Gato, Zhun Wang, Pengcheng Chang, Yang Zhao, et al. 2017. “YAP1 Regulates Prostate Cancer Stem Cell-like Characteristics to Promote Castration Resistant Growth.” *Oncotarget* 8 (70): 115054–67. https://doi.org/10.18632/oncotarget.23014.

Joseph, Diya B., Gervaise H. Henry, Alicia Malewska, Nida S. Iqbal, Hannah M. Ruetten, Anne E. Turco, Lisa L. Abler, et al. 2020. “Urethral Luminal Epithelia Are Castration-Insensitive Cells of the Proximal Prostate.” *The Prostate* 80 (11): 872–84. https://doi.org/10.1002/pros.24020.

Karthaus, Wouter R., Matan Hofree, Danielle Choi, Eliot L. Linton, Mesruh Turkekul, Alborz Bejnood, Brett Carver, et al. 2020. “Regenerative Potential of Prostate Luminal Cells Revealed by Single-Cell Analysis.” *Science* 368 (6490): 497–505. https://doi.org/10.1126/science.aay0267.

Karthaus, Wouter R., Phillip J. Iaquinta, Jarno Drost, Ana Gracanin, Ruben van Boxtel, John Wongvipat, Catherine M. Dowling, et al. 2014. “Identification of Multipotent Luminal Progenitor Cells in Human Prostate Organoid Cultures.” *Cell* 159 (1): 163–75. https://doi.org/10.1016/j.cell.2014.08.017.

Kato, Manabu, Kenichiro Ishii, Yoichi Iwamoto, Takeshi Sasaki, Hideki Kanda, Yasushi Yamada, Kiminobu Arima, Taizo Shiraishi, and Yoshiki Sugimura. 2013. “Activation of FGF2-FGFR Signaling in the Castrated Mouse Prostate Stimulates the Proliferation of Basal Epithelial Cells.” *Biology of Reproduction* 89 (4). https://doi.org/10.1095/biolreprod.112.107516.

Katz, David, Emma Ito, Ken S. Lau, Joseph D. Mocanu, Carlo Bastianutto, Aaron D. Schimmer, and Fei-Fei Liu. 2008. “Increased Efficiency for Performing Colony Formation Assays in 96-Well Plates: Novel Applications to Combination Therapies and High-Throughput Screening.” *BioTechniques* 44 (2S): ix–xiv. https://doi.org/10.2144/000112757.

Keil, Kimberly P., Vatsal Mehta, Lisa L. Abler, Pinak S. Joshi, Christopher T. Schmitz, and Chad M. Vezina. 2012. “Visualization and Quantification of Mouse Prostate Development by in Situ Hybridization.” *Differentiation; Research in Biological Diversity* 84 (3): 232–39. https://doi.org/10.1016/j.diff.2012.07.005.

Kelly, P N, and A Strasser. 2011. “The Role of Bcl-2 and Its pro-Survival Relatives in Tumourigenesis and Cancer Therapy.” *Cell Death and Differentiation* 18 (9): 1414–24. https://doi.org/10.1038/cdd.2011.17.

Kim, Eric H., John A. Brockman, and Gerald L. Andriole. 2018. “The Use of 5-Alpha Reductase Inhibitors in the Treatment of Benign Prostatic Hyperplasia.” *Asian Journal of Urology* 5 (1): 28–32. https://doi.org/10.1016/j.ajur.2017.11.005.

Kim, Eric H., Jeffrey A. Larson, and Gerald L. Andriole. 2016. “Management of Benign Prostatic Hyperplasia.” *Annual Review of Medicine* 67: 137–51. https://doi.org/10.1146/annurev-med-063014-123902.

Kim, Ju-Ha, Hyemin Lee, Eun Ah Shin, Dong Hee Kim, Jhin Baek Choi, and Sung-Hoon Kim. 2017. “Implications of Bcl-2 and Its Interplay with Other Molecules and Signaling Pathways in Prostate Cancer Progression.” *Expert Opinion on Therapeutic Targets* 21 (9): 911–20. https://doi.org/10.1080/14728222.2017.1369044.

Kim, Kwang-Youn, Kwang-Il Park, Sang-Hun Kim, Sun-Nyoung Yu, Sul-Gi Park, Young Woo Kim, Young-Kyo Seo, Jin-Yeul Ma, and Soon-Cheol Ahn. 2017. “Inhibition of Autophagy Promotes Salinomycin-Induced Apoptosis via Reactive Oxygen Species-Mediated PI3K/AKT/MTOR and ERK/P38 MAPK-Dependent Signaling in Human Prostate Cancer Cells.” *International Journal of Molecular Sciences* 18 (5). https://doi.org/10.3390/ijms18051088.

Koul, Hari K., Mintu Pal, and Sweaty Koul. 2013. “Role of P38 MAP Kinase Signal Transduction in Solid Tumors.” *Genes & Cancer* 4 (9–10): 342–59. https://doi.org/10.1177/1947601913507951.

Krämer, Andreas, Jeff Green, Jack Pollard, and Stuart Tugendreich. 2014. “Causal Analysis Approaches in Ingenuity Pathway Analysis.” *Bioinformatics (Oxford, England)* 30 (4): 523–30. https://doi.org/10.1093/bioinformatics/btt703.

Kuser-Abali, Gamze, Ahmet Alptekin, Michael Lewis, Isla P. Garraway, and Bekir Cinar. 2015. “YAP1 and AR Interactions Contribute to the Switch from Androgen-Dependent to Castration-Resistant Growth in Prostate Cancer.” *Nature Communications* 6 (September): 8126. https://doi.org/10.1038/ncomms9126.

Kwast, Th H van der, C Lopes, C Santonja, C-G Pihl, I Neetens, P Martikainen, S Di Lollo, L Bubendorf, and R F Hoedemaeker. 2003. “Guidelines for Processing and Reporting of Prostatic Needle Biopsies.” *Journal of Clinical Pathology* 56 (5): 336–40.

Kwon, Oh-Joon, Joseph Valdez, Li Zhang, Boyu Zhang, Xing Wei, Qingtai Su, Michael M Ittmann, Chad J Creighton, and Li Xin. 2014. “Increased Notch Signaling

Inhibits Anoikis and Stimulates Proliferation of Prostate Luminal Epithelial Cells." *Nature Communications* 5 (July): 4416. https://doi.org/10.1038/ncomms5416.

Kwon, Oh-Joon, Yiqun Zhang, Yumei Li, Xing Wei, Li Zhang, Rui Chen, Chad J. Creighton, and Li Xin. 2019. "Functional Heterogeneity of Mouse Prostate Stromal Cells Revealed by Single-Cell RNA-Seq." *IScience* 13 (March): 328–38. https://doi.org/10.1016/j.isci.2019.02.032.

Lee, Christine H., Oluyemi Akin-Olugbade, and Alexander Kirschenbaum. 2011. "Overview of Prostate Anatomy, Histology, and Pathology." *Endocrinology and Metabolism Clinics of North America*, Hormones and Cancer: Breast and Prostate, 40 (3): 565–75. https://doi.org/10.1016/j.ecl.2011.05.012.

Lee, Suk Hyung, Daniel T. Johnson, Richard Luong, Eun Jeong Yu, Gerald R. Cunha, Roel Nusse, and Zijie Sun. 2015. "Wnt/β-Catenin-Responsive Cells in Prostatic Development and Regeneration." *Stem Cells (Dayton, Ohio)* 33 (11): 3356–67. https://doi.org/10.1002/stem.2096.

Lepor, Herbert. 2005. "Pathophysiology of Lower Urinary Tract Symptoms in the Aging Male Population." *Reviews in Urology* 7 (Suppl 7): S3–11.

———. 2007. "Alpha Blockers for the Treatment of Benign Prostatic Hyperplasia." *Reviews in Urology* 9 (4): 181–90.

Levesque, Christine, and Peter S. Nelson. 2018. "Cellular Constituents of the Prostate Stroma: Key Contributors to Prostate Cancer Progression and Therapy Resistance." *Cold Spring Harbor Perspectives in Medicine* 8 (8). https://doi.org/10.1101/cshperspect.a030510.

Li, Jia J., and Michael M. Shen. 2019. "Prostate Stem Cells and Cancer Stem Cells." *Cold Spring Harbor Perspectives in Medicine* 9 (6). https://doi.org/10.1101/cshperspect.a030395.

Lim, Kok Bin. 2017. "Epidemiology of Clinical Benign Prostatic Hyperplasia." *Asian Journal of Urology* 4 (3): 148–51. https://doi.org/10.1016/j.ajur.2017.06.004.

Litvinov, Ivan V., Donald J. Vander Griend, Yi Xu, Lizamma Antony, Susan L. Dalrymple, and John T. Isaacs. 2006. "Low-Calcium Serum-Free Defined Medium Selects for Growth of Normal Prostatic Epithelial Stem Cells." *Cancer Research* 66 (17): 8598–8607. https://doi.org/10.1158/0008-5472.CAN-06-1228.

Liu, Teresa T., Samuel Thomas, Dalton T. Mclean, Alejandro Roldan-Alzate, Diego Hernando, Emily A. Ricke, and William A. Ricke. 2019. “Prostate Enlargement and Altered Urinary Function Are Part of the Aging Process.” *Aging (Albany NY)* 11 (9): 2653–69. https://doi.org/10.18632/aging.101938.

Liu, Wennuan, Chunmei Carol Xie, Yi Zhu, Tao Li, Jishan Sun, Yu Cheng, Charles M. Ewing, et al. 2008. “Homozygous Deletions and Recurrent Amplifications Implicate New Genes Involved in Prostate Cancer.” *Neoplasia (New York, N.Y.)* 10 (8): 897–907. https://doi.org/10.1593/neo.08428.

Livak, K. J., and T. D. Schmittgen. 2001. “Analysis of Relative Gene Expression Data Using Real-Time Quantitative PCR and the 2(-Delta Delta C(T)) Method.” *Methods (San Diego, Calif.)* 25 (4): 402–8. https://doi.org/10.1006/meth.2001.1262.

Long, Ronan M., Colm Morrissey, John M. Fitzpatrick, and R. William G. Watson. 2005. “Prostate Epithelial Cell Differentiation and Its Relevance to the Understanding of Prostate Cancer Therapies.” *Clinical Science (London, England: 1979)* 108 (1): 1–11. https://doi.org/10.1042/CS20040241.

Macosko, Evan Z., Anindita Basu, Rahul Satija, James Nemesh, Karthik Shekhar, Melissa Goldman, Itay Tirosh, et al. 2015. “Highly Parallel Genome-Wide Expression Profiling of Individual Cells Using Nanoliter Droplets.” *Cell* 161 (5): 1202–14. https://doi.org/10.1016/j.cell.2015.05.002.

Maundrell, K., B. Antonsson, E. Magnenat, M. Camps, M. Muda, C. Chabert, C. Gillieron, et al. 1997. “Bcl-2 Undergoes Phosphorylation by c-Jun N-Terminal Kinase/Stress-Activated Protein Kinases in the Presence of the Constitutively Active GTP-Binding Protein Rac1.” *The Journal of Biological Chemistry* 272 (40): 25238–42. https://doi.org/10.1074/jbc.272.40.25238.

McAuley, Erin M., Devkumar Mustafi, Brian W. Simons, Rebecca Valek, Marta Zamora, Erica Markiewicz, Sophia Lamperis, et al. 2017. “Magnetic Resonance Imaging and Molecular Characterization of a Hormone-Mediated Murine Model of Prostate Enlargement and Bladder Outlet Obstruction.” *The American Journal of Pathology* 187 (11): 2378–87. https://doi.org/10.1016/j.ajpath.2017.07.014.

McAuley, Erin, Daniel Moline, Calvin VanOpstall, Sophia Lamperis, Ryan Brown, and Donald J. Vander Griend. 2019. “Sox2 Expression Marks Castration-Resistant Progenitor Cells in the Adult Murine Prostate.” *Stem Cells (Dayton, Ohio)* 37 (5): 690–700. https://doi.org/10.1002/stem.2987.

McCray, Tara, Daniel Moline, Bethany Baumann, Donald Vander Griend, and Larisa Nonn. 2019. “Single-Cell RNA-Seq Analysis Identifies a Putative Epithelial Stem Cell Population in Human Primary Prostate Cells in Monolayer and Organoid Culture Conditions.” *National Journal of Clinical and Experimental Urology* 7 (3).

McCray, Tara, Zachary Richards, Joseph Marsili, Gail S. Prins, and Larisa Nonn. 2019. “Handling and Assessment of Human Primary Prostate Organoid Culture.” *Journal of Visualized Experiments: JoVE*, no. 143 (17). https://doi.org/10.3791/59051.

Moad, Mohammad, Edouard Hannezo, Simon J. Buczacki, Laura Wilson, Amira El-Sherif, David Sims, Robert Pickard, et al. 2017. “Multipotent Basal Stem Cells, Maintained in Localized Proximal Niches, Support Directed Long-Ranging Epithelial Flows in Human Prostates.” *Cell Reports* 20 (7): 1609–22. https://doi.org/10.1016/j.celrep.2017.07.061.

Montoro, Daniel T., Adam L. Haber, Moshe Biton, Vladimir Vinarsky, Brian Lin, Susan E. Birket, Feng Yuan, et al. 2018. “A Revised Airway Epithelial Hierarchy Includes CFTR-Expressing Ionocytes.” *Nature* 560 (7718): 319–24. https://doi.org/10.1038/s41586-018-0393-7.

Nadiminty, Nagalakshmi, Ramakumar Tummala, Chengfei Liu, Joy Yang, Wei Lou, Christopher P. Evans, and Allen C. Gao. 2013. “NF-KB2/P52 Induces Resistance to Enzalutamide in Prostate Cancer: Role of Androgen Receptor and Its Variants.” *Molecular Cancer Therapeutics* 12 (8): 1629–37. https://doi.org/10.1158/1535-7163.MCT-13-0027.

Neelam, Sudha, Morgan M. Brooks, and Patrick R. Cammarata. 2013. “Lenticular Cytoprotection. Part 1: The Role of Hypoxia Inducible Factors-1α and -2α and Vascular Endothelial Growth Factor in Lens Epithelial Cell Survival in Hypoxia.” *Molecular Vision* 19: 1–15.

Newman, M. E. J. 2006. “Modularity and Community Structure in Networks.” *Proceedings of the National Academy of Sciences of the United States of America* 103 (23): 8577–82. https://doi.org/10.1073/pnas.0601602103.

Nicholson, Tristan M., and William A. Ricke. 2011. “Androgens and Estrogens in Benign Prostatic Hyperplasia: Past, Present and Future.” *Differentiation; Research in Biological Diversity* 82 (4–5): 184–99. https://doi.org/10.1016/j.diff.2011.04.006.

Niranjan, Birunthi, Mitchell G. Lawrence, Melissa M. Papargiris, Michelle G. Richards, Shirin Hussain, Mark Frydenberg, John Pedersen, Renea A. Taylor, and Gail P. Risbridger. 2013. “Primary Culture and Propagation of Human Prostate Epithelial Cells.” *Methods in Molecular Biology (Clifton, N.J.)* 945: 365–82. https://doi.org/10.1007/978-1-62703-125-7_22.

Notara, Maria, and Aamir Ahmed. 2012. “Benign Prostate Hyperplasia and Stem Cells: A New Therapeutic Opportunity.” *Cell Biology and Toxicology* 28 (6): 435–42. https://doi.org/10.1007/s10565-012-9234-x.

Oliveira, Daniel S. M., Sijana Dzinic, Alan I. Bonfil, Allen D. Saliganan, Shijie Sheng, and R. Daniel Bonfil. 2016. “The Mouse Prostate: A Basic Anatomical and Histological Guideline.” *Bosnian Journal of Basic Medical Sciences* 16 (1): 8–13. https://doi.org/10.17305/bjbms.2016.917.

Ornitz, David M., and Nobuyuki Itoh. 2015. “The Fibroblast Growth Factor Signaling Pathway.” *Wiley Interdisciplinary Reviews. Developmental Biology* 4 (3): 215–66. https://doi.org/10.1002/wdev.176.

Paule, Bernard, Stéphane Terry, Laurence Kheuang, Pascale Soyeux, Francis Vacherot, and Alexandre de la Taille. 2007. “The NF-KappaB/IL-6 Pathway in Metastatic Androgen-Independent Prostate Cancer: New Therapeutic Approaches?” *World Journal of Urology* 25 (5): 477–89. https://doi.org/10.1007/s00345-007-0175-6.

Peehl, D. M., and T. A. Stamey. 1986. “Serum-Free Growth of Adult Human Prostatic Epithelial Cells.” *In Vitro Cellular & Developmental Biology: Journal of the Tissue Culture Association* 22 (2): 82–90. https://doi.org/10.1007/BF02623537.

Peehl, D. M., S. T. Wong, and T. A. Stamey. 1988. “Clonal Growth Characteristics of Adult Human Prostatic Epithelial Cells.” *In Vitro Cellular & Developmental Biology: Journal of the Tissue Culture Association* 24 (6): 530–36. https://doi.org/10.1007/BF02629087.

Peehl, Donna M. 2003. “Growth of Prostatic Epithelial and Stromal Cells in Vitro.” *Methods in Molecular Medicine* 81: 41–57. https://doi.org/10.1385/1-59259-372-0:41.

———. 2004. “Are Primary Cultures Realistic Models of Prostate Cancer?” *Journal of Cellular Biochemistry* 91 (1): 185–95. https://doi.org/10.1002/jcb.10691.

Peng, Yu-Ching, and Alexandra L. Joyner. 2015. “Hedgehog Signaling in Prostate Epithelial-Mesenchymal Growth Regulation.” *Developmental Biology* 400 (1): 94–104. https://doi.org/10.1016/j.ydbio.2015.01.019.

Portillo-Lara, Roberto, and Mario Moisés Alvarez. 2015. “Enrichment of the Cancer Stem Phenotype in Sphere Cultures of Prostate Cancer Cell Lines Occurs through Activation of Developmental Pathways Mediated by the Transcriptional Regulator ΔNp63α.” *PloS One* 10 (6): e0130118. https://doi.org/10.1371/journal.pone.0130118.

Ramsey, E. W. 2000. “Benign Prostatic Hyperplasia: A Review.” *The Canadian Journal of Urology* 7 (6): 1135–43.

Rawla, Prashanth. 2019. “Epidemiology of Prostate Cancer.” *World Journal of Oncology* 10 (2): 63–89. https://doi.org/10.14740/wjon1191.

Rocco, Bernardo, Giancarlo Albo, Rafael Coelho Ferreira, Matteo Spinelli, Gabriele Cozzi, Paolo Dell’Orto, Vipul Patel, and Francesco Rocco. 2011. “Recent Advances in the Surgical Treatment of Benign Prostatic Hyperplasia.” *Therapeutic Advances in Urology* 3 (6): 263–72. https://doi.org/10.1177/1756287211426301.

Salem, Omar, and Carsten G. Hansen. 2019. “The Hippo Pathway in Prostate Cancer.” *Cells* 8 (4). https://doi.org/10.3390/cells8040370.

Satija, Rahul, Jeffrey A. Farrell, David Gennert, Alexander F. Schier, and Aviv Regev. 2015. “Spatial Reconstruction of Single-Cell Gene Expression Data.” *Nature Biotechnology* 33 (5): 495–502. https://doi.org/10.1038/nbt.3192.

Schmelz, Monika, Roland Moll, Ulrike Hesse, Anil R. Prasad, Jay A. Gandolfi, Shirin R. Hasan, Marty Bartholdi, and Anne E. Cress. 2005. “Identification of a Stem Cell Candidate in the Normal Human Prostate Gland.” *European Journal of Cell Biology* 84 (2–3): 341–54. https://doi.org/10.1016/j.ejcb.2004.12.019.

Schneider, Andre, Thomas Brand, Robert Zweigerdt, and Hans-Henning Arnold. 2000. “Targeted Disruption of the Nkx3.1 Gene in Mice Results in Morphogenetic Defects of Minor Salivary Glands: Parallels to Glandular Duct Morphogenesis in Prostate.” *Mechanisms of Development* 95 (1): 163–74. https://doi.org/10.1016/S0925-4773(00)00355-5
.

Siegel, Rebecca L., Kimberly D. Miller, and Ahmedin Jemal. 2017. “Cancer Statistics, 2017.” *CA: A Cancer Journal for Clinicians* 67 (1): 7–30. https://doi.org/10.3322/caac.21387.

Sobel, R. E., and M. D. Sadar. 2005a. “Cell Lines Used in Prostate Cancer Research: A Compendium of Old and New Lines--Part 1.” *The Journal of Urology* 173 (2): 342–59. https://doi.org/10.1097/01.ju.0000141580.30910.57.

———. 2005b. “Cell Lines Used in Prostate Cancer Research: A Compendium of Old and New Lines--Part 2.” *The Journal of Urology* 173 (2): 360–72. https://doi.org/10.1097/01.ju.0000149989.01263.dc.

Song, Shumei, Min Xie, Ailing W. Scott, Jiankang Jin, Lang Ma, Xiaochuan Dong, Heath D. Skinner, Randy L. Johnson, Sheng Ding, and Jaffer A. Ajani. 2018. “A Novel YAP1 Inhibitor Targets CSC-Enriched Radiation-Resistant Cells and Exerts Strong Antitumor Activity in Esophageal Adenocarcinoma.” *Molecular Cancer Therapeutics* 17 (2): 443–54. https://doi.org/10.1158/1535-7163.MCT-17-0560.

Sugimura, Y., G. R. Cunha, and A. A. Donjacour. 1986a. “Morphogenesis of Ductal Networks in the Mouse Prostate.” *Biology of Reproduction* 34 (5): 961–71. https://doi.org/10.1095/biolreprod34.5.961.

———. 1986b. “Morphological and Histological Study of Castration-Induced Degeneration and Androgen-Induced Regeneration in the Mouse Prostate.” *Biology of Reproduction* 34 (5): 973–83.

Sugimura, Y., G. R. Cunha, A. A. Donjacour, R. M. Bigsby, and J. R. Brody. 1986. “Whole-Mount Autoradiography Study of DNA Synthetic Activity during Postnatal Development and Androgen-Induced Regeneration in the Mouse Prostate.” *Biology of Reproduction* 34 (5): 985–95. https://doi.org/10.1095/biolreprod34.5.985.

Sugimura, Y., B. A. Foster, Y. K. Hom, J. H. Lipschutz, J. S. Rubin, P. W. Finch, S. A. Aaronson, N. Hayashi, J. Kawamura, and G. R. Cunha. 2003. “Keratinocyte Growth Factor (KGF) Can Replace Testosterone in the Ductal Branching Morphogenesis of the Rat Ventral Prostate.” *International Journal of Developmental Biology* 40 (5): 941–51. https://doi.org/10.1387/ijdb.8946242.

Suh, Junghan, and Arnold B. Rabson. 2004. “NF-KappaB Activation in Human Prostate Cancer: Important Mediator or Epiphenomenon?” *Journal of Cellular Biochemistry* 91 (1): 100–117. https://doi.org/10.1002/jcb.10729.

Suvarna, Vasanti, Vikas Singh, and Manikanta Murahari. 2019. “Current Overview on the Clinical Update of Bcl-2 Anti-Apoptotic Inhibitors for Cancer Therapy.” *European Journal of Pharmacology* 862 (November): 172655. https://doi.org/10.1016/j.ejphar.2019.172655.

Teo, Min Yuen, Dana E. Rathkopf, and Philip Kantoff. 2019. “Treatment of Advanced Prostate Cancer.” *Annual Review of Medicine* 70: 479–99. https://doi.org/10.1146/annurev-med-051517-011947.

Thomson, A. A., and G. R. Cunha. 1999. “Prostatic Growth and Development Are Regulated by FGF10.” *Development* 126 (16): 3693–3701.

Timms, Barry G., Tom J. Mohs, and Liberato J. A. Didio. 1994. “Ductal Budding and Branching Patterns in the Developing Prostate.” *The Journal of Urology* 151 (5): 1427–32. https://doi.org/10.1016/S0022-5347(17)35273-4.

Toivanen, Roxanne, Adithi Mohan, and Michael M. Shen. 2016. “Basal Progenitors Contribute to Repair of the Prostate Epithelium Following Induced Luminal Anoikis.” *Stem Cell Reports* 6 (5): 660–67. https://doi.org/10.1016/j.stemcr.2016.03.007.

Toivanen, Roxanne, and Michael M. Shen. 2017. “Prostate Organogenesis: Tissue Induction, Hormonal Regulation and Cell Type Specification.” *Development (Cambridge, England)* 144 (8): 1382–98. https://doi.org/10.1242/dev.148270.

Tokar, Erik J., Brooke B. Ancrile, Gerald R. Cunha, and Mukta M. Webber. 2005. “Stem/Progenitor and Intermediate Cell Types and the Origin of Human Prostate Cancer.” *Differentiation* 73 (9): 463–73. https://doi.org/10.1111/j.1432-0436.2005.00047.x.

Torrealba, Norelia, Raúl Vera, Benito Fraile, Pilar Martínez-Onsurbe, Ricardo Paniagua, and Mar Royuela. 2019. “TGF-β/PI3K/AKT/MTOR/NF-KB Pathway. Clinicopathological Features in Prostate Cancer.” *The Aging Male: The Official Journal of the International Society for the Study of the Aging Male*, April, 1–11. https://doi.org/10.1080/13685538.2019.1597840.

Trapnell, Cole, Davide Cacchiarelli, Jonna Grimsby, Prapti Pokharel, Shuqiang Li, Michael Morse, Niall J. Lennon, Kenneth J. Livak, Tarjei S. Mikkelsen, and John L. Rinn. 2014. “Pseudo-Temporal Ordering of Individual Cells Reveals Dynamics and Regulators of Cell Fate Decisions.” *Nature Biotechnology* 32 (4): 381–86. https://doi.org/10.1038/nbt.2859.

Tsujimura, Akira, Yasuhiro Koikawa, Sarah Salm, Tetsuya Takao, Sandra Coetzee, David Moscatelli, Ellen Shapiro, Herbert Lepor, Tung-Tien Sun, and E. Lynette Wilson. 2002. “Proximal Location of Mouse Prostate Epithelial Stem Cells.” *The Journal of Cell Biology* 157 (7): 1257–65. https://doi.org/10.1083/jcb.200202067.

Uzgare, Aarti R., Yi Xu, and John T. Isaacs. 2004. “In Vitro Culturing and Characteristics of Transit Amplifying Epithelial Cells from Human Prostate Tissue.” *Journal of Cellular Biochemistry* 91 (1): 196–205. https://doi.org/10.1002/jcb.10764.

Valkenburg, Kenneth C., and Bart O. Williams. 2011. “Mouse Models of Prostate Cancer.” *Prostate Cancer* 2011: 895238. https://doi.org/10.1155/2011/895238.

Visakorpi, T., E. Hyytinen, P. Koivisto, M. Tanner, R. Keinänen, C. Palmberg, A. Palotie, T. Tammela, J. Isola, and O. P. Kallioniemi. 1995. “In Vivo Amplification of the Androgen Receptor Gene and Progression of Human Prostate Cancer.” *Nature Genetics* 9 (4): 401–6. https://doi.org/10.1038/ng0495-401.

Vlaeminck-Guillem, Virginie, Germain Gillet, and Ruth Rimokh. 2014. “SRC: Marker or Actor in Prostate Cancer Aggressiveness.” *Frontiers in Oncology* 4: 222. https://doi.org/10.3389/fonc.2014.00222.

Wallach, Thomas, and James R Bayrer. 2017. “Intestinal Organoids: New Frontiers in the Study of Intestinal Disease and Physiology.” *Journal of Pediatric Gastroenterology and Nutrition* 64 (2): 180–85. https://doi.org/10.1097/MPG.0000000000001411.

Wang, Bu-er, Xi Wang, Jason E. Long, Jeff Eastham-Anderson, Ron Firestein, and Melissa R. Junttila. 2015. “Castration-Resistant Lgr5+ Cells Are Long-Lived Stem Cells Required for Prostatic Regeneration.” *Stem Cell Reports* 4 (5): 768–79. https://doi.org/10.1016/j.stemcr.2015.04.003.

Wang, Guocan, Zhiwei Wang, Fazlul H. Sarkar, and Wenyi Wei. 2012. “Targeting Prostate Cancer Stem Cells for Cancer Therapy.” *Discovery Medicine* 13 (69): 135–42.

Wang, Xi, Marianna Kruithof-de Julio, Kyriakos D. Economides, David Walker, Hailong Yu, M. Vivienne Halili, Ya-Ping Hu, Sandy M. Price, Cory Abate-Shen, and Michael M. Shen. 2009. “A Luminal Epithelial Stem Cell That Is a Cell of Origin

for Prostate Cancer." *Nature* 461 (7263): 495–500. https://doi.org/10.1038/nature08361.

Wei, John T., Elizabeth Calhoun, and Steven J. Jacobsen. 2005. "Urologic Diseases in America Project: Benign Prostatic Hyperplasia." *The Journal of Urology* 173 (4): 1256–61. https://doi.org/10.1097/01.ju.0000155709.37840.fe.

Wen, Y., M. C. Hu, K. Makino, B. Spohn, G. Bartholomeusz, D. H. Yan, and M. C. Hung. 2000. "HER-2/Neu Promotes Androgen-Independent Survival and Growth of Prostate Cancer Cells through the Akt Pathway." *Cancer Research* 60 (24): 6841–45.

Willis, Simon, Catherine L. Day, Mark G. Hinds, and David C. S. Huang. 2003. "The Bcl-2-Regulated Apoptotic Pathway." *Journal of Cell Science* 116 (20): 4053–56. https://doi.org/10.1242/jcs.00754.

Wu, Angela R, Norma F Neff, Tomer Kalisky, Piero Dalerba, Barbara Treutlein, Michael E Rothenberg, Francis M Mburu, et al. 2014. "Quantitative Assessment of Single-Cell RNA-Sequencing Methods." *Nature Methods* 11 (1): 41–46. https://doi.org/10.1038/nmeth.2694.

Wuidart, Aline, Marielle Ousset, Steffen Rulands, Benjamin D. Simons, Alexandra Van Keymeulen, and Cédric Blanpain. 2016. "Quantitative Lineage Tracing Strategies to Resolve Multipotency in Tissue-Specific Stem Cells." *Genes & Development* 30 (11): 1261–77. https://doi.org/10.1101/gad.280057.116.

Xin, L. 2013. "Cells of Origin for Cancer: An Updated View from Prostate Cancer." *Oncogene* 32 (32): 3655–63. https://doi.org/10.1038/onc.2012.541.

Xin, Li, Hisamitsu Ide, Yoon Kim, Purnima Dubey, and Owen N. Witte. 2003. "In Vivo Regeneration of Murine Prostate from Dissociated Cell Populations of Postnatal Epithelia and Urogenital Sinus Mesenchyme." *Proceedings of the National Academy of Sciences* 100 (suppl 1): 11896–903. https://doi.org/10.1073/pnas.1734139100.

Xiong, Xiaozhong, Markus Schober, Evelyne Tassone, Alireza Khodadadi-Jamayran, Ana Sastre-Perona, Hua Zhou, Aristotelis Tsirigos, et al. 2018. "KLF4, A Gene Regulating Prostate Stem Cell Homeostasis, Is a Barrier to Malignant Progression and Predictor of Good Prognosis in Prostate Cancer." *Cell Reports* 25 (11): 3006-3020.e7. https://doi.org/10.1016/j.celrep.2018.11.065.

Yoo, Jae Kwang, Jae Ho Cho, Seung Woo Lee, and Young Chul Sung. 2002. “IL-12 Provides Proliferation and Survival Signals to Murine CD4+ T Cells Through Phosphatidylinositol 3-Kinase/Akt Signaling Pathway.” *The Journal of Immunology* 169 (7): 3637–43. https://doi.org/10.4049/jimmunol.169.7.3637.

Yoo, Young A., Meejeon Roh, Anum F. Naseem, Barbara Lysy, Mohamed M. Desouki, Kenji Unno, and Sarki A. Abdulkadir. 2016. “Bmi1 Marks Distinct Castration-Resistant Luminal Progenitor Cells Competent for Prostate Regeneration and Tumour Initiation.” *Nature Communications* 7 (October): 12943. https://doi.org/10.1038/ncomms12943.

Yu, Jindan, Jianjun Yu, Ram-Shankar Mani, Qi Cao, Chad J. Brenner, Xuhong Cao, Xiaoju Wang, et al. 2010. “An Integrated Network of Androgen Receptor, Polycomb, and TMPRSS2-ERG Gene Fusions in Prostate Cancer Progression.” *Cancer Cell* 17 (5): 443–54. https://doi.org/10.1016/j.ccr.2010.03.018.

Zhao, Bin, Xiaomu Wei, Weiquan Li, Ryan S. Udan, Qian Yang, Joungmok Kim, Joe Xie, et al. 2007. “Inactivation of YAP Oncoprotein by the Hippo Pathway Is Involved in Cell Contact Inhibition and Tissue Growth Control.” *Genes & Development* 21 (21): 2747–61. https://doi.org/10.1101/gad.1602907.